AD_____
(Leave blank)

Award Number: W81XWH-04-1-0286
(Enter Army Award number assigned to research, i.e., DAMD17-00-1-0296)

TITLE: The Role of the Sonic Hedgehog Pathway for Prostate Cancer Progression
(Enter title of award)

PRINCIPAL INVESTIGATOR: Jingwu Xie, PhD
(Enter the name and degree of Principal Investigator and any Associates)

CONTRACTING ORGANIZATION: University of Texas Medical Branch, Galveston, TX 77555-0136
(Enter the Name, City, State and Zip Code of the Contracting Organization)

REPORT DATE: February 2006
(Enter month and year, i.e., January 2001)

TYPE OF REPORT: Annual
(Enter type of report, i.e., annual, midterm, annual summary, final)

PREPARED FOR: U.S. Army Medical Research and Materiel Command
Fort Detrick, Maryland 21702-5012

DISTRIBUTION STATEMENT: (Check one)

- ✓ Approved for public release; distribution unlimited

- Distribution limited to U.S. Government agencies only; report contains proprietary information

REPORT DOCUMENTATION PAGE

Form Approved
OMB No. 074-0188

1. Agency Use Only (Leave blank)	2. Report Date	3. Report Type and Period Covered (i.e., annual 1 Jun 00 - 31 May 01)
	Feb. 25, 2006	Annual, 30 Jan 05 – 31 Jan 06

4. Title and Subtitle
The role of the sonic hedgehog pathway for prostate cancer progression

5. Award Number
W81XWH-04-1-0286

6. Author(s)
Jingwu Xie

7. Performing Organization Name (Include Name, City, State, Zip Code and Email for Principal Investigator)
Jingwu Xie
University of Texas Medical Branch
Galveston, TX 77555-1048
E-Mail: jinxie@utmb.edu

8. Performing Organization Report Number (Leave Blank)

9. Sponsoring/Monitoring Agency Name and Address
U.S. Army Medical Research and Materiel Command
Fort Detrick, Maryland 21702-5012

10. Sponsoring/Monitoring Agency Report Number (Leave Blank)

11. Supplementary Notes (i.e., report contains color photos, report contains appendix in non-print form, etc.)
Publication: Appendix 1: Cancer Letter 2006, **2**: Journal of Biological Chemistry, 2005

12a. Distribution/Availability Statement (check one)
☑ Approved for public release; distribution unlimited
☐ Distribution limited to U.S. Government agencies only - report contains proprietary information

12b. Distribution Code
(Leave Blank)

13. Abstract ***(Maximum 200 Words)*** *(abstract should contain no proprietary or confidential information)*

The hedgehog pathway plays a critical role in the development of prostate. In the previous funding period, we reported activation of hedgehog signaling in advanced and metastatic tumors. Here we report molecular mechanisms by which activated hedgehog signaling alter cell functions. In one cancer cell line, NCI-H209, we detected promoter methylation of *Su(Fu)*. Ectopic expression of Su(Fu) in NCI-H209 cells down-regulates hedgehog target gene expression and leads to inhibition of BrdU incorporation, a marker for cell proliferation. Thus, inactivation of Su(Fu) is a mechanism by which hedgehog signaling is activated in human cancer. We also investigated the molecular basis by which PKA affects Gli1 activity. We find that activation of PKA retains Gli1 in the cytoplasm. Conversely, inhibition of PKA activity promotes nuclear accumulation of Gli1. Mutation analysis identifies T374 as a major PKA site determining Gli1 protein localization. In the three dimension structure, T374 resides adjacent to the basic-residue cluster of the nuclear localization signal (NLS). Mutation of this residue to Asp (Gli1/T374D) results in more cytoplasmic Gli1 whereas a mutation to Lys (Gli1/T374K) leads to more nuclear Gli1. These data provide evidence to support a model that PKA regulates Gli1 localization, in part, through modulating the NLS function.

14. Subject Terms (keywords previously assigned to proposal abstract or terms which apply to this award)
Prostate cancer, Suppressor of fused, hedgehog, Patched

15. Number of Pages (count all pages including appendices) 39

16. Price Code

17. Security Classification of Report	18. Security Classification of this Page	19. Security Classification of Abstract	20. Limitation of Abstract
Unclassified	Unclassified	Unclassified	Unlimited

NSN 7540-01-280-5500

Standard Form 298 (Rev. 2-89)
Prescribed by ANSI Std. Z39-18
298-102

Table of Contents

Introduction

This proposal is to evaluate the role of the hedgehog pathway in prostate cancer in clinical specimens, and to identify the molecular basis of hedgehog mediated tumor formation.

Body

Good progress has been made on this project in the last funding period. We have two manuscripts directed associated with this proposal and two manuscripts relevant to the proposed research areas accepted for publication in last year. Specifically, we revealed that the same mechanism for activated hedgehog signaling exists in lung cancer (Cancer Letters, 2006, see Appendix for details). Furthermore, we found a novel mechanism by which PKA regulates Gli1 localization (Journal of Biological Chemistry, 2006, see Appendix for details). These findings are very important for our understanding of hedgehog-mediated prostate cancer development. In addition, with support of this grant, we were able to identify hedgehog signaling in gastrointestinal cancers, with two manuscripts published (Carcinogenesis, 2005 and Int. Journal of Cancer, 2006).

Task 1: (completed last year)

Task 2: (partially completed last year)

The role of Su(Fu) on cell proliferation

In NCI-H209 cells (a lung cancer cell line), the only cancer cell line with no detectable expression of Su(Fu). we demonstrated that re-expression of Su(Fu) slowed cell growth of this cell line, and reduced the percentage of S phase cell population (see Fig. 1).

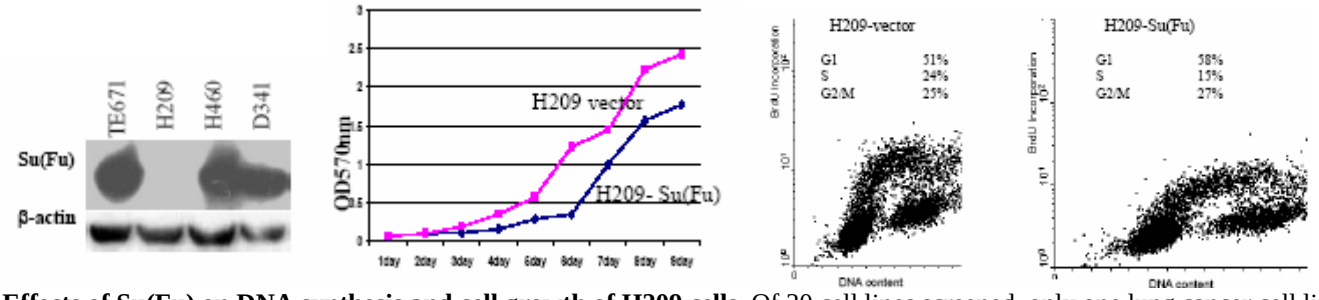

Fig. 1 Effects of Su(Fu) on DNA synthesis and cell growth of H209 cells. Of 30 cell lines screened, only one lung cancer cell line, H209, was shown to lack Su(Fu) protein expression by Western blotting (**left**). Stable expression of Su(Fu) leads to reduced cell growth (**middle**). In consistence with cell growth, Su(Fu) reduced the percentage of S phase cell population (**right**).

Currently, we are still trying to inactivate Su(Fu) in a normal prostate epithelial cell line, RWPE-1, using inducible expression of SiRNA. Since RWPE-1 cells grow slowly, we are planning to express activating SMO in this cell line using an inducible retrovirus system. Once the technical difficulties are resolved, we will examine the effects of inducible activation of hedgehog signaling in this prostate cell line using cell biology techniques.

Inhibition of Gli1 function by PKA through interfering with protein localization

Gli1 is not only a downstream effector, but also a target gene of the hedgehog pathway. Thus, identification of the mechanism by which PKA phosphorylation regulates Gli1 functions will help us understand signal transduction of the hedgehog pathway in cancer.

First, we tested whether Gli1 protein localization can be altered by accumulation of the cellular cAMP level in COS7 cells. After transient transfection, the protein localization of Gli1 was detected by immunofluorescent staining of the C-MYC tag at the Gli1 N-terminus and by cell fractionation. In the presence of 20 μM forskolin, which directly activates adenylyl cyclase and raises the cyclic AMP level (41), we observed that the percentage of cytoplasmic Gli1 was increased over 5 fold whereas the percentage of nuclear Gli1 was reduced by 80% (Fig. 1A, 1B). The effect seems to be direct because the change in Gli1 localization can be observed 20 min after forskolin treatment. Conversely, addition of PKA inhibitor H89 led to a shift of Gli1 localization to the nucleus (Fig. 1A, 1B). As a consequence of forskolin treatment, the cellular PKA activity was increased two fold (Fig. 1C). Conversely, addition of H89 into the medium inhibited the cellular PKA activity by 70% (Fig. 1C). Thus, Gli1 localization was correlated with the cellular PKA activity. To confirm the data from the

immunofluorescent staining, we performed cell fractionation analysis. As shown in Fig.1B, more Gli1 were in the nuclear fraction following H89 treatment whereas forskolin caused an increase of cytoplasmic Gli1 (Fig. 1B). Furthermore, we monitored localization of Gli1-GFP fusion protein with a time-lapse microscope in the presence of H89 or forskolin. Forskolin retained Gli1-GFP in the cytoplasm whereas H89 promoted nuclear accumulation of this fusion protein (data not shown). All these data indicate that Gli1 localization can be regulated by modulating the cellular PKA activity.

Gli1 protein shuttling between the nucleus and the cytoplasm was interrupted by inhibition of nuclear export with leptomycin B (LMB), a specific inhibitor for CRM1-mediated nuclear export, resulting in nuclear accumulation of all Gli1 proteins (Fig. 1A, 1B), supporting that Gli1 localization is a dynamic process and is tightly regulated. Our data suggest that direct phosphorylation of Gli1 by PKA is responsible for regulation of Gli1 protein localization.

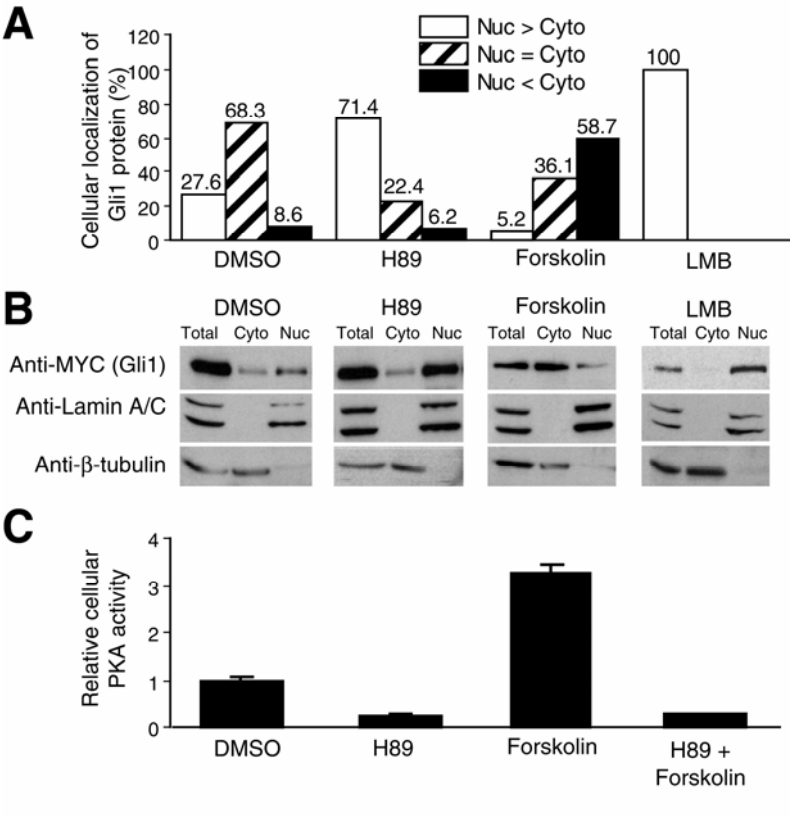

Fig. 2 Regulation of Gli1 localization by forskolin-mediated PKA activation in Cos7 cells. 1A, Gli1 was detected by immunofluorescent staining. Following treatment with forskolin (8 hours), H89 (8 hours) or leptomycin B (LMB, 8 hours) (see Methods for details), Gli1 protein \localization was assessed under a fluorescent microscope in over 200 Gli1-expressing cells, and the experiment was repeated three times with similar results. The percentage of Gli1 in each cellular compartment was calculated from these experiments (see Supplementary Figure for typical pictures of Gli1 staining). Nuc>Cyto indicates preferential nuclear localization, Nuc=Cyto indicates localization both in the nucleus and in the cytoplasm, and Nuc<Cyto indicates predominant cytoplasmic localization. **1B**, Gli1 was detected after cell fractionation (see Methods for details). Both the nuclear fraction and the cytoplasmic fraction were collected for Western blotting analysis. The purity of cell fractionation was assessed using lamin A/C for the nuclear fraction and β-tubulin for the cytoplasmic fraction. **1C**, The cellular PKA activity in COS7 cells was determined using a kit from Upstate Biotechnology Inc. The high PKA activity (**1C**) was correlated with a higher level of cytoplasmic Gli1.

Sequence analysis predicts five putative PKA sites in Gli1. The sequence around these PKA sites is highly conserved among Gli proteins (Fig. 2A). Several point mutations of Gli1 were made to test Gli1 regulation by PKA (see the diagram in Fig. 2B). These mutations were made by *in situ*-mutagenesis in our DNA Recombinant Laboratory Core Facility or by PCR-based mutagenesis.

Using these mutant constructs, we assessed Gli1 localization in cultured cells. We found that mutation at T374 (Gli1/T374V) significantly affects Gli1 localization (Fig. 2C). Furthermore, the response of Gli1/T374V to forskolin treatment was nearly diminished (in response to forskolin treatment, 5 fold increase in cytoplasmic protein for wild type Gli1 but only 40% increase for Gli1/T374V) (also see Supplementary Figure). In contrast, the protein localization of Gli1/S544G and Gli1/S544G/S560A was not different from the wild type Gli1 (Supplementary Figure). A mutant Gli1 (Gli1/T374V/S544G/S560A) with triple mutations at PKA sites behaved like Gli1/T374V (Supplementary Figure), indicating that S544 and S560 are not involved in regulation of Gli1 localization. On the other hand, a mutation at S640A had only slight effects on Gli1 protein localization in response to forskolin (Supplementary Figure). These data indicate that T374 is the major site responsible for Gli1 protein localization in cultured cells.

Consistent with the role of T374 for Gli1 protein localization, we also confirmed that T374 can be phosphorylated by recombinant PKA *in vitro (*Fig. 2D). We performed PKA phosphorylation with Gli1 protein purified by immunoprecipitation in the presence of [r-^{32}P] ATP and recombinant PKA in test tube, and found that Gli1 was highly phosphorylated by PKA *in vitro* (Fig. 2D left, first lane). Gli1 with mutations of all five PKA sites (PKAΔ) could not be phosphorylated by PKA (Fig. 2D, left, right lane). To test if the T374 site of Gli1 is phosophorylated by recombinant PKA, we used a Gli1 fragment containing only two PKA sites: T296 and T374. We found that this Gli1 fragment (1-514

AA) with a mutation at T374 was not able to be phosphorylated by recombinant PKA *in vitro* (Fig. 2D, center). Even a single point mutation at T374 significantly reduced PKA-mediated phosphorylation of full-length Gli1 (Fig. 2D, right), indicating that T374 site is a major PKA site of Gli1 phosphorylation. In addition, our data also suggested that S544, S560 and S640 can be phosphorylated by PKA *in vitro* (data not shown here). The above data indicate that T374 is a major PKA site involved in regulation of Gli1 protein localization.

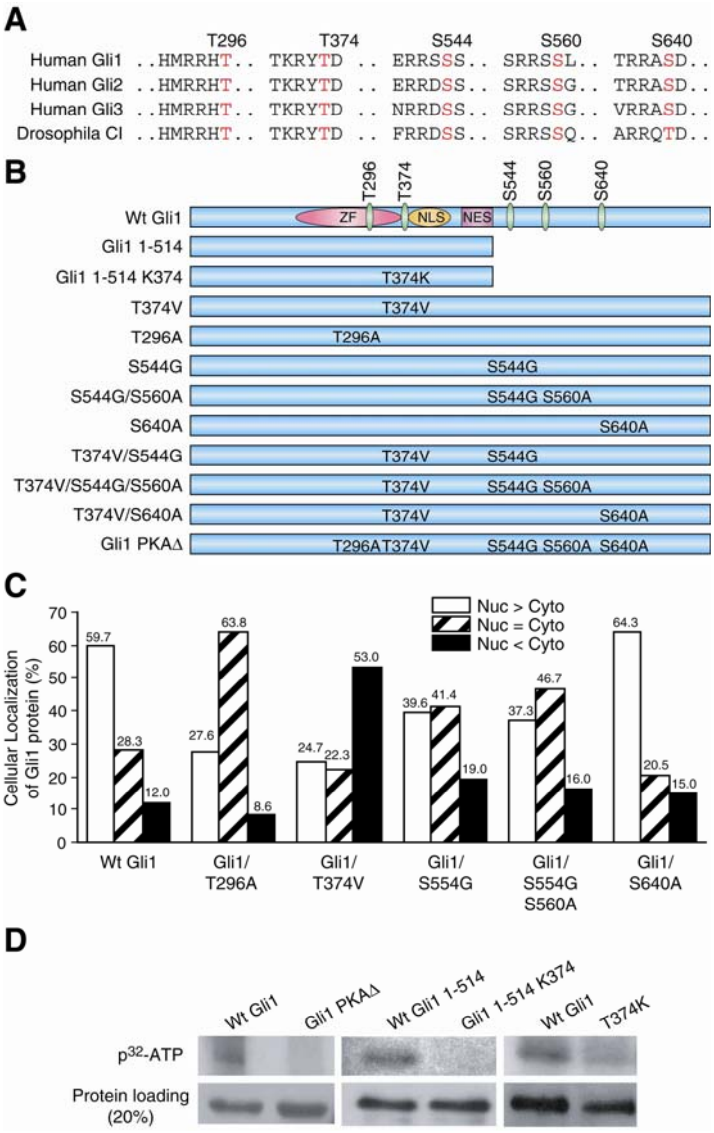

Fig. 3 Regulation of PKA phosphorylation and localization by cAMP/PKA. The five putative sites are conserved in all Gli molecules. **2A** shows the sequence alignment of CI, human Gli1, Gli2 and Gli3 at the five putative PKA sites. **2B** shows the Gli1 constructs used in this study. Gli1 molecules with point mutations of one or more PKA sites were expressed in COS7 cells and their localization was detected by immunofluorescent staining. Full-length Gli1 with a mutation at T374 (T374V) had the most significant effect on Gli1 protein localization (Fig. **2C**). In contrast, a mutation at S544 or other sites (Fig. **2C**) had little effects on Gli1 protein localization. A Gli1 mutant Gli1/T374V /S544G/S560A with triple mutations at PKA sites behaved like Gli1/T374V (data not shown), indicating that T374 is a critical PKA site for determining Gli1 protein localization. Over 200 Gli1 positive cells were counted under a fluorescent microscope for Gli1 protein localization, and the experiment was repeated three times with similar results. The data was the average result from these experiments. **2D** shows Gli1 phosphorylation *in vitro* by recombinant PKA. Wild type Gli1 and its mutant forms were expressed in COS7 cells, and subsequently purified through immunoprecipitation. The ability of PKA to phosphorylate immunoprecipitated Gli1 proteins were performed *in vitro* (see Methods for details). The full-length Gli1, but not Gli1-PKAΔ (See Fig. **2B** the mutation sites), was highly phosphorylated by PKA *in vitro* (**2D left**). A single point mutation in a Gli1 fragment (1-514 AA, shown in Fig. **2B**) prevented protein phosphorylation by PKA (**2D Center**). This same mutation in the full-length Gli1 also dramatically reduced the level of phosphorylation (**2D right**).

In the three dimension structure, T374, together with the adjacent D375, is close to the first basic-residue cluster (R380/K381/H382) of the bipartite motif (the classic NLS) in Gli1 (Fig. 3A) (42). It is known that protein phosphorylation at the residue next to the bipartite motif inhibits its binding affinity to importins, leading to reduced nuclear localization of the target protein (43). We predict that phosphorylation of T374 will increase the local negative charge, leading to reduced NLS functions and accumulation of Gli1 in the cytoplasm. Indeed, Gli1/T374D was preferentially localized to the cytoplasm (Fig. 3B). Conversely, Gli1/T374K has a high local positive charge near the NLS, and we found that Gli1/T374K predominantly localized to the nucleus (Fig. 3B). Localization of these Gli1 proteins was further confirmed by cell fractionation (Fig. 3B). These data support our hypothesis that one mechanism by which the cellular PKA activity regulates Gli1 localization is through altering the local charge nearby the NLS of Gli1.

If Gli1 nuclear localization is regulated by PKA phosphorylation through a NLS-dependent mechanism, disruption of the NLS should affect localization of these mutant Gli1 molecules. As shown in Fig. 3C, we found that Gli1/K381E, which is predicted to disrupt the NLS, was predominantly localized to the cytoplasm, confirming the role of NLS in Gli1 localization (12). Although Gli1/T374K localizes predominantly to the nucleus, additional mutation at K381 (K381E) retained Gli1/T374K to the cytoplasm (Fig. 3C), suggesting that regulation of Gli1 localization by T374 phosphorylation requires the intact NLS.

The ultimate effect of Gli1 is transcriptional activation of the downstream target genes. To assess whether Gli1 localization affects its transcriptional activity, we established stable expression of Gli1 luciferase reporter under the control of Gli responsive elements in NIH3T3 cells (13). By measuring the reporter luciferase activity, we examined the association of Gli1 localization with its transcriptional activity (Fig. 3D). Gli1/K381E remains preferentially in the cytoplasm, the transcriptional activity was low. In contrast, Gli1 with a defective NES (Gli1/L496V/L498V), which localizes predominantly in the nucleus, was more active (Fig. 3D). Thus, the Gli1 luciferase reporter activity in these cells is very sensitive to Gli1 localization. We examined the effects of forskolin to Gli1-mediated transcriptional activity in this NIH3T3 stable cell line. Like the wild type Gli1, Gli1/T374V can activate the Gli luciferase reporter (Fig. 3E). Consistent with its cytoplasmic localization, the luciferase activity in cells expressing the wild type Gli1 was reduced after forskolin treatment (Fig. 3E). In contrast, Gli1/T374V mediated reporter gene activity was not affected by forskolin (Fig. 3E). These data suggest that T374 is an important PKA site responsible for PKA phosphorylation and for the transcriptional activity of Gli1.

Based on these data, we proposed a mechanism by which the cAMP/PKA signaling axis mediates regulation of Gli1 localization. Gli1 enters nucleus through a nuclear localization signal. With the accumulation of cAMP in the cell, T374 gets phosphorylated. Phosphorylation of T374 will increase the local negative charge nearby the NLS, which results in inhibition of NLS function. Consequently, Gli1 is retained in the cytoplasm and is unable to activate the target genes. Since this Thr residue is highly conserved among Gli proteins, we anticipate the same mechanism is applicable to PKA regulation of other Gli molecules.

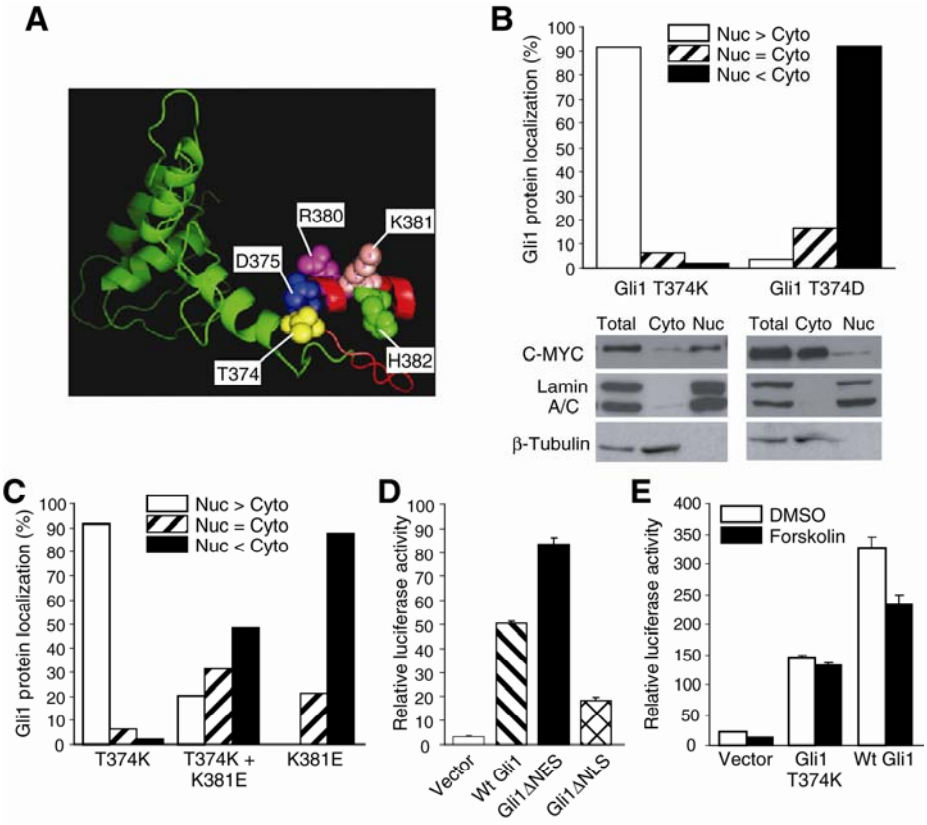

Fig. 4 Demonstration of T374 as the major site for Gli1 regulation. 3A, A 3D model of Gli1 fragment, showing the proximity of T374/D375 to the basic residue cluster (R380/K381/H382) of the Gli1 NLS. **3B** shows the preferential nuclear localization of Gli1/T374K and the predominant cytoplasmic localization of Gli1/T374D. Localization was confirmed by cell fractionation. Immunofluorescent staining was done as in Fig. **1A**. **3C** shows Gli1/T374K localization following an additional mutation at K381. These experiments suggest that T374 is responsible for cAMP/PKA-mediated regulation of Gli1 localization, which may be achieved through affecting the NLS function. **3D,** Correlation of Gli1 localization with its transcriptional activity was examined in NIH3T3 cells with stable expression of a luciferase reporter under the control of Gli-responsive elements. Gli1 with a Lys to Glu mutation at K381 (K381E) of the NLS motif, which predominantly localizes to the cytoplasm, was unable to activate this reporter. In contrast, Gli1 with mutations in the NES motif, which predominantly localizes to the nucleus, was more active than the wild type Gli1. **3E**, Transcriptional activity of Gli1/T374V was not responsive to forskolin treatment whereas the transcriptional activity of wild type Gli1 was reduced by 60% following forskolin treatment.

<u>Task 3</u>: Because nearly 50% of Ptch1+/- mice die of medulloblastomas or rhabdomyosarcomas, we have established a novel system for activated hedgehog signaling in the prostate. In this system, we have inducible expression of activating SMO using lox-P system. With expression of cre, SMO will be induced to express in the prostate. We have talked with Professor Hong Wu from UCLA to collaborate on mouse model of prostate cancer using activated hedgehog signaling. Eventually, this mouse model will help us to understand hedgehog signaling for development of prostate cancer. Furthermore, Professor Leland Chung has started collaboration with my laboratory on the effects of hedgehog signaling for prostate cancer metastasis. All these long-term studies are necessary for us to design novel therapeutic approaches to treat prostate cancer.

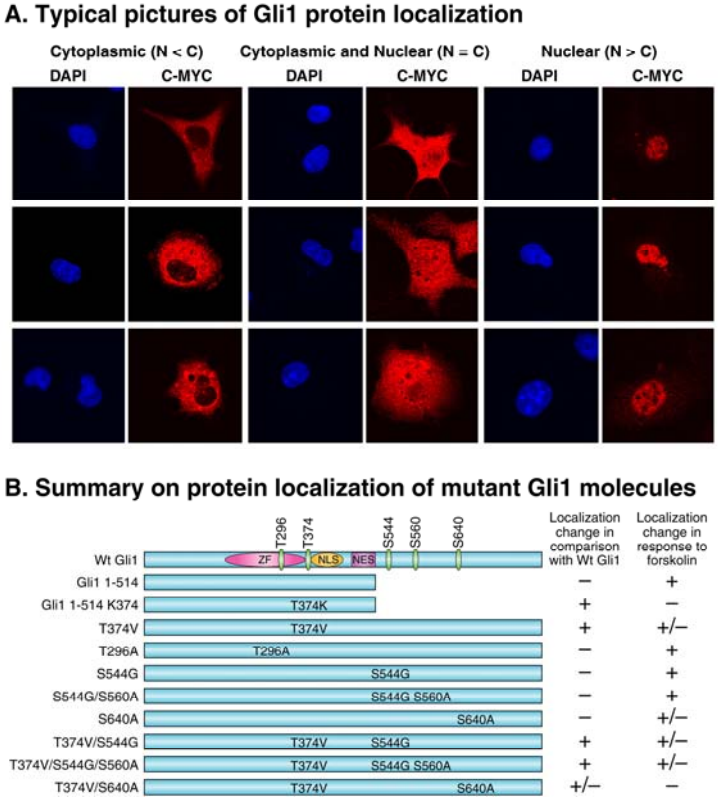

Supplementary Figure shows typical pictures of Gli1 protein localization in cultured cells (630X). The nucleus was stained with DAPI (in blue). Localization of Gli1 molecules was detected by immunofluorescent staining with the N-terminal tag (C-MYC) of Gli1 (in red). **B** shows a summary of our data from different Gli1 constructs. + indicates a significant change in protein localization (>50%, i.e. a change from 50% to 75% in nuclear Gli1 would be a significant change); -indicates an insignificant change of protein -localization (<30%, i.e. a change from 50% to -60% in nuclear Gli1 is not a significant change) -and +/- indicates a slight alteration of protein -localization (30-50%). The data was the average -result from three independent experiments.

Key Research Accomplishments

With support from DOD, we have demonstrated that activation of the hedgehog pathway occurs not only in advanced and metastatic prostate cancers, but also in subsets of gastrointestinal and lung cancers (***Carcinogenesis*** 26:1698-1705, 2005; ***International Journal of Cancer*** 118(1):139-48, 2006; ***Cancer Letters***, 2006). In addition, we found a novel mechanism by which PKA regulates Gli1 localization (***J. Biological Chemistry*** 2005 Nov. 17; [Epub ahead of time]). Based on these findings, we may be able to design better ways to inhibit hedgehog signaling activation in several types of human cancer, particularly in prostate cancer. Two long-term collaborations (with Drs. Hong Wu and Leland Chung) have been established.

Reportable outcomes

Four research papers (***Carcinogenesis*** 26:1698-1705, 2005; ***International Journal of Cancer*** 118(1):139-48, 2006; ***Cancer Letters***, 2006; ***J. Biological Chemistry*** 2005 Nov. 17; [Epub ahead of time])

Conclusion

We have demonstrated that hedgehog pathway activation occurs frequently in advanced prostate cancer as well as other common cancers. Inhibition of hedgehog signaling in these cancers may be achieved through inhibition of Gli1 activity. Several long-term collaboration have been established to investigate hedgehog signaling for development of prostate cancer.

References

1. Ma, X.L., Sheng, T., Zhang, Y.X., Huang S.H., He, J., Chen, K., Zhang, X., Zhang H.W. and **Xie J.** Hedgehog signaling is activated in subsets of esophageal cancers ***International Journal of Cancer*** 118(1):139-48, 2006. Epub 2005 July 7.

2. Ma, X.L., Chen, K., Huang S.H., Sheng, T., Zhang, X., Evers, B.M., Adegboyega, P., Zhang H.W. and **Xie J (2005).** Frequent activation of the hedgehog pathway in advanced gastric adenocarcinomas. ***Carcinogenesis*** 26(10):1698-1705. Epub 2005 May 19.

3. Sheng T, Chi S, Zhang X and **Xie J (2006)**. Regulation of Gli1 localization by the cAMP/ PKA signaling axis through a site near the nuclear localization signal. ***J. Biological Chemistry*** 281: 9-12.

4. Huang, S-H, Chi, S., Li, C-X, Zhang, X., Haque, A.K., Zwischenberger, J., Tyring, S.K., Logrono, R., Bhutani, M., Zhang, H-W and **Xie, J** (2006). Expression of sonic hedgehog and its target genes in lung cancers. ***Cancer Letters*** 2006 Jan. 27, [Epub ahead of print].

Appendices

1. Reprint of Carcinogenesis, 2005.
2. Reprint of JBC, 2006.
3. Copy of the accepted manuscript in Cancer Letters, 2005.
4. Reprint of Int J. Cancer, 2006.

Carcinogenesis vol.26 no.10 pp.1698–1705, 2005
doi:10.1093/carcin/bgi130
Advance Access publication May 19, 2005

Frequent activation of the hedgehog pathway in advanced gastric adenocarcinomas

Xiaoli Ma[1,†], Kai Chen[2,†], Shuhong Huang[1,†], Xiaoli Zhang[2], Patrick A.Adegboyega[3], B.Mark Evers[4], Hongwei Zhang[1] and Jingwu Xie[2,*]

[1]Institute of Developmental Biology, School of Life Sciences, Shandong University, Jinan, PR China, [2]Department of Pharmacology, [3]Department of Pathology and [4]Department of Surgery, Sealy Center for Cancer Cell Biology, University of Texas Medical Branch, Galveston, TX 77555-1048, USA

[*]To whom correspondence should be addressed. Tel: +1 409 747 1845; Fax: +1 409 747 1938;
Email: jinxie@utmb.edu or zhw@sdu.edu.cn

The hedgehog pathway plays a critical role in the development of the foregut. Recent studies indicate that the hedgehog pathway activation occurs in the stomach and other gastrointestinal cancers. However, the association of hedgehog pathway activation with tumor stage, differentiation and tumor subtype is not well documented. Here, we report our findings that the elevated expression of hedgehog target genes human patched gene 1 (PTCH1) or Gli1 occurs in 63 of the 99 primary gastric cancers. Activation of the hedgehog pathway is associated with poorly differentiated and more aggressive tumors. The sonic hedgehog (Shh) transcript is localized to the cancer tissue, whereas expression of Gli1 and PTCH1 is observed both in the cancer and in the surrounding stroma. Treatment of gastric cancer cells with KAAD-cyclopamine, a hedgehog signaling inhibitor, decreases expression of Gli1 and PTCH1, resulting in cell growth inhibition and apoptosis. Overexpression of Gli1 under the control of the cytomegalovirus (CMV) promoter renders these cells resistant to cyclopamine-induced apoptosis. Thus, our analysis of *in vivo* tissues indicates that the hedgehog pathway is frequently activated in advanced gastric adenocarcinomas; our *in vitro* studies suggest that hedgehog signaling contributes to gastric cancer cell growth. These data predict that targeted inhibition of the hedgehog pathway may be effective in the prevention and treatment of advanced gastric adenocarcinomas.

Introduction

The hedgehog pathway plays a critical role in embryonic development, tissue polarity and carcinogenesis (1,2). Secreted hedgehog molecules bind to the receptor patched (PTC–PTCH1, PTCH2), thereby alleviating PTC-mediated suppression of smoothened (SMO), a putative seven-transmembrane protein. SMO signaling triggers a cascade of intracellular events, leading to the activation of the pathway through GLI-dependent transcription (2). Activation of hedgehog signaling, through loss-of-function mutations of PTCH1 or activated mutations of SMO, occurs frequently in human basal cell carcinomas (BCCs) and medulloblastomas (3–7). More recently, abnormal activation of the sonic hedgehog pathway has been reported in subsets of small cell lung cancer, pancreatic cancer, prostate cancer and gastrointestinal (GI) cancers (8–14).

Gastric cancer is the second most common cancer worldwide in terms of incidence and mortality (15). Patients with gastric cancer usually present at late stages and have a poor prognosis. Thus, identification of specific drug targets in the tumor is an essential step to reduce the mortality. A previous study indicated that activation of the hedgehog pathway occurred in all nine primary gastric cancers (10). To determine if hedgehog signaling activation can be utilized for the diagnosis and treatment of gastric cancer, we performed a comprehensive study to assess the hedgehog pathway activation in 99 primary gastric cancers using *in situ* hybridization, real-time PCR and immunohistochemistry.

Through the assessment of sonic hedgehog and its target genes Gli1 and PTCH1, we find that activation of the hedgehog pathway varies among different subtypes of gastric cancer. Tubular and papillary adenocarcinomas, but not signet-ring cell carcinomas, frequently harbor activated hedgehog signaling. Protein expression of the hedgehog and its target genes is not only detected in the tumor, but also in the stroma. We further demonstrate that targeted inhibition of the hedgehog pathway slows cell growth and induces apoptosis in gastric cancer cells. Thus, our studies indicate that activation of the hedgehog pathway is an important event during the progression of gastric cancer. We predict that targeted inhibition of the hedgehog pathway may be an effective method for the treatment of patients with gastric cancer.

Materials and methods

Tumor samples

A total of 117 specimens of gastric tissues were used in our study (99 cancer specimens and 18 normal or inflamed gastric tissues). From the Surgery Department at the Shan Dong Qi Lu Hospital, Jinan, China, or from the UTMB Surgical Pathology, 54 specimens were received as discarded materials with the approval from the Institutional Review Board (IRB). In addition, we purchased a tissue microarray, which contains 63 specimens of gastric cancer, from Chaoying Biotechnology Co., Ltd (Xi'an, China). Pathological reports, H and E staining of each specimen were reviewed to determine the nature of the disease and the tumor histology. In addition, immunohistochemistry with keratin antibodies was used to confirm the tumor pathology. The randomly sorted samples with masked identity were evaluated by at least two independent certified pathologists. Gastric cancers were divided into three major subtypes according to the WHO guideline (16): tubular adenocarcinoma, papillary adenocarcinoma and signet-ring cell carcinomas. This study also includes specimens for normal stomach tissues ($n = 11$), gastritis ($n = 4$) and other stomach tissues ($n = 3$) (see Supplementary Table 1A for more information).

In situ hybridization

Gli1 (X07384) was cloned into pBluescript M13+KS, the direction of insert is *Hind*III-5′ and *Xba*I-3′. The plasmid was digested with *Nru*I to generate the

Abbreviations: BCC, basal cell carcinoma; CMV, cytomegalovirus; PTC, patched; PTCH1, human patched gene 1; Shh, sonic hedgehog; SMO, smoothened; Su(Fu), suppressor of fused.

[†]These authors contributed equally to this work.

sense fragment (412 bp) and with *Nde*I to generate the antisense fragment (682 bp). PTCH1 (U59464) (cloned into *Xba*I5′ and *Cla*I3′ of pRK5) was digested with *Dra*III to generate a small cDNA fragment (590 bp). Gli3 (M57609) was initially cloned into *Sst*I (5′) and *Sal*I (3′) of pBluescript-SK. *Sna*BI was used to generate the sense fragment (552 bp) and *Psh*AI to generate the antisense fragment (770 bp). Sense and antisense probes were obtained by T3 and T7 *in vitro* transcription using a DIG RNA labeling kit from Roche (Mannheim, Germany). Tissue sections (6 μm thick) were mounted onto poly-L-lysine slides (19). Following deparaffinization, the tissue sections were rehydrated in a series of dilutions of ethanol. To enhance the signal and facilitate probe penetration, sections were immersed in 0.3% Triton X-100 solution for 15 min at room temperature and in proteinase K (20 μg/ml) solution for 20 min at 37°C, respectively. The sections were then incubated with 4% (v/v) paraformaldehyde/phosphate-buffered saline (PBS) for 5 min at 4°C. After washing with PBS and 0.1 M triethanolamine, the slides were incubated with prehybridization solution (50% formamide, 50% 4× SSC) for 2 h at 37°C. The probe was added to each tissue section at a concentration of 1 μg/ml and hybridized overnight at 42°C. After high stringency washing (2× SSC twice, 1× standard saline citrate twice and 0.5× SSC twice at 37°C) the sections were incubated with an alkaline phosphatase-conjugated sheep anti-digoxigenin antibody, which catalyzed a color reaction with the NBT/BCIP (Nitro-Blue-Tetrazolium/5-bromo-4-chloro-3-indolyl phosphate) substrate (Roche, Mannheim, Germany). Blue indicated strong hybridization. As negative controls, sense probes were used in all hybridizations and no positive signal was observed.

RNA isolation and quantitative PCR

Total RNA of the cells was extracted using an RNA extraction kit from Promega according to the manufacturer's instruction (Promega, Madison, WI). For this analysis, we selected only tumors in which 70% of the tissue mass was actually tumor tissue. For quantitative PCR analyses, we detected transcripts of sonic hedgehog, Gli1 and PTCH1 using the Applied Biosystems' assays-by-demand assay mixtures (the sequences for human Gli1, HIP and PTCH1 have been patented by Applied Biosystems, Foster City, CA) and pre-developed 18S rRNA (VIC™-dye labeled probe) TaqMan® assay reagent (P/N 4319413E) as an internal control. The primers were designed to span exon–exon junctions so as not to detect genomic DNA, and the primers and probe sequences were searched against the Celera database to confirm specificity. To obtain the relative quantitation of gene expression, a validation experiment was performed to test the efficiency of the target amplification and the efficiency of the reference amplification. All absolute values of the slope of log input amount versus ΔC_T were <0.1. Separate tubes (single-plex) one-step RT–PCR was performed with 20 ng RNA for both target genes and the endogenous control using TaqMan one-step RT–PCR master mix reagent kit (P/N 4309169). The cycling parameters for one-step RT–PCR were reverse transcription at 48°C for 30 min, AmpliTaq activation at 95°C for 10 min, denaturation at 95°C for 15 s and annealing/extension at 60°C for 1 min (repeat 40 times) on ABI7000. Triplicate C_T values were analyzed in Microsoft Excel using the comparative $C_T(\Delta\Delta C_T)$ method as described by the manufacturer (Applied Biosystems, Foster City, CA). The amount of target ($2^{-\Delta\Delta CT}$) was obtained by normalization to an endogenous reference (18S RNA) and relative to a calibrator.

Immunohistochemistry

Representative formalin fixed and paraffin embedded tissue sections (6 μm thickness) were used for immunohistochemistry with specific antibodies to human Shh and PTCH1 (Cat. no. 9024 for Shh and Cat. no. 6149 for PTCH1, Santa Cruz Biotechnology Inc., Santa Cruz, CA). First, tissue sections were deparaffinized, followed by rehydration with decreased concentrations of ethanol, and immersed in 3% H_2O_2 (in distilled H_2O) for 10 min (to inhibit endogenous peroxidase activity). Following antigen retrieval in citrate buffer (pH 6.0), the tissue sections were incubated with normal goat serum to block nonspecific antibody binding (20 min at room temperature). The sections were then incubated with primary antibodies (at 1:200 dilution) at 37°C in humid chambers for 2 h. After washing with PBS three times, the sections were incubated with the biotinylated secondary antibody (goat anti-rabbit IgG or monkey anti-goat IgG) and streptavidin conjugated to horseradish peroxidase for 20 min at 37°C, followed by PBS wash. The sections were incubated with the DAB substrate for less than 30 min. Haematoxylin was used for counterstaining. Negative controls were performed in all cases by omitting the first antibodies. All primary antibodies have been previously tested for immunohistostaining (9,11,18).

Cell culture, MTT assay and TUNEL assay

Cell lines (AGS, SIIA and RKO) were cultured in F12 Medium with 10% FBS (AGS and SIIA) or DMEM with 10% FBS (RKO), respectively. Colorimetric MTT assay was performed according to our published protocol in the presence of 0.5% FBS (19). Cells were treated with 2 μM of Keto-*N*-aminoethylaminocaproyldihydrocinnamoyl-cyclopamine (KAAD-cyclopamine) for specific times (see Figure 6 for details). Ectopic expression of Gli1, under the control of the cytomegalovirus (CMV) promoter, in AGS cells was achieved by the transient transfection with LipofectAmine 2000 (20,21), and Gli1 was detected by immunofluorescent staining with the Myc tag antibody 9e10 (Sigma, St Louis, MO) (19). TUNEL assay was performed using a kit from Roche according to the manufacturer's instructions (19,21).

Statistical analysis

Student's *t*-test for two samples was performed for the difference between the tumor groups: $P < 0.05$ was considered statistically significant. For example (Table I), the difference between Stage I and Stage III tumors for expression of Shh and PTCH1 was statistically significant with a *P* value of 0.01923. Similarly, the difference between well-differentiated (WD) and poorly differentiated (PD) tumors for expression of Shh and PTCH1 was significantly

Table I. Summary of gastric specimens: clinical pathological data and the hedgehog pathway activation*

	Tumor number	Expression of Shh	Expression of PTCH1	Expression of Gli1
Overall	99	64/99 (∼65%)	63/99 (∼64%)	22/32 (∼69%)
Gender				
Male	77	50/77 (∼65%)	47/77 (∼61%)	15/25 (60%)
Female	22	14/22 (∼64%)	16/22 (∼73%)	7/8
Stage[a]				
I	22	12/22 (∼55%)	11/22 (50%)	5/6
II	22	17/22 (∼77%)	15/22 (∼68%)	4/6
III	41	30/41 (∼73%)	32/41 (∼78%)	11/16 (∼69%)
IV	5	5/5	5/5	2/2
WHO classification				
Adenocarcinomas	90	64/90 (∼71%)	63/90 (70%)	22/28 (79%)
Tubular	43	27/43 (∼63%)	25/43 (∼58%)	7/12 (∼58%)
Papillary	7	5/7	4/7	3/4
PD	40	32/40 (80%)	34/40 (85%)	11/11 (100%)
Signet-ring cell carcinomas	9	0/9	0/9	0/9
Differentiation[b]				
Well differentiated (WD)	18	7/18 (∼39%)	7/18 (∼39%)	1/4
Moderately differentiated (MD)	25	20/25 (80%)	18/25 (72%)	7/9
Poorly differentiated (PD)	40	32/40 (80%)	34/40 (85%)	11/11 (100%)

*Statistical analysis was performed using student's *t*-test for two samples: $P < 0.05$ was considered statistically significant (see Materials and methods for details).
[a]Signet-ring cell carcinomas were excluded from this analysis.
[b]Only tubular adenocarcinomas were used in this analysis.

different (P value = 0.006028). The P value comparing WD and moderately differentiated (MD) tumors for Shh and PTCH1 expression was 0.02993. Furthermore, the difference between tubular and PD tumors on Shh and PTCH1 expression was significant with a P value of 0.01059. There was no significant difference between MD and PD tumors in Shh and PTCH1 expression (P value = 1).

Results

Increased hedgehog target gene expression in gastric cancers

Hedgehog is a critical endodermal signal for the epithelial–mesodermal interactions during the development of the vertebrate gut. In the adult stomach, hedgehog signaling is either undetectable or its expression is restricted to the fundus (18). A previous report using nine primary gastric cancers identified hedgehog pathway activation in all tumors (10). To test whether hedgehog signaling activation can be used for diagnosis of gastric cancers, a comprehensive study is needed to examine the frequency of hedgehog signaling activation in a large number of primary gastric cancers. Toward that end, we examined expression of hedgehog target genes Gli1 and PTCH1 in 117 gastric specimens (99 cancer specimens and 18 non-cancerous specimens, see Supplementary Table 1A for more information). As the target genes of the hedgehog pathway, increased levels of PTCH1 and Gli1 transcripts indicates hedgehog signaling activation (1). We used three methods to assess hedgehog signaling activation in our collected tissues ($n = 54$): *in situ* hybridization, immunohistochemistry and real-time PCR analyses. Expression of sonic hedgehog and PTCH1 was also examined in the tissue array specimens ($n = 63$) by *in situ* hybridization and immunohistostaining (Supplementary Table 1A and B).

Using *in situ* hybridization, we detected PTCH1 expression in 63 of the 99 (~64%) tumor specimens, suggesting that activation of the hedgehog pathway is quite common in gastric cancer (Figure 1A and B and Supplementary Figure A). In contrast, all normal stomach tissues did not have a detectable level of PTCH1, indicating that the hedgehog pathway is not activated in these normal tissues (Figure 1C). Our data are consistent with a previous report that Shh signaling is restricted to the fundic stomach of humans and mice (18). The results of Gli1 expression were consistent with those of PTCH1 expression (see Figure 1E and F, Supplementary Figure B and Supplementary Table 1A). The frequency of hedgehog signaling activation appears to differ in different subtypes of gastric cancer (see Table I). In adenocarcinomas of gastric cancer, 63 of the 90 (70%) specimens demonstrated high levels of PTCH1 (or Gli1) transcripts (Figure 1 and Table I for details). However, signet-ring cell carcinomas ($n = 9$) had no detectable expression of these target genes, suggesting that activation of the hedgehog pathway may not be a frequent event in this subtype of gastric cancer (Table I). Thus, our results indicate that the hedgehog pathway is frequently activated in gastric cancer and the frequency of activation varies among different subtypes of tumors.

Further analysis of the data revealed an association of hedgehog signaling activation with poor differentiation in tubular adenocarcinomas. Only 7 out of 18 (~39%) well-differentiated adenocarcinomas had a high level of PTCH1 transcript, whereas 18 out of 25 (72%) moderately differentiated adenocarcinomas and 34 out of the 40 (85%) poorly differentiated adenocarcinomas expressed the target genes (see Table I). Thus, activation of hedgehog signaling appears to be inversely associated with tumor differentiation. As poor differentiation of the tumor is often associated with prognosis, our findings suggest that activation of the hedgehog pathway may serve as a valuable prognostic biomarker for gastric cancer. This hypothesis predicts that activation of the hedgehog pathway may be more common in advanced stages of gastric cancer. Indeed, 11 out of the 22 Stage I gastric adenocarcinomas (50%) had elevated levels of the target gene transcripts, 78% of Stage III tumors had detectable expression of the target genes (Table I).

To confirm the *in situ* hybridization data, we performed real-time PCR analyses in selected tumors, in which >70% of the tissue mass was actually tumor tissue, to detect the levels of Gli1 and PTCH1 expression. In the tumors with elevated Gli1 and PTCH1 transcripts, we found an approximate 5- to 20-fold increase in levels of Gli1 and PTCH1 expression compared with the matched normal tissues (Figure 2), indicating that the *in situ* hybridization results are in agreement with real-time PCR data. Furthermore, we detected the PTCH1 protein by immunohistochemistry (11). We found that PTCH1 protein was detected in primary gastric cancer, but not in the normal tissues (Figure 3). The data from the immunohistochemical analysis are consistent with the results from real-time PCR and *in situ* hybridization analyses. Taken together, these data indicate that the hedgehog pathway is frequently activated in advanced gastric adenocarcinomas.

Expression of sonic hedgehog in gastric cancer

It is reported that overexpression of sonic hedgehog may be responsible for the activation of the hedgehog pathway in pancreatic cancer, subsets of small cell lung cancer, prostate cancer and several primary gastric cancers (8–14). To test this possibility, we examined expression of sonic hedgehog in gastric specimens by *in situ* hybridization. Many cancers had a high level of sonic hedgehog transcript (Figure 4, Supplementary Figure C and Supplementary Table 1A). In most of the cases, elevated levels of Shh were consistent with elevated levels of PTCH1 and Gli1 expression (see Supplementary Table 1A and B). We found that elevated sonic hedgehog expression is associated with poor differentiation of the tumor and higher tumor grades (Table I). Also in agreement with lack of PTCH1 and Gli1 expression in signet-ring cell carcinomas, there was no detectable expression of sonic hedgehog in any of the signet-ring cell carcinomas analyzed (Table I). In contrast, sonic hedgehog expression was undetectable or very low in normal and inflamed gastric tissues (Figure 4). To confirm the *in situ* hybridization data, we detected the sonic hedgehog protein by immunohistochemistry (9,11). In agreement with the *in situ* hybridization data, we found that tumors with increased sonic hedgehog mRNA expression had high levels of the sonic hedgehog protein (Figure 5). The correlation of sonic hedgehog expression with Gli1 and PTCH1 transcripts indicates an important role of sonic hedgehog in the activation of the hedgehog pathway in gastric adenocarcinomas.

Hedgehog signaling and cellular functions of gastric cancers

If hedgehog pathway activation is required for gastric cancer development, gastric cancer cells should be susceptible to the treatment using the SMO antagonist, cyclopamine. All available gastric cancer cell lines have elevated hedgehog signaling (10), we chose a GI cancer cell line RKO as the negative control [RKO cells do not have elevated levels of Gli1 and

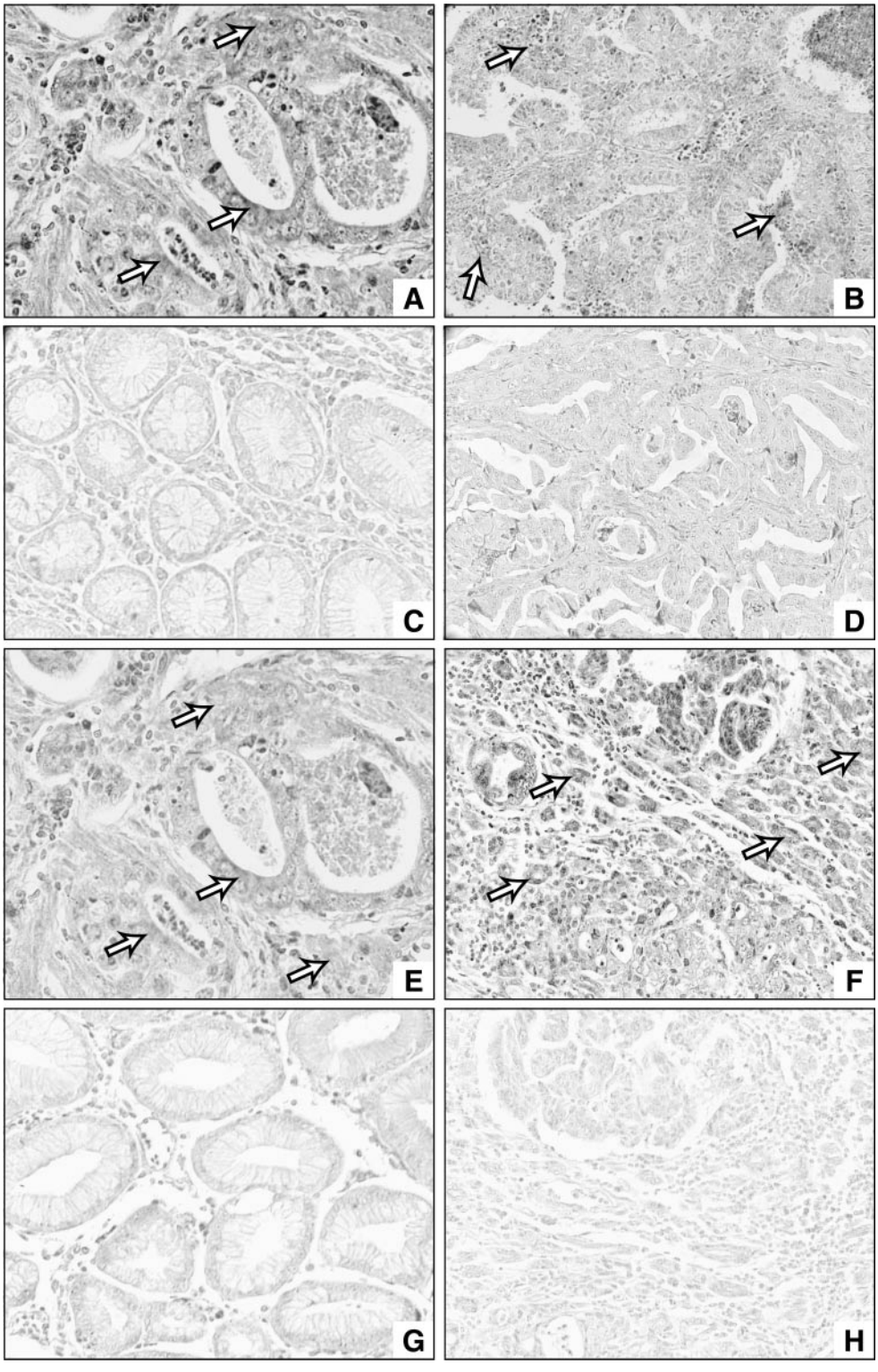

Fig. 1. Detection of Gli1 and PTCH1 expression in primary gastric cancers by *in situ* hybridization. *In situ* hybridization detection of PTCH1 expression (denoted by arrows) in gastric cancers (**A** and **B**) and normal gastric tissue (**C**). **D** is the sense probe control of **B**. Expression of Gli1 was similar to PTCH1 in gastric cancer (**E** and **F**) and normal gastric tissue (**G**) (denoted by arrows). **H** is the sense probe control of **F**. The pattern of Gli1 and PTCH1 expression is very similar in the same tumor (comparing **A** and **E**), further affirming that the hedgehog pathway is activated in the tumor. See online Supplementary material for a color version of this figure.

PTCH1, unpublished data and (10)]. In this experiment, we used two gastric cancer cell lines (AGS and SIIA) to test KAAD-cyclopamine sensitivity.The addition of KAAD-cyclopamine (2 μM) greatly decreased the levels of Gli1 and PTCH1 mRNA expression in both the cell lines (Figure 6A shows the data for Gli1 expression in SIIA and RKO cells), indicating inhibition of the hedgehog pathway by KAAD-cyclopamine. The closely related compound tomatidine,

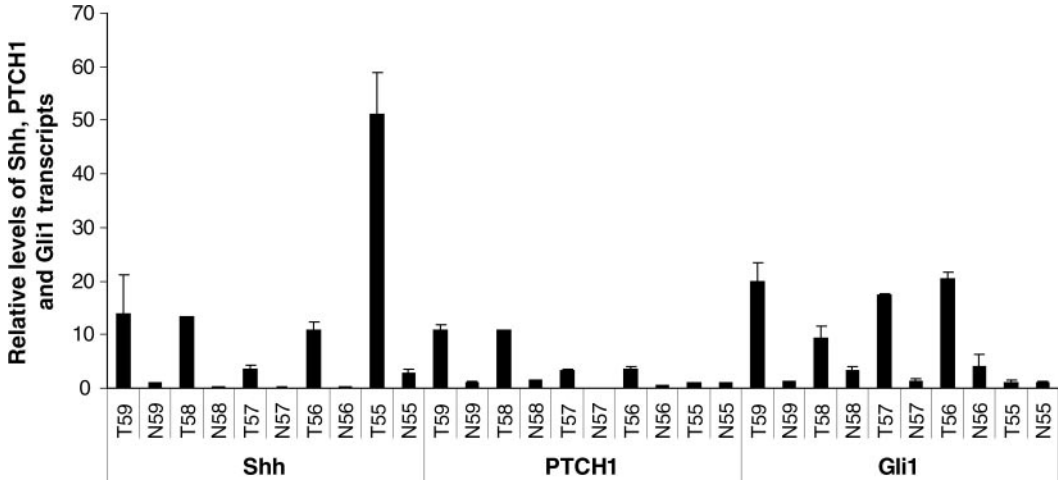

Fig. 2. Real-time PCR analysis of Shh, Gli1 and PTCH1 transcripts in primary gastric cancers. Total RNAs were extracted from the primary tumors in which 70% of the tissue mass was actually tumor tissue. The levels of Shh, Gli1 and PTCH1 were measured in our Real-time PCR Core Facility (see Materials and methods for details), and the experiment was repeated twice with similar results. The relative amount of target was obtained by normalization to an endogenous reference (18S RNA) and relative to a calibrator. T59 stands for tumor from patient no. 59 and N59 stands for the matched normal control from patient no. 59. The data from this analysis are consistent with those from *in situ* hybridization.

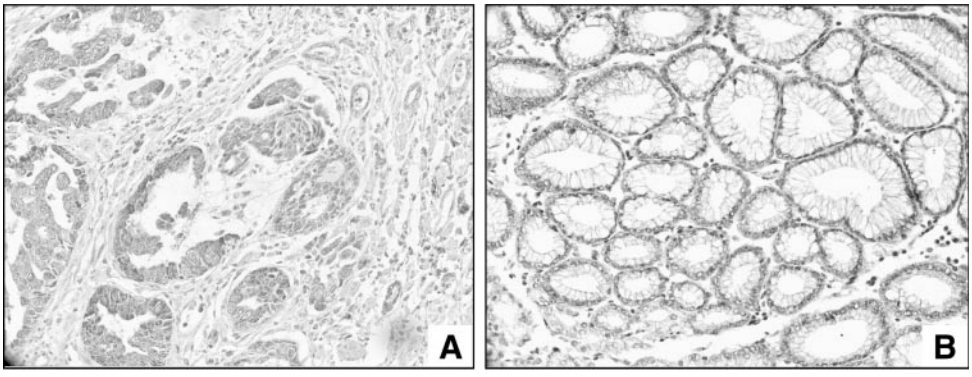

Fig. 3. Detection of PTCH1 protein in gastric tissues. Ptch1 protein was detected by immunohistostaining in gastric cancer (**A**) and normal tissue (**B**). See online Supplementary material for a color version of this figure.

which does not affect SMO signaling and thus served as a negative control, had little discernible effect on these target genes. As expected, we found that cell growth of SIIA and AGS (Figure 6B) cells was inhibited by KAAD-cyclopamine (2 μM). In addition, we detected apoptosis in AGS cells following the treatment with cyclopamine (Figure 6C). Tomatidine did not induce apoptosis in AGS cells (Figure 6C). Similar data were also observed in SIIA cells (data not shown). In contrast, RKO cells, which do not have active hedgehog signaling, were not affected by KAAD-cyclopamine treatment (Figure 6B), with no detectable apoptosis (Figure 6C). These data indicate that inhibition of the hedgehog pathway by KAAD-cyclopamine dramatically decreases cell growth, and induces apoptosis in gastric cancer cells.

Our model predicts that overexpression of Gli1 in AGS cells under the control of a strong promoter (such as the CMV promoter) would constitutively activate the hedgehog pathway, which could render these cancer cells resistant to cyclopamine treatment. Indeed, cyclopamine did not induce apoptosis in constitutive Gli1-expressing AGS cells, as indicated by lack of TUNEL staining in all Gli1 positive cells ($n = 500$) (Figure 6D). Thus, ectopic expression of Gli1 under the control of the CMV promoter prevents KAAD-cyclopamine-induced apoptosis in gastric cancer cells.

Taken together, our findings indicate that activation of the hedgehog pathway is quite common in advanced gastric adenocarcinomas, and this activation differs among different subtypes of gastric cancer. Elevated expression of Gli1 and PTCH1 is associated with decreased tumor differentiation and more advanced tumor stages in tubular adenocarcinomas. Inhibition of the hedgehog pathway in gastric cancer cell lines, however, decreases cell growth and induces apoptosis. Thus, our data indicate that activation of the hedgehog pathway may be an important event in the progression of gastric adenocarcinomas.

Discussion

Activation of the hedgehog pathway in gastric cancer

Hedgehog signaling pathway regulates cell proliferation, tissue polarity and cell differentiation during normal development. Abnormal signaling of this pathway has been reported in a variety of human cancers, including BCCs, medulloblastomas, small cell lung cancer, pancreatic cancer, prostate cancer and

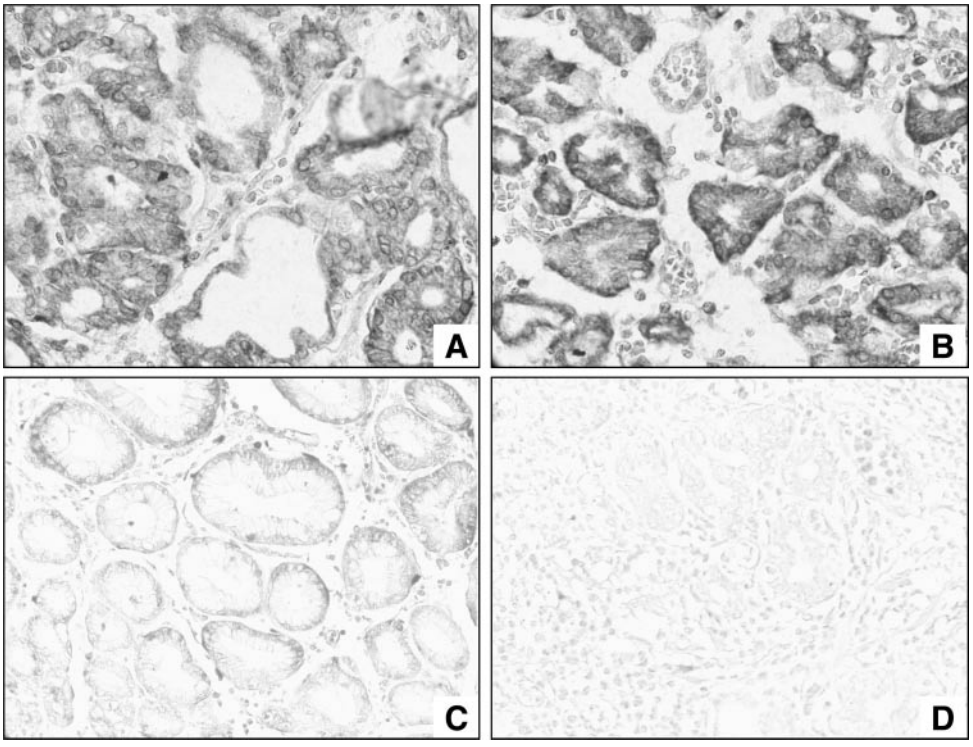

Fig. 4. Expression of Shh in primary gastric cancers. *In situ* hybridization was performed to detect Shh expression in gastric cancers (**A** and **B**) and normal gastric tissue (**C**). (**D**) The sense probe control for the sample shown in (**B**) and did not reveal any positive signals. See online Supplementary material for a color version of this figure.

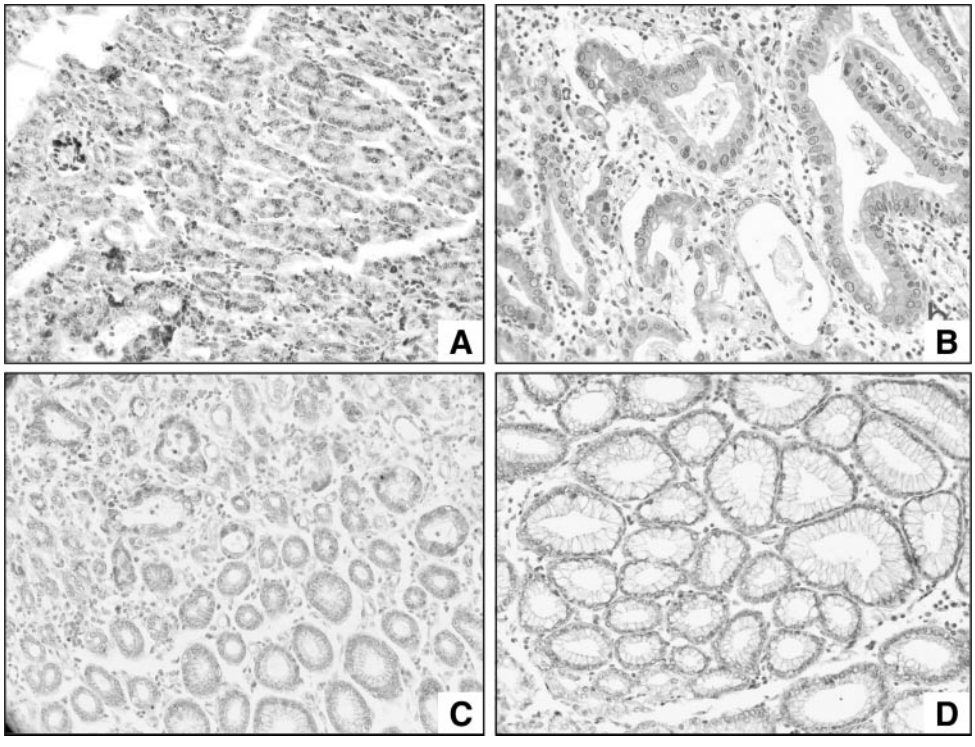

Fig. 5. Protein expression of Shh in primary gastric cancers. *In situ* hybridization was confirmed by immunohistostaining in gastric cancers (**A**–**C**) and normal gastric tissue (**D**). See online Supplementary material for a color version of this figure.

several primary gastric tumors (3–14). Our findings in this report indicate that activation of the hedgehog pathway occurs frequently in advanced gastric adenocarcinomas. We have detected high levels of hedgehog targets PTCH1 and Gli1 in $>60\%$ of gastric cancers. Further analyses of our data indicate an association of the hedgehog pathway activation with poor differentiation of gastric tumors. In a previous report, hedgehog signaling activation was detected in all nine primary

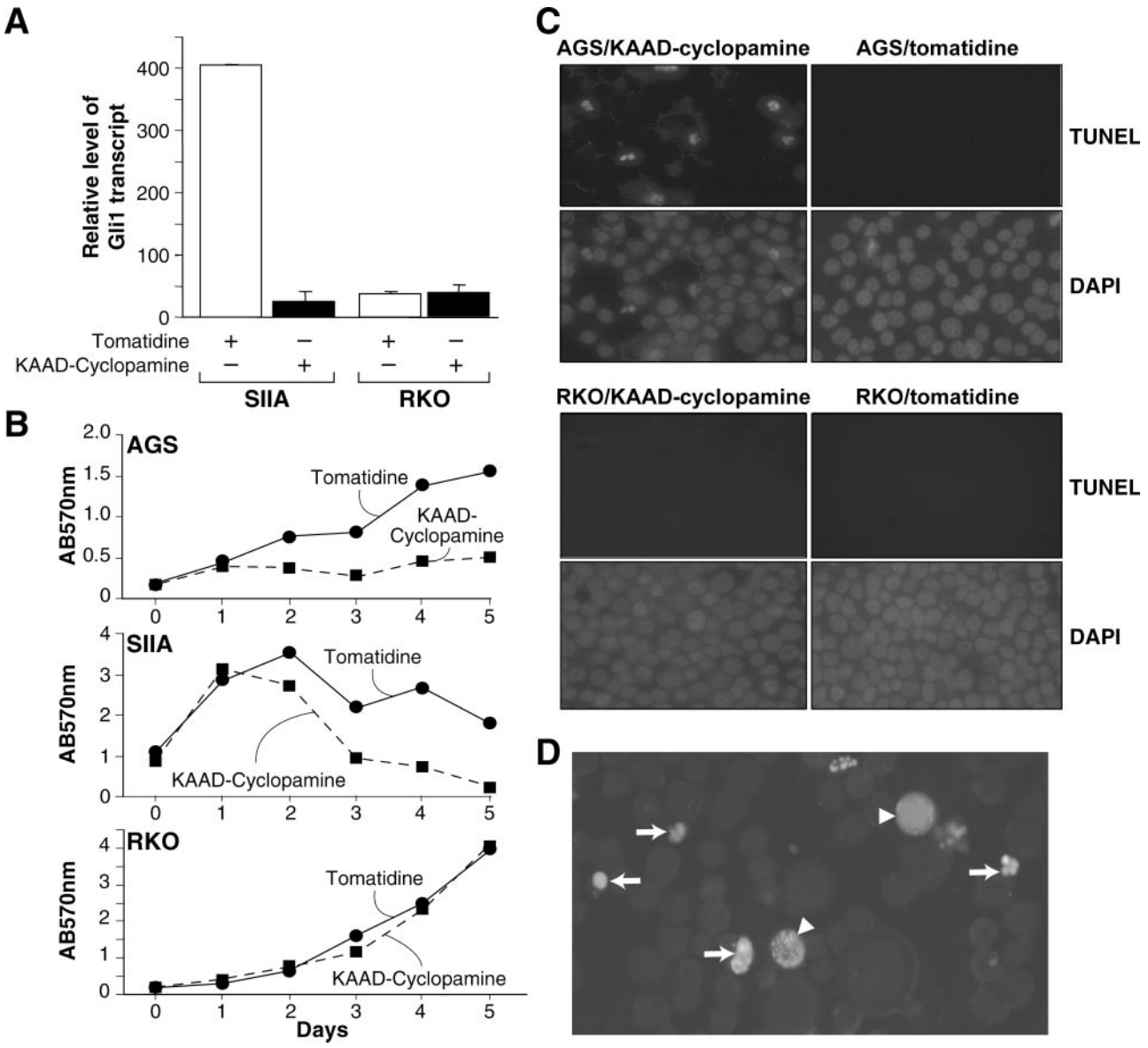

Fig. 6. Hedgehog signaling is required for growth of gastric cancer cells. In the presence of the SMO antagonist KAAD-cyclopamine (2 μM), Gli1 expression was decreased in SIIA cells (**A**). Unlike RKO cells, which do not have active hedgehog signaling, AGS and SIIA cells are sensitive to KAAD-cyclopamine treatment (2 μM) (**B**). TUNEL assay revealed apoptosis (indicated by arrows) in AGS cells but not in RKO cells (**C**). Following the expression of Gli1 under the control of the CMV promoter, AGS cells became resistant to KAAD-cyclopamine treatment (**D**). No apoptosis was detected in >500 Gli1 over-expressing cells (indicated by arrowheads), whereas 10–20% of Gli1 negative cells underwent apoptosis after the cyclopamine treatment (indicated by arrows). See online Supplementary material for a color version of this figure.

tumors using real-time PCR analysis (10). This discrepancy may be owing to specimen selection. As we have indicated in our study, hedgehog signaling activation is associated with poorly differentiated tumors (tubular adenocarcinoma subtype). Another factor may be the sample size. Since signet-ring carcinomas are not a common subtype of gastric cancer, a large number of tumor specimens may be necessary to verify the results in our study.

In all the tumors with elevated levels of Gli1 and PTCH1 we detected expression of Shh, thus suggesting that overexpression of Shh may be responsible for elevated expression of Gli1 and PTCH1 in gastric cancer. However, a high level of sonic hedgehog expression was not always accompanied by elevated Gli1 and PTCH1 expression in tumors (Table I and Supplementary Table 1A), suggesting additional regulatory mechanisms for the hedgehog pathway activation. We speculate that, in addition to the hedgehog overexpression, other genetic alterations are required to activate the hedgehog pathway in gastric cancers.

Therapeutic perspective of gastric cancer through targeted inhibition of the hedgehog pathway

Our studies using gastric cancer cells indicate that the SMO antagonist, cyclopamine, may be effective in the future treatment of gastric cancers. We further demonstrate that over-expression of Gli1 under the control of the CMV promoter prevents cyclopamine-mediated apoptosis, further supporting the specificity of cyclopamine. Our recent studies indicate that chronic oral administration of cyclopamine to Ptch1$^{+/-}$ mice did not affect the overall survival of the mice (21), which

provides a possibility of clinical trials using cyclopamine for gastric cancers. Thus, in the future, it may be possible to treat the subsets of gastric cancer in which the hedgehog pathway is activated with a specific SMO antagonist (e.g. cyclopamine).

Supplementary material

Supplementary material can be found at: http://carcin.oxfordjournals.org/

Acknowledgements

This research was supported by grants from the NIH (R01-CA94160), Department of Defense (DOD-PC030429), the Sealy Foundation for Biomedical Sciences and National Science Foundation of China (30228031). We thank Huiping Guo for technical support in real-time PCR analysis, Karen K.Martin, Brenda Rubio and David Gosky for helping with the manuscript.

Conflict of Interest Statement: None declared.

References

1. Pasca di Magliano,M. and Hebrok,M. (2003) Hedgehog signalling in cancer formation and maintenance. *Nat. Rev. Cancer*, **3**, 903–911.
2. Taipale,J. and Beachy,P.A. (2001) The Hedgehog and Wnt signalling pathways in cancer. *Nature*, **411**, 349–354.
3. Johnson,R.L., Rothman,A.L., Xie,J. *et al.* (1996) Human homolog of patched, a candidate gene for the basal cell nevus syndrome. *Science*, **272**, 1668–1671.
4. Hahn,H., Wicking,C., Zaphiropoulous,P.G. *et al.* (1996) Mutations of the human homolog of *Drosophila* patched in the nevoid basal cell carcinoma syndrome. *Cell*, **85**, 841–851.
5. Xie,J., Murone,M., Luoh,S.M. *et al.* (1998) Activating smoothened mutations in sporadic basal-cell carcinoma. *Nature*, **391**, 90–92.
6. Xie,J., Johnson,R.L., Zhang,X. *et al.* (1997) Mutations of the PATCHED gene in several types of sporadic extracutaneous tumors. *Cancer Res.*, **57**, 2369–2372.
7. Berman,D.M., Karhadkar,S.S., Hallahan,A.R. *et al.* (2002) Medulloblastoma growth inhibition by hedgehog pathway blockade. *Science*, **297**, 1559–1561.
8. Watkins,D.N., Berman,D.M., Burkholder,S.G., Wang,B., Beachy,P.A. and Baylin,S.B. (2003) Hedgehog signaling within airway epithelial progenitors and in small-cell lung cancer. *Nature*, **422**, 313–317.
9. Thayer,S.P., Di Magliano,M.P., Heiser,P.W. *et al.* (2003) Hedgehog is an early and late mediator of pancreatic cancer tumorigenesis. *Nature*, **425**, 851–856.
10. Berman,D.M., Karhadkar,S.S., Maitra,A. *et al.* (2003) Widespread requirement for Hedgehog ligand stimulation in growth of digestive tract tumours. *Nature*, **425**, 846–851.
11. Sheng,T., Li,C.-X., Zhang,X., Chi,S., He,N., Chen,K., McCormick,F., Gatalica,Z. and Xie,J. (2004) Activation of the hedgehog pathway in advanced prostate cancer. *Mol. Cancer*, **3**, 29.
12. Sanchez,P., Hernandez,A.M., Stecca,B. *et al.* (2004) Inhibition of prostate cancer proliferation by interference with SONIC HEDGEHOG-GLI1 signaling. *Proc. Natl Acad. Sci. USA*, **101**, 12561–12566.
13. Fan,L., Pepicelli,C.V., Dibble,C.C. *et al.* (2004) Hedgehog signaling promotes prostate xenograft tumor growth. *Endocrinology*, **145**, 3961–3970.
14. Karhadkar,S., Bova,G., Abdallah,N. *et al.* (2004) Hedgehog signaling in prostate regeneration, neoplasia and metastasis. *Nature*, **2431**(7009), 707–712.
15. Pisani,P., Parkin,D.M., Bray,F. and Ferlay,J. (1999) Estimates of the worldwide mortality from 25 cancers in 1990. *Int. J. Cancer*, **83**, 18–29.
16. Borchard,F. (1990) Classification of gastric carcinoma. *Hepatogastroenterology*, **37**, 223–232.
17. Unden,A.B., Zaphiropoulos,P.G., Bruce,K., Toftgard,R. and Stahle-Backdahl,M. (1997) Human patched (PTCH) mRNA is overexpressed consistently in tumor cells of both familial and sporadic basal cell carcinoma. *Cancer Res.*, **57**, 2336–2340.
18. van den Brink,G.R., Hardwick,J.C., Nielsen,C., Xu,C., ten Kate,F.J., Glickman,J., van Deventer,S.J., Roberts,D.J. and Peppelenbosch,M.P. (2002) Sonic hedgehog expression correlates with fundic gland differentiation in the adult gastrointestinal tract. *Gut*, **51**, 628–633.
19. Li,C., Chi,S., He,N., Zhang,X., Guicherit,O., Wagner,R., Tyring,S. and Xie,J. (2004) IFNalpha induces Fas expression and apoptosis in hedgehog pathway activated BCC cells through inhibiting Ras-Erk signaling. *Oncogene*, **23**, 1608–1617.
20. Xie,J., Aszterbaum,M., Zhang,X., Bonifas,J.M., Zachary,C., Epstein,E. and McCormick,F. (2001) A role of PDGFRalpha in basal cell carcinoma proliferation. *Proc. Natl Acad. Sci. USA*, **98**, 9255–9259.
21. Athar,M., Li,C.-X., Chi,S. *et al.* (2004) Inhibition of smoothened signaling prevents ultraviolet B-induced basal cell carcinomas through induction of fas expression and apoptosis. *Cancer Res.*, **60**, 7545–7552.

Received January 28, 2005; revised May 4, 2005; accepted May 13, 2005

ACCELERATED PUBLICATION

This paper is available online at www.jbc.org

THE JOURNAL OF BIOLOGICAL CHEMISTRY VOL. 281, NO. 1, pp. 9–12, January 6, 2006

Regulation of Gli1 Localization by the cAMP/Protein Kinase A Signaling Axis through a Site Near the Nuclear Localization Signal*[S]

Received for publication, June 28, 2005, and in revised form, November 14, 2005
Published, JBC Papers in Press, November 17, 2005, DOI 10.1074/jbc.C500300200

Tao Sheng, Sumin Chi, Xiaoli Zhang, and Jingwu Xie[1]

From the Sealy Center for Cancer Cell Biology and Department of Pharmacology, University of Texas Medical Branch, Galveston, Texas 7555-1048

The *hedgehog* (Hh) pathway plays a critical role during development of embryos and cancer. Although the molecular basis by which protein kinase A (PKA) regulates the stability of hedgehog downstream transcription factor cubitus interruptus, the *Drosophila* homologue of vertebrate Gli molecules, is well documented, the mechanism by which PKA inhibits the functions of Gli molecules in vertebrates remains elusive. Here, we report that activation of PKA retains Gli1 in the cytoplasm. Conversely, inhibition of PKA activity promotes nuclear accumulation of Gli1. Mutation analysis identifies Thr^{374} as a major PKA site determining Gli1 protein localization. In the three-dimensional structure, Thr^{374} resides adjacent to the basic residue cluster of the nuclear localization signal (NLS). Phosphorylation of this Thr residue is predicted to alter the local charge and consequently the NLS function. Indeed, mutation of this residue to Asp (Gli1/T374D) results in more cytoplasmic Gli1 whereas a mutation to Lys (Gli1/T374K) leads to more nuclear Gli1. Disruption of the NLS causes Gli1/T374K to be more cytoplasmic. We find that the change of Gli1 localization is correlated with the change of its transcriptional activity. These data provide evidence to support a model that PKA regulates Gli1 localization and its transcriptional activity, in part, through modulating the NLS function.

Hedgehog (Hh)[2] proteins are a group of secreted proteins whose active forms are derived from a unique protein cleavage process and at least two post-translational modifications (1, 2). Secreted Hh molecules bind to the receptor patched (PTC), thereby alleviating PTC-mediated suppression of smoothened (SMO) (2, 3). Expression of sonic hedgehog (Shh) appears to stabilize SMO protein possibly through post-translational modification of SMO (4). The effect of hedgehog molecules can be inhibited by hedgehog-interacting protein (HIP) through competitive association with PTC (5, 6). In *Drosophila*, SMO stabilization triggers complex formation with Costal-2, Fused, and Gli homologue cubitus interruptus (CI), which prevents CI degradation and formation of a transcriptional repressor (7–10). SMO ultimately activates transcription factors of the Gli family. Gli molecules enter nucleus through a nuclear localization signal (11, 12), but little is known about the regulatory mechanism for this process. As transcriptional factors, Gli molecules can regulate target gene expression by direct association with a consensus binding site (5′-tgggtggtc-3′) located in the promoter region of the target genes (13, 14).

Protein kinase A (PKA) was first identified as an inhibitory component of the Hh pathway in *Drosophila* (15–19). PKA fulfills its negative role by phosphorylating full-length Ci (Ci155) at several Ser/Thr residues, priming it for further phosphorylation by glycogen synthase kinase 3 (GSK3) and casein kinase I (CKI) (20–22). Hyperphosphorylation of Ci155 targets it for proteolytic processing to generate the repressor form (Ci75) (23). Consistent with this, overexpressing a constitutively active form of PKA catalytic subunit (PKAc), mC*, blocks Ci155 accumulation and Hh target gene expression (24). In addition to its inhibitory effects, PKA phosphorylation at the C terminus of SMO in *Drosophila*, but not in mammals, enhances hedgehog-mediated signaling (25, 26).

While the regulation of CI cleavage by PKA phosphorylation is well documented, very little is known about the role of PKA in Gli regulation. In vertebrates, there are three Gli molecules, Gli1, Gli2, and Gli3. Gli3 can be processed in a manner similar to CI, a process regulated by PKA (27, 28). The fact that Gli3 expression is often not detectable in human cancer suggests that Gli3 does not play a significant role in hedgehog-driven carcinogenesis (29–31). In contrast, Gli1 and Gli2 are expressed in tumors with activated hedgehog signaling (2, 29–36). Here, we report that the cAMP/PKA signaling axis regulates Gli1 protein localization, in part, through phosphorylation of Gli1 at a site near the nuclear localization signal (NLS). We propose that this unique regulation is an important mechanism by which PKA inhibits transcriptional activity of Gli molecules.

MATERIALS AND METHODS

Cell Culture and Plasmids—COS7 and NIH3T3 cells were purchased from the American Type Culture Collection (Manassas, VA) and were maintained in Dulbecco's modified Essential medium supplemented with 10% fetal bovine serum (Invitrogen). Transfection was performed using Lipofectamine 2000 (Invitrogen) according to the manufacturer's instructions (the ratio of plasmid (μg) to lipid (μl) was 1:2.5). Stable expression of a luciferase reporter under the control of Gli responsive elements in NIH3T3 cells was achieved through selection with G418 for 3 weeks after transient transfection with Lipofectamine 2000 (Invitrogen). Two clones with good responses to Gli1 expression (over 20-fold) were selected from a total of 80 clones.

Cells with expression of Gli1 (with C-MYC tag) were treated with 10 μM H89 (Calbiochem) or 0.4 ng/ml leptomycin B (LMB, Sigma) for 8 h. For forskolin treatment (20 μM for 8 h), cells were pretreated with phosphodiesterase inhibitor IBMX (100 μM) for 30 min before addition of forskolin. Immunofluorescent detection of C-MYC-tagged Gli1 was performed as described previously with Cy3-conjugated MYC antibody 9e10 (Sigma) (1:100 dilution) (37). Gli1 localization was detected under a fluorescent microscope; the percentage of Gli1 in the nucleus or the cytoplasm was calculated for each experiment from over 200 Gli1-expressing cells, and the experiment was repeated three times.

Gli1 cDNA was generously provided by Dr. Bert Vogelstein and cloned into pCDNA3.1 with a C-MYC tag at the N terminus. Gli1-GFP construct was made by subcloning Gli1 cDNA into pEGFP-3C using *BamHI* (5′) and NotI (3′) sites. Point mutations of Gli1 were made by *in situ* mutagenesis in our DNA Recombinant Laboratory Core Facility or by PCR-based mutagenesis. All mutations were confirmed by sequencing of the entire coding region. Clones containing only the targeted mutations were used in the studies.

Immunoprecipitation and in Vitro Kinase Assay—Cells were lysed using Nonidet P-40 cell lysis buffer 48 h following Gli1 transfection. C-MYC-tagged Gli1 proteins were immunoprecipitated with an anti-MYC 9B11 antibody (Cell Signaling Inc.) for 3 h followed by incubation with A/G plus beads (Bethyl Laboratories, Inc.) for 1 h. The immunocomplexes were divided into two portions. One portion (20%) was separated by 10% SDS-PAGE and analyzed by Western blotting using an anti-MYC antibody 9B11. The remaining 80% of them were incubated with 0.6 ng of recombinant PKA catalytic subunit with ADBI buffer (20 mM MOPS, pH 7.2, 25 mM β-glycerol phosphate, 5 mM EGTA, 1 mM sodium orthovanadate, 1 mM dithionthreitol) containing 1 mg/ml bovine serum albumin, and 10 μCi of [γ-^{32}P]ATP at 30 °C for 30 min. The kinase reactions were terminated by adding 4× SDS sample buffer, and the samples were separated by 10% SDS-PAGE. Gels were dried on Whatman

* This work was supported by NCI/National Institutes of Health Grant R01CA94160, Department of Defense Grant DOD-PC030429, and NIEHS/National Institutes of Health Grant ES06676. The costs of publication of this article were defrayed in part by the payment of page charges. This article must therefore be hereby marked "*advertisement*" in accordance with 18 U.S.C. Section 1734 solely to indicate this fact.

[S] The on-line version of this article (available at http://www.jbc.org) contains a supplemental figure.

[1] To whom correspondence should be addressed: Sealy Center for Cancer Cell Biology, MRB 9.104, UTMB, 301 University Blvd., Galveston, TX 77555-1048. Tel.: 409-747-1845; Fax: 409-747-1938; E-mail: jinxie@utmb.edu.

[2] The abbreviations used are: Hh, hedgehog; PTC, patched; SMO, smoothened; PKA, protein kinase A; CI, cubitus interruptus; Shh, sonic hedgehog; NLS, nuclear localization signal; NES, nuclear export signal; aa, amino acid; LMB, leptomycin B; IBMX, isobutylmethylxanthine; GFP, green fluorescent protein; MOPS, 4-morpholinepropanesulfonic acid.

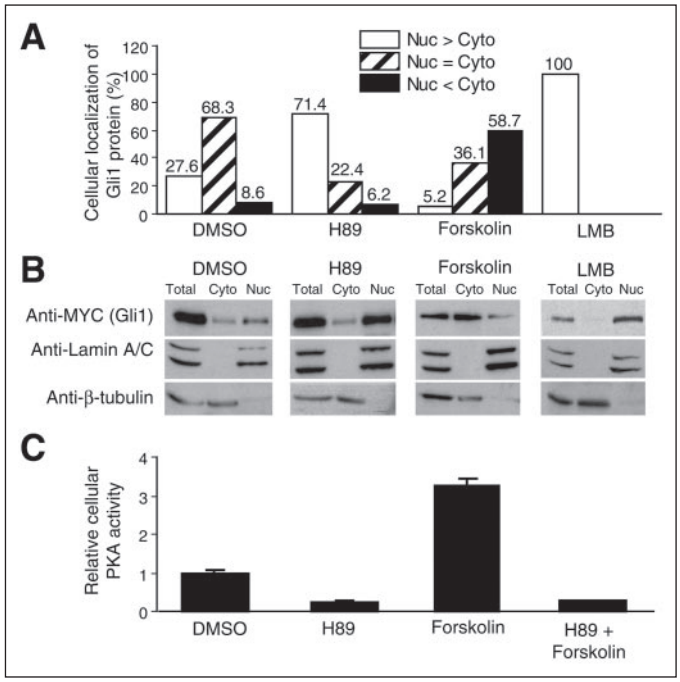

FIGURE 1. **Regulation of Gli1 localization by forskolin-mediated PKA activation in COS7 cells.** *A*, Gli1 was detected by immunofluorescent staining. Following treatment with forskolin (8 h), H89 (8 h), or LMB (8 h) (see "Materials and Methods"), Gli1 protein localization was assessed under a fluorescent microscope in over 200 Gli1-expressing cells, and the experiment was repeated three times with similar results. The percentage of Gli1 in each cellular compartment was calculated from these experiments (see supplemental figure for typical pictures of Gli1 staining). *Nuc > Cyto* indicates preferential nuclear localization, *Nuc = Cyto* indicates localization both in the nucleus and in the cytoplasm, and *Nuc < Cyto* indicates predominant cytoplasmic localization. *B*, Gli1 was detected after cell fractionation (see "Materials and Methods"). Both the nuclear fraction and the cytoplasmic fraction were collected for Western blotting analysis. The purity of cell fractionation was assessed using lamin A/C for the nuclear fraction and β-tubulin for the cytoplasmic fraction. *C*, the cellular PKA activity in COS7 cells was determined using a kit from Upstate Biotechnology Inc. The high PKA activity (*C*) was correlated with a higher level of cytoplasmic Gli1.

paper, followed by autoradiography. Western blotting analysis was performed according to a previously published procedure (37).

Cellular PKA Activation Assay—COS7 cells were seeded into 6-well plates the day before the experiment. Cells were serum-starved for 12 h and then treated with 20 μM H89, 20 μM forskolin or both for 45 min. 100 μM IBMX was added for 30 min prior to treatment with forskolin. Cellular PKA activity in the above-described conditions was determined using a PKA activation assay (Upstate Biotechnology Inc.), in which Leu-Arg-Arg-Ala-Ser-Leu-Gly (Kemptide) was used as the substrate (38). In brief, cell lysates were prepared using Nonidet P-40 lysis buffer. After sonication, the cell lysates were collected at 12,000 rpm for 5 min. 10-μl cell lysates were incubated with 10 μM ATP containing 10μCi [γ-^{32}P]ATP (3,000 Ci/mmol)], 250 μM Kemptide substrate in ADBI buffer at 30 °C for 10 min. Background was determined from reactions without substrate, and the total PKA activity was estimated in reactions containing 20 μM dibutyryl-cAMP. Aliquots were spotted onto Whatman P-81 paper, and the filters were washed in 0.75% phosphoric acid three times for 5 min per wash. ^{32}P incorporation was determined by liquid scintillation counting. Protein concentration of the cell lysates was determined by a kit from Bio-Rad (Bio-Rad protein assay). Data are representative of three independent experiments.

Cell Fractionation—Following transfection, the COS7 cells were maintained in 10 cm cell culture dishes for 48 h. Before harvest, the cells were rinsed twice with cold phosphate-buffered saline, harvested by scraping with 1 ml of cold phosphate-buffered saline for each 10-cm dish, and collected by centrifugation at 3,000 × *g* for 30 s. One-fifth of the lysates were collected for detection of Gli1 expression by Western blotting. The cell pellets were incubated with 60 μl of buffer A (50 mM HEPES, pH 7.4, 10 mM KCl, 1 mM EDTA, 1 mM EGTA, 1 mM dithiothreitol, 0.1 μg of phenylmethylsulfonyl fluoride/ml, 1 μg of pepstatin A/ml, 1 μg of leupeptin/ml, 10 μg of soybean trypsin inhibitor/ml, 10 μg of aprotinin/ml, and 0.1% IGEPAL CA-630). After 10 min on ice, the lysates were centrifuged at 6,000 × *g* for 30 s at 4 °C. The supernatant fractions were saved as the cytoplasmic fraction. The pellet (containing the nuclei) was resuspended in buffer B (buffer A containing 1.0 M sucrose) and centrifuged at 15,000 × *g* for 10 min at 4 °C. The purified nuclei (pellets) were incubated in 30 μl buffer C (10% glycerol, 50 mM HEPES, pH 7.4, 400 mM KCl, 1 mM EDTA, 1 mM EGTA, 1 mM dithiothreitol, 0.1 μg of phenylmethylsulfonyl fluoride/ml, 1 μg of pepstatin A/ml, 1 μg of leupeptin/ml, 10 μg of soybean trypsin inhibitor/ml, 10 μg of aprotinin/ml) after vigorous vortex and centrifuged at 15,000 × *g* for 20 min at 4 °C, and supernatant fractions were collected. All extracts were normalized for protein amounts determined by Bio-Rad protein assay (Bio-Rad) and separated by 10% SDS-PAGE for further analysis (39). Antibodies to β-tubulin (Sigma) and Lamin A/C (Santa Cruz Biotechnology Inc.) were used to detect the purity of cytoplasmic (β-tubulin) and nuclear (Lamin A/C) fractions using Western blotting analysis.

Luciferase Reporter Gene Assay—For luciferase assay, NIH3T3 cells with stable expression of the Gli luciferase reporter were transfected with Gli1 constructs (0.5 μg/well) and the TK-*Renilla* control plasmid (5 ng/well) using Lipofectamine 2000. After 5 h, the medium was replaced with fresh growth medium and the cells were incubated in 5% CO_2 at 37 °C overnight. Following treatment with forskolin or other compounds, the cells were harvested, and luciferase activity was measured with the dual luciferase reporter assay system (Promega) according to the manufacturer's instruction. In brief, the transfected cells were lysed in the 6-well plates with 100 μl of reporter lysis buffer and the lysate transferred into Eppendorf tubes. Cell debris was removed by centrifugation at top speed for 10 min in a microcentrifuge. 20 μl of the supernatant was mixed with 100 μl of buffer LAR II, and the absorbance was immediately measured (the first reading). After 3 s, 100 μl of Stop & Glo® Reagent was added to measure the Renillar luciferase activity (the second reading). The value from the first reading was divided by the value from the second reading of each sample to obtain the luciferase activity. Each experiment was repeated three times with similar results.

RESULTS

Gli1 is not only a downstream effector but also a target gene of the hedgehog pathway (40). Thus, identification of the mechanism by which PKA phosphorylation regulates Gli1 functions will help us understand signal transduction of the hedgehog pathway in cancer.

First, we tested whether Gli1 protein localization can be altered by accumulation of the cellular cAMP level in COS7 cells. After transient transfection, the protein localization of Gli1 was detected by immunofluorescent staining of the C-MYC tag at the Gli1 N terminus and by cell fractionation. In the presence of 20 μM forskolin, which directly activates adenylyl cyclase and raises the cyclic AMP level (41), we observed that the percentage of cytoplasmic Gli1 was increased over 5-fold, whereas the percentage of nuclear Gli1 was reduced by 80% (Fig. 1, *A* and *B*). The effect seems to be direct because the change in Gli1 localization can be observed 20 min after forskolin treatment. Conversely, addition of PKA inhibitor H89 led to a shift of Gli1 localization to the nucleus (Fig. 1, *A* and *B*). As a consequence of forskolin treatment, the cellular PKA activity was increased 2-fold (Fig. 1*C*). Conversely, addition of H89 into the medium inhibited the cellular PKA activity by 70% (Fig. 1*C*). Thus, Gli1 localization was correlated with the cellular PKA activity. To confirm the data from the immunofluorescent staining, we performed cell fractionation analysis. As shown in Fig. 1*B*, more Gli1 were in the nuclear fraction following H89 treatment whereas forskolin caused an increase of cytoplasmic Gli1 (Fig. 1*B*). Furthermore, we monitored localization of Gli1-GFP fusion protein with a time-lapse microscope in the presence of H89 or forskolin. Forskolin retained Gli1-GFP in the cytoplasm whereas H89 promoted nuclear accumulation of this fusion protein (data not shown). All these data indicate that Gli1 localization can be regulated by modulating the cellular PKA activity.

Gli1 protein shuttling between the nucleus and the cytoplasm was interrupted by inhibition of nuclear export with LMB, a specific inhibitor for CRM1-mediated nuclear export, resulting in nuclear accumulation of all Gli1 proteins (Fig. 1, *A* and *B*), supporting that Gli1 localization is a dynamic process and is tightly regulated. Our data suggest that direct phosphorylation of Gli1 by PKA is responsible for regulation of Gli1 protein localization.

Sequence analysis predicts five putative PKA sites in Gli1. The sequence around these PKA sites is highly conserved among Gli proteins (Fig. 2*A*). Several point mutations of Gli1 were made to test Gli1 regulation by PKA (see the diagram in Fig. 2*B*). These mutations were made by *in situ* mutagenesis in our DNA Recombinant Laboratory Core Facility or by PCR-based mutagenesis.

Using these mutant constructs, we assessed Gli1 localization in cultured

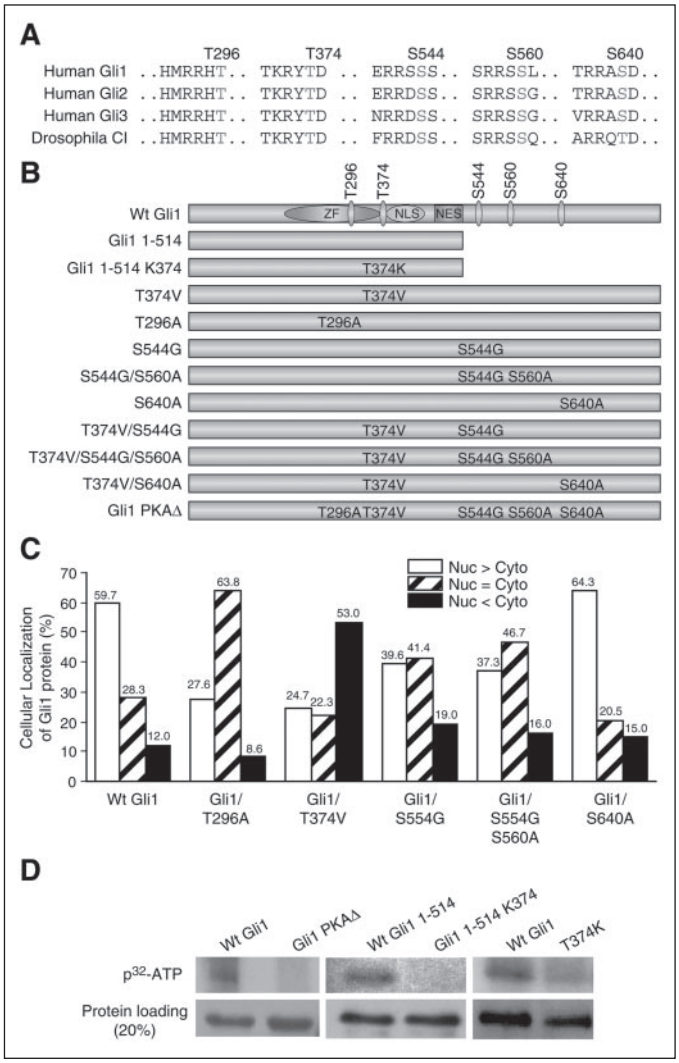

FIGURE 2. **Regulation of PKA phosphorylation and localization by cAMP/PKA. The five putative sites are conserved in all Gli molecules.** *A* shows the sequence alignment of CI and human Gli1, Gli2, and Gli3 at the five putative PKA sites. *B* shows the Gli1 constructs used in this study. Gli1 molecules with point mutations of one or more PKA sites were expressed in COS7 cells and their localization was detected by immunofluorescent staining. Full-length Gli1 with a mutation at Thr^{374} (T374V) had the most significant effect on Gli1 protein localization (*C*). In contrast, a mutation at Ser^{544} or other sites (*C* and see supplemental figure) had little effects on Gli1 protein localization. A Gli1 mutant Gli1/T374V/S544G/S560A with triple mutations at PKA sites behaved like Gli1/T374V (supplemental figure), indicating that Thr^{374} is a critical PKA site for determining Gli1 protein localization. Over 200 Gli1-positive cells were counted under a fluorescent microscope for Gli1 protein localization, and the experiment was repeated three times with similar results. The data were the average result from these experiments. *D* shows Gli1 phosphorylation *in vitro* by recombinant PKA. Wild type Gli1 and its mutant forms were expressed in COS7 cells and subsequently purified through immunoprecipitation. The ability of PKA to phosphorylate immunoprecipitated Gli1 proteins were performed *in vitro* (see "Materials and Methods"). The full-length Gli1, but not Gli1-PKAΔ (see *B*, the mutation sites), was highly phosphorylated by PKA *in vitro* (*D*, *left panels*). A single point mutation in a Gli1 fragment (1–514 aa, shown in *B*) prevented protein phosphorylation by PKA (*D*, *center panels*). This same mutation in the full-length Gli1 also dramatically reduced the level of phosphorylation (*D*, *right panels*).

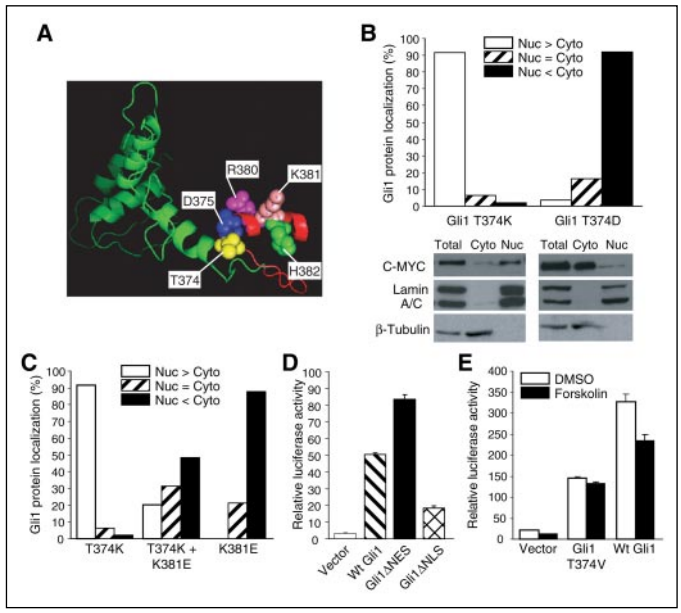

FIGURE 3. **Demonstration of Thr^{374} as the major site for Gli1 regulation.** *A*, a three-dimensional model of Gli1 fragment, showing the proximity of Thr^{374}/Asp^{375} to the basic residue cluster (Arg^{380}/Lys^{381}/His^{382}) of the Gli1 NLS. *B* shows the preferential nuclear localization of Gli1/T374K and the predominant cytoplasmic localization of Gli1/T374D. Localization was confirmed by cell fractionation. Immunofluorescent staining was done as described for Fig. 1*A*. *C* shows Gli1/T374K localization following an additional mutation at Lys^{381}. These experiments suggest that Thr^{374} is responsible for cAMP/PKA-mediated regulation of Gli1 localization, which may be achieved through affecting the NLS function. *D*, correlation of Gli1 localization with its transcriptional activity was examined in NIH3T3 cells with stable expression of a luciferase reporter under the control of Gli-responsive elements (see "Materials and Methods" for details). Gli1 with a Lys to Glu mutation at Lys^{381} (K381E) of the NLS motif, which predominantly localizes to the cytoplasm, was unable to activate this reporter. In contrast, Gli1 with mutations in the NES motif, which predominantly localizes to the nucleus, was more active than the wild type Gli1. *E*, transcriptional activity of Gli1/T374V was not responsive to forskolin treatment whereas the transcriptional activity of wild type Gli1 was reduced by 60% following forskolin treatment.

cells. We found that mutation at Thr^{374} (Gli1/T374V) significantly affects Gli1 localization (Fig. 2*C*). Furthermore, the response of Gli1/T374V to forskolin treatment was nearly diminished (in response to forskolin treatment, 5-fold increase in cytoplasmic protein for wild type Gli1 but only 40% increase for Gli1/T374V) (also see the supplemental figure). In contrast, the protein localization of Gli1/S544G and Gli1/S544G/S560A was not different from the wild type Gli1 (supplemental figure). A mutant Gli1 (Gli1/T374V/S544G/S560A) with triple mutations at the PKA sites behaved like Gli1/T374V (supplemental figure), indicating that Ser^{544} and Ser^{560} are not involved in regulation of Gli1 localization. On the other hand, a mutation at S640A had only slight effects on Gli1 protein localization in response to forskolin (supplemental figure). These data indicate that Thr^{374} is the major site responsible for Gli1 protein localization in cultured cells.

Consistent with the role of Thr^{374} for Gli1 protein localization, we also confirmed that Thr^{374} can be phosphorylated by recombinant PKA *in vitro* (Fig. 2*D*). We performed PKA phosphorylation with Gli1 protein purified by immunoprecipitation in the presence of [γ-^{32}P]ATP and recombinant PKA in test tube and found that Gli1 was highly phosphorylated by PKA *in vitro* (Fig. 2*D*, *left panels*, *first lane*). Gli1 with mutations of all five PKA sites (PKAΔ) could not be phosphorylated by PKA (Fig. 2*D*, *left panels*, *right lane*). To test whether the Thr^{374} site of Gli1 is phosophorylated by recombinant PKA, we used a Gli1 fragment containing only two PKA sites: Thr^{296} and Thr^{374}. We found that this Gli1 fragment (1–514 aa) with a mutation at Thr^{374} was not able to be phosphorylated by recombinant PKA *in vitro* (Fig. 2*D*, *center panels*). Even a single point mutation at Thr^{374} significantly reduced PKA-mediated phosphorylation of full-length Gli1 (Fig. 2*D*, *right panels*), indicating that the Thr^{374} site is a major PKA site of Gli1 phosphorylation. In addition, our data also suggested that Ser^{544}, Ser^{560}, and Ser^{640} can be phosphorylated by PKA *in vitro* (data not shown here). The above data indicate that Thr^{374} is a major PKA site involved in regulation of Gli1 protein localization.

In the three-dimensional structure, Thr^{374}, together with the adjacent Asp^{375}, is close to the first basic residue cluster (Arg^{380}/Lys^{381}/His^{382}) of the bipartite motif (the classic NLS) in Gli1 (Fig. 3*A*) (42). It is known that protein phosphorylation at the residue next to the bipartite motif inhibits its binding affinity to importins, leading to reduced nuclear localization of the target protein (43). We predict that phosphorylation of Thr^{374} will increase the local negative charge, leading to reduced NLS functions and accumulation of Gli1 in the cytoplasm. Indeed, Gli1/T374D was preferentially localized to the cytoplasm (Fig. 3*B*). Conversely, Gli1/T374K has a high local positive charge near the NLS, and we found that Gli1/T374K predominantly localized to the nucleus (Fig. 3*B*). Localization of these Gli1 proteins was further confirmed by

cell fractionation (Fig. 3*B*). These data support our hypothesis that one mechanism by which the cellular PKA activity regulates Gli1 localization is through altering the local charge nearby the NLS of Gli1.

If Gli1 nuclear localization is regulated by PKA phosphorylation through a NLS-dependent mechanism, disruption of the NLS should affect localization of these mutant Gli1 molecules. As shown in Fig. 3*C*, we found that Gli1/K381E, which is predicted to disrupt the NLS, was predominantly localized to the cytoplasm, confirming the role of NLS in Gli1 localization (12). Although Gli1/T374K localizes predominantly to the nucleus, additional mutation at K381 (K381E) retained Gli1/T374K to the cytoplasm (Fig. 3*C*), suggesting that regulation of Gli1 localization by T374 phosphorylation requires the intact NLS.

The ultimate effect of Gli1 is transcriptional activation of the downstream target genes. To assess whether Gli1 localization affects its transcriptional activity, we established stable expression of Gli1 luciferase reporter under the control of Gli responsive elements in NIH3T3 cells (13). By measuring the reporter luciferase activity, we examined the association of Gli1 localization with its transcriptional activity (Fig. 3*D*). If Gli1/K381E remains preferentially in the cytoplasm, the transcriptional activity was low. In contrast, Gli1 with a defective NES (Gli1/L496V/L498V), which localizes predominantly in the nucleus, was more active (Fig. 3*D*). Thus, the Gli1 luciferase reporter activity in these cells is very sensitive to Gli1 localization. We examined the effects of forskolin to Gli1-mediated transcriptional activity in this NIH3T3 stable cell line. Like the wild type Gli1, Gli1/T374V can activate the Gli luciferase reporter (Fig. 3*E*). Consistent with its cytoplasmic localization, the luciferase activity in cells expressing the wild type Gli1 was reduced after forskolin treatment (Fig. 3*E*). In contrast, Gli1/T374V-mediated reporter gene activity was not affected by forskolin (Fig. 3*E*). These data suggest that Thr^{374} is an important PKA site responsible for PKA phosphorylation and for the transcriptional activity of Gli1.

Based on these data, we proposed a mechanism by which the cAMP/PKA signaling axis mediates regulation of Gli1 localization. Gli1 enters the nucleus through a nuclear localization signal. With the accumulation of cAMP in the cell, Thr^{374} gets phosphorylated. Phosphorylation of Thr^{374} will increase the local negative charge nearby the NLS, which results in inhibition of NLS function. Consequently, Gli1 is retained in the cytoplasm and is unable to activate the target genes. Since this Thr residue is highly conserved among Gli proteins, we anticipate that the same mechanism is applicable to PKA regulation of other Gli molecules.

DISCUSSION

In our study, we provide direct evidence to support that the cAMP/PKA signaling axis regulates Gli1 protein localization primarily through a site at Thr^{374}. Our data further indicate that PKA-mediated regulation of Gli1 localization is through Thr^{374}, possibly through interfering with the NLS function.

Although our studies demonstrated that Thr^{374} is a major site for PKA-mediated regulation of Gli1 localization (Figs. 2 and 3 and supplemental figure), mutation at this site did not completely abolish the effects of forskolin (supplemental figure). To identify an additional site required for this regulation, we made double and triple point mutations of Gli1 at the PKA sites (Fig. 2*B*). Our data indicate that mutations at Thr^{374} and Ser^{640} completely abolished the response to forskolin treatment, indicating that Ser^{640} is another site involving PKA-mediated regulation of Gli1 localization (supplemental figure). However, mutation at Ser^{640} alone had no effect on Gli1 protein localization and had only a slight effect in response to forskolin treatment, suggesting that Ser^{640} is not a primary site for Gli1 regulation. This hypothesis was further supported by the fact that Gli1/S640E and Gli1/S640R, unlike Gli1/T374D and Gli1/T374K, did not alter Gli1 protein localization (data not shown here). Thus, we believe that additional structural information of Gli1 near the Ser^{640} region is required to understand the molecular mechanism by which PKA phosphorylation at Ser^{640} affects Gli1 localization.

Further studies of Gli1 phosphorylation can be facilitated by measuring the stoichiometry of phosphorylation for Gli1. Currently, a large amount of purified Gli1 protein is not available, making it difficult to calculate the stoichiometry of phosphorylation for such a large protein (150 kDa for Gli1). This issue may be addressed in the future using highly purified Gli1 fragments from bacteria.

In addition, our data indicate that Ser^{544} and Ser^{560} residues are not involved in regulation of Gli1 protein localization. It will be interesting to know how these two sites are involved in regulation of Gli1 functions.

Acknowledgments—We thank Drs. James Lee, Yigong Shi, Xiaodong Cheng, Mark Evers, and Min Chen for help with this project, Drs. H. Sasaki and Bert Vogelstein for providing reagents, and Karen Martin and Brenda Rubio for help with the manuscript.

REFERENCES

1. Taipale, J., and Beachy, P. A. (2001) *Nature* **411,** 349–354
2. Pasca di Magliano, M., and Hebrok, M. (2003) *Nat. Rev. Cancer* **3,** 903–911
3. Stone, D. M., Hynes, M., Armanini, M., Swanson, T. A., Gu, Q., Johnson, R. L., Scott, M. P., Pennica, D., Goddard, A., Phillips, H., Noll, M., Hooper, J. E., de Sauvage, F., and Rosenthal, A. (1996) *Nature* **384,** 129–134
4. Hooper, J. E., and Scott, M. P. (2005) *Nat. Rev. Mol. Cell Biol.* **6,** 306–317
5. Chuang, P. T., and McMahon, A. P. (1999) *Nature* **397,** 617–621
6. Lum, L., and Beachy, P. A. (2004) *Science* **304,** 1755–1759
7. Jia, J., Tong, C., and Jiang, J. (2003) *Genes Dev.* **17,** 2709–2720
8. Lum, L., Zhang, C., Oh, S., Mann, R. K., von Kessler, D. P., Taipale, J., Weis-Garcia, F., Gong, R., Wang, B., and Beachy, P. A. (2003) *Mol. Cell* **12,** 1261–1274
9. Ogden, S. K., Ascano, M., Jr., Stegman, M. A., Suber, L. M., Hooper, J. E., and Robbins, D. J. (2003) *Curr. Biol.* **13,** 1998–2003
10. Ruel, L., Rodriguez, R., Gallet, A., Lavenant-Staccini, L., and Therond, P. P. (2003) *Nat. Cell Biol.* **5,** 907–913
11. Kogerman, P., Grimm, T., Kogerman, L., Krause, D., Unden, A. B., Sandstedt, B., Toftgard, R., and Zaphiropoulos, P. G. (1999) *Nat. Cell Biol.* **1,** 312–319
12. Wang, Q. T., and Holmgren, R. A. (1999) *Development* (*Camb.*) **126,** 5097–5106
13. Sasaki, H., Hui, C., Nakafuku, M., and Kondoh, H. (1997) *Development* (*Camb.*) **124,** 1313–1322
14. Kinzler, K. W., and Vogelstein, B. (1990) *Mol. Cell. Biol.* **10,** 634–642
15. Jiang, J., and Struhl, G. (1995) *Cell* **80,** 563–572
16. Lepage, T., Cohen, S. M., Diaz-Benjumea, F. J., and Parkhurst, S. M. (1995) *Nature* **373,** 711–715
17. Li, W., Ohlmeyer, J. T., Lane, M. E., and Kalderon, D. (1995) *Cell* **80,** 553–562
18. Pan, D., and Rubin, G. M. (1995) *Cell* **80,** 543–552
19. Strutt, D. I., Wiersdorff, V., and Mlodzik, M. (1995) *Nature* **373,** 705–709
20. Chen, Y., Gallaher, N., Goodman, R. H., and Smolik, S. M. (1998) *Proc. Natl. Acad. Sci. U. S. A.* **95,** 2349–2354
21. Wang, G., Wang, B., and Jiang, J. (1999) *Genes Dev.* **13,** 2828–2837
22. Jia, J., Amanai, K., Wang, G., Tang, J., Wang, B., and Jiang, J. (2002) *Nature* **416,** 548–552
23. Aza-Blanc, P., Ramirez-Weber, F. A., Laget, M. P., Schwartz, C., and Kornberg, T. B. (1997) *Cell* **89,** 1043–1053
24. Kiger, J. A., Jr., and O'Shea, C. (2001) *Genetics* **158,** 1157–1166
25. Jia, J., Tong, C., Wang, B., Luo, L., and Jiang, J. (2004) *Nature* **432,** 1045–1050
26. Zhang, C., Williams, E. H., Guo, Y., Lum, L., and Beachy, P. A. (2004) *Proc. Natl. Acad. Sci. U. S. A.* **101,** 17900–17907
27. Wang, B., Fallon, J. F., and Beachy, P. A. (2000) *Cell* **100,** 423–434
28. Ruiz i Altaba, A. (1999) *Development* (*Camb.*) **126,** 3205–3216
29. Zhu, Y., James, R. M., Peter, A., Lomas, C., Cheung, F., Harrison, D. J., and Bader, S. A. (2004) *Cancer Lett.* **207,** 205–214
30. Ma, X., Chen, K., Huang, S., Zhang, X., Adegboyega, P. A., Evers, B. M., Zhang, H., and Xie, J. (2005) *Carcinogenesis* **26,** 1698–1705
31. Ma, X., Sheng, T., Zhang, Y., Zhang, X., He, J., Huang, S., Chen, K., Sultz, J., Adegboyega, P. A., Zhang, H., and Xie, J. (2006) *Int. J. Cancer* **118,** 139–148
32. Dahmane, N., Lee, J., Robins, P., Heller, P., and Ruiz i Altaba, A. (1997) *Nature* **389,** 876–881
33. Bonifas, J. M., Pennypacker, S., Chuang, P. T., McMahon, A. P., Williams, M., Rosenthal, A., De Sauvage, F. J., and Epstein, E. H., Jr. (2001) *J. Invest. Dermatol* **116,** 739–742
34. Xie, J., Aszterbaum, M., Zhang, X., Bonifas, J. M., Zachary, C., Epstein, E., and McCormick, F. (2001) *Proc. Natl. Acad. Sci. U. S. A.* **98,** 9255–9259
35. Toftgard, R. (2000) *Cell Mol. Life Sci.* **57,** 1720–1731
36. Regl, G., Neill, G. W., Eichberger, T., Kasper, M., Ikram, M. S., Koller, J., Hintner, H., Quinn, A. G., Frischauf, A. M., and Aberger, F. (2002) *Oncogene* **21,** 5529–5539
37. Athar, M., Li, C., Tang, X., Chi, S., Zhang, X., Kim, A. L., Tyring, S. K., Kopelovich, L., Hebert, J., Epstein, E. H., Jr., Bickers, D. R., and Xie, J. (2004) *Cancer Res.* **64,** 7545–7552
38. Cheng, X., Ma, Y., Moore, M., Hemmings, B. A., and Taylor, S. S. (1998) *Proc. Natl. Acad. Sci. U. S. A.* **95,** 9849–9854
39. He, N., Li, C., Zhang, X., Sheng, T., Chi, S., Chen, K., Wang, Q., Vertrees, R., Logrono, R., and Xie, J. (2005) *Mol. Carcinog* **42,** 18–28
40. Stecca, B., Mas, C., and Ruiz i Altaba, A. (2005) *Trends Mol. Med.* **11,** 199–203
41. Laurenza, A., Sutkowski, E. M., and Seamon, K. B. (1989) *Trends Pharmacol. Sci.* **10,** 442–447
42. Pavletich, N. P., and Pabo, C. O. (1993) *Science* **261,** 1701–1707
43. Harreman, M. T., Kline, T. M., Milford, H. G., Harben, M. B., Hodel, A. E., and Corbett, A. H. (2004) *J. Biol. Chem.* **279,** 20613–20621

Available online at www.sciencedirect.com
SCIENCE DIRECT
ELSEVIER
Cancer Letters xx (2006) 1–8
CANCER Letters
www.elsevier.com/locate/canlet

Activation of the hedgehog pathway in a subset of lung cancers

Sumin Chi [a,1], Shuhong Huang [b,1], Chengxin Li [a,1], Xiaoli Zhang [b], Nonggao He [a], Manoop S. Bhutani [c], Dennie Jones [c], Claudia Y. Castro [d], Roberto Logrono [d], Abida Haque [d], Joseph Zwischenberger [e], Stephen K. Tyring [f], Hongwei Zhang [a,*], Jingwu Xie [b,*]

[a] *School of Life Sciences, Institute of Developmental Biology, Shandong University, Jinan, People's Republic of China*
[b] *Department of Pharmacology, Sealy Centers for Cancer Cell Biology, University of Texas Medical Branch, 301 University Boulevard, Galveston, TX 77555-1048, USA*
[c] *Department of Internal Medicine, Sealy Centers for Cancer Cell Biology, University of Texas Medical Branch, 301 University Boulevard, Galveston, TX 77555-1048, USA*
[d] *Department of Pathology, Sealy Centers for Cancer Cell Biology, University of Texas Medical Branch, 301 University Boulevard, Galveston, TX 77555-1048, USA*
[e] *Department of Surgery, Sealy Centers for Cancer Cell Biology, University of Texas Medical Branch, 301 University Boulevard, Galveston, TX 77555-1048, USA*
[f] *Department of Dermatology, University of Texas Health Science Center, Houston, TX 77030, USA*

Received 12 July 2005; received in revised form 19 October 2005; accepted 28 November 2005

Abstract

Activation of the hedgehog pathway is reported in lung cancer, but its frequency remains unknown. We examine activation of this pathway in lung cancers by in situ hybridization and immunohistochemstry, and find that less than 10% of the tumors have elevated hedgehog target gene expression. We further identify a cell line NCI-H209 and two primary tumors with no detectable Su(Fu), a negative regulator of the pathway. Ectopic expression of Su(Fu) in NCI-H209 cells down-regulates hedgehog target gene expression and leads to inhibition of cell proliferation. These data indicate that activation of the hedgehog pathway is activated through Shh over-expression or Su(Fu) inactivation in only a subset of lung cancers.

Keywords: Hedgehog; Lung cancer; Gli1; Su(Fu); PTCH1

1. Introduction

The hedgehog pathway plays a critical role in embryonic development and tissue formation, including foregut [1]. Targeted deletions of sonic hedgehog, Gli2 or Gli3 result in foregut malformation and embryo lethality in mice [2–4]. Secreted Hh molecules bind to the receptor patched (PTC-PTCH1, PTCH2), thereby alleviating PTC-mediated suppression of smoothened (SMO), a putative seven-transmembrane protein. SMO signaling triggers a cascade of intracellular events,

Abbreviations PTC, patched; PTCH1, human patched gene 1; NSCLC, non-small cell lung cancer; shh, sonic hedgehog; BCC, basal cell carcinoma; Su(Fu), suppressor of fused.

* Corresponding authors. Tel.: +1 409 747 1845; Fax: +1 409 747 1938.
E-mail addresses: zhw@sdu.edu.cn (H. Zhang), jinxie@utmb.edu (J. Xie).

[1] These authors contributed equally to this work.

0304-3835/$ - see front matter © 2005 Published by Elsevier Ireland Ltd.
doi:10.1016/j.canlet.2005.11.036

leading to activation of the pathway through GLI-dependent transcription [5,6]. Activation of Hh signaling, through loss-of-function mutations of PTCH1 or activated mutations of SMO, occurs frequently in human basal cell carcinomas (BCCs) and medulloblastomas [7–16]. More recently, abnormal activation of the sonic hedgehog pathway has been reported in subsets of small cell lung cancer, pancreatic cancer, prostate cancer, and gastrointestinal (GI) cancers [17–23].

Lung cancer is the leading cause of cancer-related death, claiming more than 150,000 lives every year in the US alone (which exceeds the combined mortality from breast, prostate, and colorectal cancers). Patients with advanced stage of lung cancer, which represents 75% of all new cases, have a median survival time of only 10 months. Thus, identifying an effective biomarker for early diagnosis of lung cancer is the first essential step to reduce the mortality. Activation of hedgehog signaling was reported in five of 10 small cell lung cancers and four of 40 non-small cell lung cancers (NSCLC) [17]. To determine if hedgehog signaling activation can be utilized for diagnosis and treatment of lung cancer, we performed a comprehensive study to assess hedgehog pathway activation in specimens from 172 lung cancer patients and five patients without lung cancer by in situ hybridization and immunohistochemistry.

2. Materials and methods

2.1. Patient material

A total of 177 patients (172 lung cancer patients and five patients without cancer) were included in our study with approval of Institutional Research Board. Specimens from 96 patients were received as discarded materials from University of Texas Medical Branch Surgical Pathology and the Shan Dong Qi Lu Hospital, Jinan, China. Lung cancers and the matched lung tissues were collected from each patient whenever possible. For tumors without matched normal tissues, a portion of lung tissue surrounding the tumor was used. Pathology reports and H&E stained slides from each specimen were reviewed to determine the nature of the disease and the tumor histology [24]. The randomly sorted samples with masked identity were evaluated by at least two independent certified pathologists. Lung cancers were divided into the following subtypes: adenocarcinoma, squamous cell carcinoma, alveolar cell carcinoma, adenosquamous cell carcinomas, large cell carcinoma, small cell carcinoma and carcinoid. For tissue microarray, we have triplicates for each specimen [25]. Both tumor tissues and the matched normal tissues (or the surrounding tissues) were included in our study.

In addition, we purchased a tissue microarray of lung cancer from Chaoying Biotechnology Co. Ltd (Xi'an, China), which contains 81 informative specimens (including five non-cancerous lung tissues as controls). Analyzes of these specimens were described in each experimental method.

2.2. In situ hybridization

Using probes for Gli1, PTCH1 and HIP, *in situ* hybridization was performed in specimens listed in Supplementary Table 1 according to our previously published protocol [26,27]. Matched normal lung tissues or tissues surrounding tumors were also included in the study. Sense and antisense probes were obtained by T3 and T7 in vitro transcription using a kit from Roche (Mannheim, Germany). Blue indicated strong hybridization. As negative controls, sense probes were used in all hybridization and no positive signals were observed.

2.3. RNA isolation, quantitative PCR and northern blotting

Total RNAs were extracted using a RNA extraction kit from Promega according to the manufacturer (Promega, Madison, WI). Real-time PCR analyzes were performed according to Ma et al. [26,27]. Northern blotting was performed as previously reported [28].

2.4. Immunohistochemistry

Representative formalin-fixed and paraffin embedded tissue sections (6 μm thickness) were used for immunohistochemistry with specific antibodies to human Shh, PTCH1, Su(Fu) and HIP [Cat. No. 9024 for Shh and Cat. No. 6149 for PTCH1, Cat. No. 10934 for Su(Fu), Santa Cruz Biotechnology, Inc.; Cat. No. AF1568 for HIP antibodies, R&D Systems, Inc.]. All primary antibodies have been previously tested for immunohistostaining [22,23]. Immunohistochemistry of PTCH1 and Shh was carried out as previously reported [22,29] on specimens listed in Supplementary Tables 1 and 2. HIP protein expression was also detected by immunohistochemistry in the specimens listed in Supplementary Table 2. Detection of Su(Fu) protein was only performed in several specimens with activated hedgehog signaling.

2.5. Cell culture, colony formation assay, BrdU labeling and MTT assay

Human lung cancer cell lines (A549, H82, H187, H196, H209, H460, H661, H1299, BEAS2-B and BZR-T33) were purchased from ATCC and cultured in the recommended media from ATCC [28]. Expression of Su(Fu), under the control of the CMV promoter, in NCI-H209 cells was achieved by retrovirus-mediated gene transfer [29]. BrdU labeling was performed as previously described [29]. Flow cytometry was performed in our core facility [28].

Colorimetric MTT assay was performed according to our published protocol in the presence of 0.5% FBS [30,31].

Student's *t*-test for two samples was performed for the difference between tumor groups: $P<0.05$ was considered statistically significant.

3. Results

To assess the frequency of hedgehog signaling activation in primary lung cancers, we initially examined expression of hedgehog target genes Gli1 and PTCH1 in 81 cases of lung specimens in a tissue microarray (see Supplementary Table 1 for specimen information). Increased levels of both PTCH1 and Gli1 transcripts indicate activation of the hedgehog pathway [5].

We first detected Gli1 and PTCH1 transcripts using in situ hybridization. In agreement with a published report [17], we did not detect Gli1 and PTCH1 in normal lung tissues, suggesting that the hedgehog pathway is not normally activated in adult normal lung tissues (Fig. 1A and A′). In contrast, we detected expression of both Gli1 and PTCH1 transcripts in 8 of 76 tumor specimens (Table 1; Fig. 1B, C, B′ and C′), suggesting that activation of the hedgehog pathway occurs in a subset of lung cancers. Further analyzes indicated that activation of the hedgehog pathway is not restricted to any specific subtypes of lung cancers (see Table 1, positive tumors include three adenocarcinomas, two squamous cell carcinomas, one small cell carcinoma, one large cell carcinoma and one alveolar cell carcinoma).

Expression of PTCH1 in lung cancer specimens (see Supplementary Table 1) was further confirmed by immunohistochemistry (Fig. 1E and F) [22,23]. All tissues with detectable PTCH1 protein had elevated PTCH1 transcript. With these data, we expanded the study to include additional 96 lung cancer specimens. Immunohistochemistry using antibodies identified additional eight tumors with detectable expression of both PTCH1 and HIP [22] (Fig. 1H; Table 2; Supplementary Table 2), indicating activation of the hedgehog pathway in 8 of 96 tumors. These data confirm that activation of the hedgehog pathway occurs only in a small subset of lung cancers.

In total, we found 15 out of 172 lung cancers (8.7%) harboring activated hedgehog signaling. Due to limited number of tumors with activated hedgehog signaling

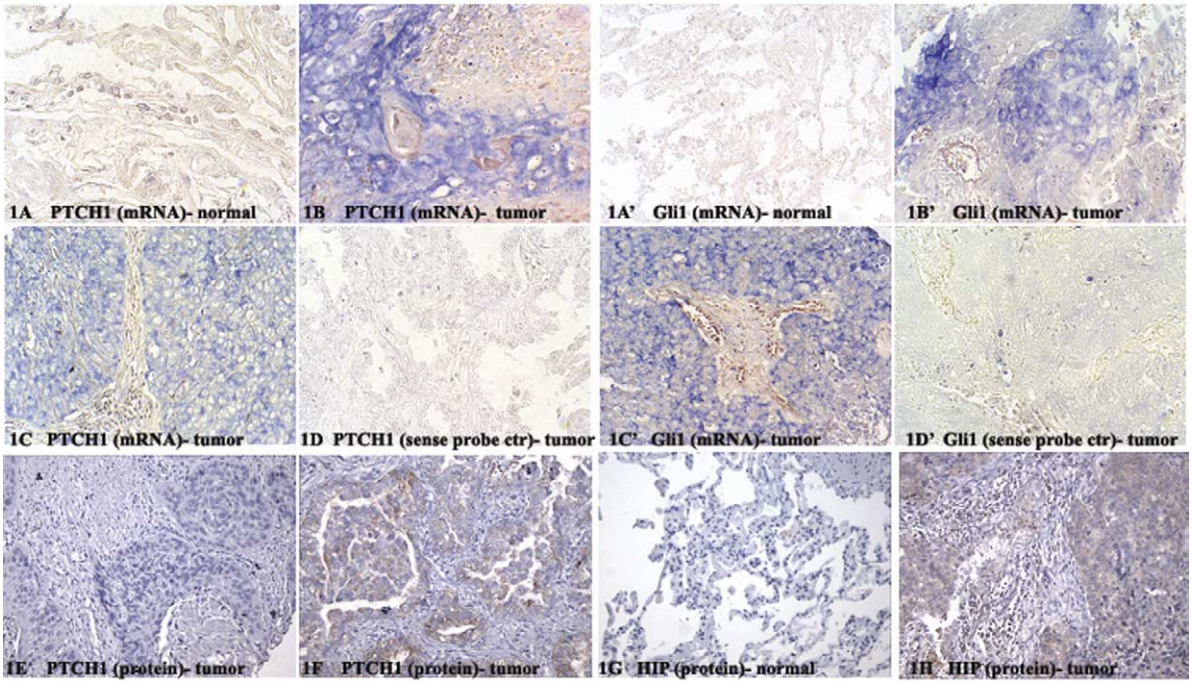

Fig. 1. Expression of hedgehog target genes in lung specimens. The levels of PTCH1 (1A–C), Gli1 (1A′–C′) transcripts (100×, blue as positive) were detected by in situ hybridization in normal and tumors (see Supplementary Table 1 for the list of specimens). The sense probe control did not give signal (see D and D′). The result was shown as '+++' for strong staining, as '++' for staining, as '+' for weak staining. Negative staining was shown as '−'. Protein expression of PTCH1 (CE and F), HIP (G and H) was detected by immunohistochemistry in all specimens with specific antibodies (see Section 2 for details, 100×) (brown–red as positive). The result was shown as '+++' for strong staining, as '++' for staining, as '+' for weak staining. Negative staining was shown as '−'. (For interpretation of the reference to colour in this legend, the reader is referred to the web version of this article.)

Table 1
Expression of Shh, PTCH1 and Gli1 in lung cancer (in situ hybridization)

	Tumor types	Total	Shh		PTCH1/Gli1	
			Positive	(%)	Positive	(%)
		76	64	84.2	8	10.5
Subtypes	Adenocarcinoma	27	21	80.8	3	11.1
	Alveolar cell carcinoma	9	7	77.8	1	11.1
	Large cell carcinoma	5	4	80.0	1	20.0
	Small cell carcinoma	10	8	80.0	1	10.0
	Squamous cell carcinoma	25	23	92.0	2	8.0
	Carcinoid	1	1		0	
Grade	Well differentiated	5	5	100	0	0
	Moderately differentiated	18	16	88.9	2	11.1
	Poorly differentiated	26	22	84.6	2	7.7
	UND[a]	27	21	77.8	4	14.8
Sex	Female	19	15	78.9	1	5.2
	Male	57	49	85.9	7	12.3

[a] Information not available.

(detectable expression of at least two hedgehog target genes, PTCH1, Gli1 or HIP), it was not possible to perform statistical analysis. We also examined expression of PTCH1 protein by immunohistochemistry in lung cancer metastases (lymph node and intra-lung metastases) and identified 4 of 38 metastases of NSCLC with PTCH1 positive staining, suggesting that activation of the hedgehog pathway is not specifically associated with lung tumor metastases. Expression of hedgehog targets resides to the tumor nest, not to the stroma, suggesting that hedgehog signaling is not very active in the stroma, which is quite different from other situations such as during lung development [1] or in gastric cancers [27].

Next, we tested expression of molecules potentially involving in hedgehog signaling activation. It is reported that Shh over-expression is responsible for activation of the hedgehog pathway in pancreatic cancer [23], gastric cancer [18,27] and lung cancer [17]. To test this possibility, we first examined expression of Shh in lung specimens by in situ hybridization in lung cancer specimens listed

Table 2
Expression of Shh, PTCH1 and HIP in lung cancer (immunohistochemistry)

	Tumor types	Total	Shh		PTCH1/Gli1	
			Positive	(%)	Positive	(%)
		96	63	65.6	8	8.3
Subtype	Adenocarcinoma	37	21	56.8	3	8.1
	Alveolar cell carcinoma	3	2		0	
	Large cell carcinoma	5	4	80.0	1	20.0
	Small cell carcinoma	3	2		0	
	Squamous cell carcinoma	42	31	73.8	4	9.5
	Carcinoid	2	1		0	
	Adenosquamous cell carcinoma	4	2		0	
Grade	Well differentiated	12	8	66.7	0	0
	Moderately differentiated	44	31	70.5	5	11.4
	Poorly differentiated	36	20	55.6	3	8.3
	UND[a]	3	3		0	
Stage	I	48	29	60.4	1	2.1
	II	24	16	66.7	3	12.5
	III/IV	20	15	75.0	4	20.0
	UND[a]	4	3		0	
Sex	Female	35	25	71.4	3	8.6
	Male	61	38	62.3	5	8.2

[a] Information not available.

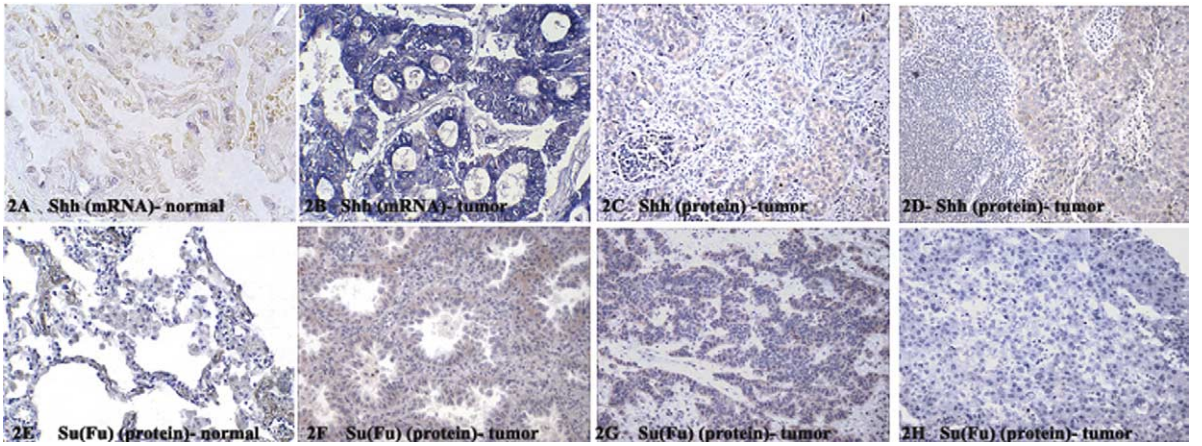

Fig. 2. Expression of Shh and Su(Fu) in lung specimens. The level of Shh transcript (A and B) was detected by in situ hybridization in the specimens listed in Supplementary Table 1 (100×, blue as positive). The proteins of Shh (C and D) and Su(Fu) (E–H) were assessed by immunohistochemistry (100×, Brown–red as positive). The result was shown as '+++' for strong staining, as '++' for staining, as '+' for weak staining. Negative staining was shown as '−'. (For interpretation of the reference to colour in this legend, the reader is referred to the web version of this article.)

in Supplementary Table 1. As expected, Shh expression was undetectable in all three normal lung tissues examined (Fig. 2A). In contrast, many primary tumors expressed Shh (Fig. 2B; Tables 1 and 2). In agreement with the in situ hybridization data, we detected Shh protein in tumors with detectable Shh transcript (Fig. 2C and D; Supplementary Table 1). Shh was detectable specifically in the tumor, not in the stroma (Fig. 2C and D), suggesting that that a paracrine signaling mechanism of sonic hedgehog does not play an important role in lung cancers. Furthermore, expression of Shh protein was also detected in specimens listed Supplementary Table 2. In all, over 73% of lung cancers had detectable Shh expression (Tables 1 and 2). We found that expression of Shh is not always associated with expression of hedgehog target genes in lung cancers ($P=0.8444$). Furthermore, 5 of the 16 tumors, which have detectable expression of at least two hedgehog target genes, did not have detectable expression of Shh (Supplementary Tables 1 and 2), suggesting that over-expression of Shh may be partially responsible for activating hedgehog signaling pathway in lung cancers.

To identify additional molecular mechanisms for hedgehog signaling activation, we detected expression of other components of the hedgehog pathway, including Su(Fu), a negative regulator of hedgehog signaling [32,33]. Like PTCH1, loss of Su(Fu) is reported to be responsible for hedgehog signaling activation in subset of medulloblastomas [12], prostate cancer [22] and basal cell carcinomas [11]. We found that two tumors with elevated levels of PTCH1 and Gli1 had no detectable levels of Su(Fu), one of the tumors had no Shh expression (Fig. 2E–H and Supplementary Table 2), suggesting that loss of Su(Fu) may be also responsible for hedgehog signaling activation in a small number of lung cancers.

To substantiate our findings in the tumors, we examined eight lung cancer cell lines for Su(Fu) expression and found one cell line NCI-H209 with no detectable Su(Fu) protein (Fig. 3A and Supplementary Fig. 1). Southern hybridization using Su(Fu) probe did not reveal dramatic genomic changes of the Su(Fu) gene in H209 cells (data not shown here). Northern analysis showed no detectable Su(Fu) transcript in NCI-H209 cells (Fig. 3A), indicating a possible transcriptional silencing mechanism, such as promoter methylation. Methylation of the promoter region causes gene transcription silencing, which can be reversed by 5-aza-2′-deoxycytidine. We found that Su(Fu) became detectable in NCI-H209 cells in the presence of 5-aza-2′-deoxycytidine for 6–8 days (Fig. 3B), confirming that the Su(Fu) gene was silenced through promoter methylation in these cells.

To demonstrate the tumor suppressing role of Su(Fu), we stably expressed wild type Su(Fu) in H209 cells using retrovirus-mediated gene transfer [29]. Protein expression was verified by western blot analysis (Fig. 3B). By comparison of the levels of PTCH1 and Gli1 transcripts using real-time PCR analysis [26], we found that stable expression of Su(Fu) caused dramatic reduction in hedgehog target genes GLi1 and PTCH1 (Fig. 3C), indicating that Su(Fu) is sufficient to inhibit hedgehog signaling in this cell line. To demonstrate the tumor suppressor activity of wild type Su(Fu), we performed colony formation analysis in Su(Fu) negative

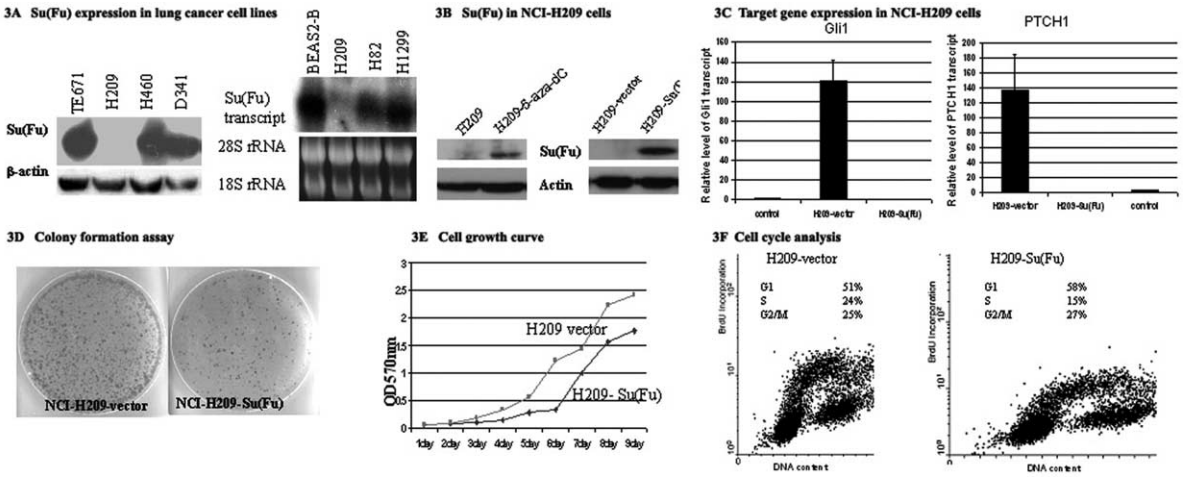

Fig. 3. Role of Su(Fu) in cancer cell lines Su(Fu) was detected by western blotting using Su(Fu) specific antibodies (see Section 2 for details). One of the eight lung cancer cell lines, NCI-H209, has no detectable Su(Fu) protein (A, also see Supplementary Fig. 1). Su(Fu) transcripts were undetectable in H209 cells by northern hybridization (A), indicating inactivation of the Su(Fu) gene. The inactivation of Su(Fu) was reversible in H209 cells in the presence of 5-aza-2′-deoxycytidine for over 6 days (B left), indicating an epigenetic mechanism of Su(Fu) silencing in these cells. Following expression of Su(Fu) in H209 cells, Su(Fu) protein was detected by western blotting (B right). Following stable expression of Su(Fu), levels of PTCH1 and Gli1 transcripts were detected by real-time PCR and found to be dramatically reduced (2C), indicating that Su(Fu) expression was sufficient to suppress the hedgehog signaling pathway. In contrast, expression of Su(Fu) has no effects on A549 cells (data not shown). Colony formation assay was performed to test the role wild type Su(Fu) on cell growth in H209 cells. Cells transfected with Su(Fu) formed small and few colonies (D). To confirm this result, the cell growth curve from Su(Fu) stably expressed H209 cell line was compared with that from the control cell line (E). Su(Fu) expression slowed cell growth. Furthermore, we performed BrdU labeling in these two cell lines (F). Following BrdU labeling for 30 min, around 24% of H209-vector cells were BrdU positive. In contrast, only 15% BrdU positive cells were observed in H209-Su(Fu) cells ($P < 0.02$), indicating that Su(Fu) inhibits cell growth and DNA synthesis in H209 cells.

H209 cells. Cells with ectopic expression of wild type Su(Fu) or the control vector were selected with G418 for 2 weeks, and cell colonies were stained with violet blue. Expression of Su(Fu) caused reduction of both the colony number and the size (Fig. 3D), indicating that ectopic expression of Su(Fu) is sufficient to suppress cell proliferation of these tumor cells.

Next, we examined cell growth using MTT assay, and found that H209-Su(Fu) cells grow slower than H209-vector cells, confirming that Su(Fu) indeed can suppress cell growth (Fig. 3E). The effect of Su(Fu) on DNA synthesis was assessed with BrdU labeling (Fig. 3F). In H209 cells, we found around 24% of cells are positive for BrdU after 30 min labeling with BrdU. In contrast, we only observed that 15% of cells with stable expression of Su(Fu) were BrdU positive. The difference is significant ($P < 0.02$). In contrast, Su(Fu) has no effects on DNA synthesis of A549 cells, which have no activated hedgehog signaling (data not shown here). These data indicate that wild type Su(Fu) can inhibit DNA synthesis and cell growth in lung cancer cells.

Taken together, our findings indicate that activation of the hedgehog signaling pathway, which occurs only in 15 out of 172 lung cancers (8.7%), is not a very common event in lung cancer although sonic hedgehog is frequently over-expressed. Our data suggest that Shh over-expression or loss of Su(Fu) may be responsible for hedgehog signaling activation in a small subset of lung cancers. Using a cell line with no detectable Su(Fu) protein, we demonstrated that expression of Su(Fu) is sufficient to inhibit the hedgehog signaling, leading to reduced DNA synthesis and inhibited cell growth. Thus, Su(Fu) inactivation appears to be another mechanism by which the hedgehog pathway is activated in subset of human lung cancer.

4. Discussion

Our data indicate that only a small proportion of lung tumors have expression of two hedgehog target genes (8.7%). We further find that loss of Su(Fu) was observed in 2 of the 16 tumors and one cell line NCI-H209, in which elevated hedgehog target genes were detected. The role of Su(Fu) is demonstrated in NCI-H209 cells. Thus, our data provide evidence that hedgehog signaling activation occurs in only a small percentage of lung cancer in which hedgehog signaling may be involved in cancer cell proliferation. Our studies further indicate that activation of the hedgehog

pathway can be achieved by either Shh over-expression or Su(Fu) inactivation in a subset of lung cancer.

While activation of hedgehog signaling occurs infrequently, Shh is frequently over-expressed in lung cancers (Tables 1 and 2). Although Shh is weakly detectable in an inflammatory lung tissue (Supplementary Table 1), all three normal lung tissues had no detectable Shh, indicating that Shh expression may be a biomarker of abnormal lung pathology. Based on the fact that the target genes were not elevated in these tissues, it will be interesting to investigate the functions of Shh in preneoplastic lesions as well as in lung cancers. We speculate that Shh expression is induced during lung cancer development long before the induction of the target genes. An early report indicates that sonic hedgehog may be involved in generating progenitor cells of lung [17]. Further investigation of hedgehog expression in a large number of inflammatory lung tissues and other pathological conditions may provide additional clues of sonic hedgehog functions in lung tissues.

Acknowledgements

This research was supported by grants from the NIH (R01-CA94160, JX), Department of Defense (DOD-PC030429, JX), the NIEHS (ES06676) and National Science Foundation of China (30228031, JX and HWZ).

Supplementary Material

Supplementary data associated with this article can be found, in the online version, at doi:10.1016/j.canlet.2005.11.036.

References

[1] D. Warburton, J. Zhao, M.A. Berberich, M. Bernfield, Molecular embryology of the lung: then, now, and in the future, Am. J. Physiol. 276 (1999) L697–L704.
[2] C.V. Pepicelli, P.M. Lewis, A.P. McMahon, Sonic hedgehog regulates branching morphogenesis in the mammalian lung, Curr. Biol. 8 (1998) 1083–1086.
[3] J. Motoyama, J. Liu, R. Mo, Q. Ding, M. Post, C.C. Hui, Essential function of Gli2 and Gli3 in the formation of lung, trachea and oesophagus, Nat. Genet. 20 (1998) 54–57.
[4] Y. Litingtung, L. Lei, H. Westphal, C. Chiang, Sonic hedgehog is essential to foregut development, Nat. Genet. 20 (1998) 58–61.
[5] M. Pasca di Magliano, M. Hebrok, Hedgehog signalling in cancer formation and maintenance, Nat. Rev. Cancer 3 (2003) 903–911.
[6] J. Xie, Hedgehog signaling in prostate cancer, Future Oncol. 1 (2005) 331–338.
[7] R. Toftgard, Hedgehog signalling in cancer, Cell. Mol. Life Sci. 57 (2000) 1720–1731.
[8] E. Epstein Jr, Genetic determinants of basal cell carcinoma risk, Med. Pediatr. Oncol. 36 (2001) 555–558.
[9] H. Hahn, C. Wicking, P.G. Zaphiropoulous, M.R. Gailani, S. Shanley, A. Chidambaram, et al., Mutations of the human homolog of Drosophila patched in the nevoid basal cell carcinoma syndrome, Cell 85 (1996) 841–851.
[10] R.L. Johnson, A.L. Rothman, J. Xie, L.V. Goodrich, J.W. Bare, J.M. Bonifas, et al., Human homolog of patched, a candidate gene for the basal cell nevus syndrome, Science 272 (1996) 1668–1671.
[11] J. Reifenberger, M. Wolter, C.B. Knobbe, B. Kohler, A. Schonicke, C. Scharwachter, et al., Somatic mutations in the PTCH, SMOH, SUFUH and TP53 genes in sporadic basal cell carcinomas, Br. J. Dermatol. 152 (2005) 43–51.
[12] M.D. Taylor, L. Liu, C. Raffel, C.C. Hui, T.G. Mainprize, X. Zhang, et al., Mutations in SUFU predispose to medulloblastoma, Nat. Genet. 31 (2002) 306–310.
[13] J. Xie, R.L. Johnson, X. Zhang, J.W. Bare, F.M. Waldman, P.H. Cogen, et al., Mutations of the PATCHED gene in several types of sporadic extracutaneous tumors, Cancer Res. 57 (1997) 2369–2372.
[14] J. Xie, M. Murone, S.M. Luoh, A. Ryan, Q. Gu, C. Zhang, et al., Activating smoothened mutations in sporadic basal-cell carcinoma, Nature 391 (1998) 90–92.
[15] J. Xie, R.L. Johnson, X. Zhang, J.W. Bare, F.M. Waldman, P.H. Cogen, et al., Mutations of the PATCHED gene in several types of sporadic extracutaneous tumors, Cancer Res. 57 (1997) 2369–2372.
[16] D.M. Berman, S.S. Karhadkar, A.R. Hallahan, J.I. Pritchard, C.G. Eberhart, D.N. Watkins, et al., Medulloblastoma growth inhibition by hedgehog pathway blockade, Science 297 (2002) 1559–1561.
[17] D.N. Watkins, D.M. Berman, S.G. Burkholder, B. Wang, P.A. Beachy, S.B. Baylin, Hedgehog signalling within airway epithelial progenitors and in small-cell lung cancer, Nature 422 (2003) 313–317.
[18] D.M. Berman, S.S. Karhadkar, A. Maitra, R. Montes De Oca, M.R. Gerstenblith, K. Briggs, et al., Widespread requirement for Hedgehog ligand stimulation in growth of digestive tract tumours, Nature 425 (2003) 846–851.
[19] L. Fan, C.V. Pepicelli, C.C. Dibble, W. Catbagan, J.L. Zarycki, R. Laciak, et al., Hedgehog signaling promotes prostate xenograft tumor growth, Endocrinology 145 (2004) 3961–3970.
[20] S.S. Karhadkar, G. Steven Bova, N. Abdallah, S. Dhara, D. Gardner, A. Maitra, et al., Hedgehog signalling in prostate regeneration, neoplasia and metastasis, Nature 431 (2004) 707–712.
[21] P. Sanchez, A.M. Hernandez, B. Stecca, A.J. Kahler, A.M. DeGueme, A. Barrett, et al., Inhibition of prostate cancer proliferation by interference with SONIC HEDGEHOG-GLI1 signaling, Proc. Natl Acad. Sci. USA 101 (2004) 12561–12566.
[22] T. Sheng, C. Li, X. Zhang, S. Chi, N. He, K. Chen, et al., Activation of the hedgehog pathway in advanced prostate cancer, Mol. Cancer 3 (2004) 29.
[23] S.P. Thayer, M.P. Di Magliano, P.W. Heiser, C.M. Nielsen, D.J. Roberts, G.Y. Lauwers, et al., Hedgehog is an early and late mediator of pancreatic cancer tumorigenesis, Nature 425 (2003) 851–856.
[24] A.K. Haque, W. Au, N. Cajas-Salazar, S. Khan, A.W. Ginzel, D.V. Jones, et al., CYP2E1 polymorphism, cigarette smoking,

p53 expression, and survival in non-small cell lung cancer: a long term follow-up study, Appl. Immunohistochem. Mol. Morphol. 12 (2004) 315–322.

[25] J. Xie, Identifying biomarkers of lung cancer in the post-genomic era, Curr. Pharmacogenomics 3 (2005) 265–274.

[26] X. Ma, T. Sheng, Y. Zhang, X. Zhang, J. He, S. Huang, et al., Hedgehog signaling is activated in subsets of esophageal cancers. Int. J. Cancer 118 (2006) 139–148.

[27] X. Ma, K. Chen, S. Huang, X. Zhang, T. Sheng, P. Adegboyega, et al., Frequent activation of the hedgehog pathway in advanced gastric adenocarcinomas, Carcinogenesis (2005).

[28] N. He, C. Li, X. Zhang, T. Sheng, S. Chi, K. Chen, et al., Regulation of lung cancer cell growth and invasiveness by beta-TRCP, Mol. Carcinog. 42 (2005) 18–28.

[29] J. Xie, M. Aszterbaum, X. Zhang, J.M. Bonifas, C. Zachary, E. Epstein, et al., A role of PDGFRalpha in basal cell carcinoma proliferation, Proc. Natl Acad. Sci. USA 98 (2001) 9255–9259.

[30] C. Li, S. Chi, N. He, X. Zhang, O. Guicherit, R. Wagner, et al., IFNalpha induces Fas expression and apoptosis in hedgehog pathway activated BCC cells through inhibiting Ras-Erk signaling, Oncogene 23 (2004) 1608–1617.

[31] M. Athar, C. Li, X. Tang, S. Chi, X. Zhang, A.L. Kim, et al., Inhibition of smoothened signaling prevents ultraviolet B-induced basal cell carcinomas through regulation of fas expression and apoptosis, Cancer Res. 64 (2004) 7545–7552.

[32] P. Kogerman, T. Grimm, L. Kogerman, D. Krause, A.B. Unden, B. Sandstedt, et al., Mammalian suppressor-of-fused modulates nuclear-cytoplasmic shuttling of Gli-1, Nat. Cell Biol. 1 (1999) 312–319.

[33] D.M. Stone, M. Murone, S. Luoh, W. Ye, M.P. Armanini, A. Gurney, et al., Characterization of the human suppressor of fused, a negative regulator of the zinc-finger transcription factor Gli, J. Cell Sci. 112 (Pt 23) (1999) 4437–4448.

Int. J. Cancer: **118,** 139–148 (2006)

Hedgehog signaling is activated in subsets of esophageal cancers

Xiaoli Ma[1], Tao Sheng[2], Yuanxin Zhang[1], Xiaoli Zhang[2], Jing He[2], Shuhong Huang[1], Kai Chen[2], Josh Sultz[2], Patrick A. Adegboyega[2], Hongwei Zhang[1]* and Jingwu Xie[2]*

[1]*Institute of Developmental Biology, School of Life Sciences, Shandong University, Jinan, China*
[2]*Sealy Center for Cancer Cell Biology, Departments of Pharmacology, Toxicology and Pathology, University of Texas Medical Branch, Galveston, TX, USA*

The hedgehog pathway plays a critical role in the development of the foregut. However, the role of the hedgehog pathway in primary esophageal cancers is not well studied. Here, we report that elevated expression of hedgehog target genes occurs in 14 of 22 primary esophageal cancers. The hedgehog signaling activation is not associated with tumor subtypes, stages, or differentiation. While the sonic hedgehog (Shh) transcript is localized to the tumor tissue, expression of *Gli1* and *PTCH1* is observed both in the tumor and in the stroma. We discovered that 4 esophageal squamous cell carcinomas, which overexpress Shh, have genomic amplification of the *Shh* gene. Treatment of esophageal cancer cells with smoothened antagonist, KAAD-cyclopamine, or the neutralizing antibodies of Shh reduces cell growth and induces apoptosis. Overexpression of Gli1 under the CMV promoter renders these cells resistant to the treatments. Thus, our results indicate that elevated expression of Shh and its target genes is quite common in esophageal cancers. Our data also indicate that downregulation of Gli1 expression may be an important mechanism by which KAAD-cyclopamine inhibits growth and induces apoptosis in esophageal cancer cells (supplementary material for this article can be found on the *International Journal of Cancer* website at http://www.interscience.wiley.com/jpages/0020-7136/suppmat/index.html).

Key words: sonic hedgehog; cyclopamine; smoothened; esophageal cancer; GI cancer

The hedgehog pathway plays a critical role in embryonic development, tissue polarity and carcinogenesis.[1] Secreted Hedgehog molecules bind to the receptor *patched* (PTC-PTCH1, PTCH2), thereby alleviating PTC-mediated suppression of *smoothened* (SMO), a putative 7-transmembrane protein. SMO signaling triggers a cascade of intracellular events, leading to activation of the pathway through GLI-dependent transcription.[2,3] Activation of Hedgehog signaling, through loss-of-function mutations of *PTCH1* or activated mutations of *SMO*, occurs frequently in human basal cell carcinomas (BCCs) and medulloblastomas.[4–9] More recently, abnormal activation of the hedgehog pathway is also reported in subsets of small cell lung cancer, pancreatic cancer, gastric cancers, prostate cancer and several esophageal cancer cell lines.[10–15]

Esophageal cancer is the 6th most frequent cause of cancer death worldwide.[16] In the United States, the incidence of esophageal adenocarcinoma has nearly quadrupled over the past few decades despite a decline in the overall incidence of cancers in esophagus. Most esophageal cancers remain clinically silent until late in the disease process. Thus, these cancers are often associated with later diagnoses, poorer prognoses, significant morbidities and high mortality rates. Although an early report indicates activation of the hedgehog pathway in several esophageal cancer cell lines, it is not clear if primary tumors of esophagus have activated hedgehog signaling.[12]

To examine the significance of hedgehog pathway activation in esophageal cancers, we have analyzed expression of sonic hedgehog (Shh) and its target genes in 22 primary esophageal tumors using *in situ* hybridization, real-time PCR and immunohistochemistry. Through the assessment of the hedgehog target genes, we find that activation of the hedgehog pathway occurs in 14 of 22 esophageal cancers. We discover genomic amplification of *Shh* in 4 squamous cell carcinomas with elevated Shh expression. These data indicate that activation of the hedgehog pathway can be used as a valuable biomarker for diagnosis and molecular classification of esophageal cancers. Our results further suggest that targeted inhibition of the hedgehog signaling by KAAD-cyclopamine or Shh neutralizing antibodies may be effective in chemoprevention and treatment of esophageal cancers.

Material and methods

Tumor sample

Specimens from 22 cases of esophageal cancers (tumors and the matched adjacent normal tissues) and 1 case of normal esophageal tissue were received as discarded materials from the Shandong Qi Lu Hospital, Jinan, China, or from University of Texas Medical Branch Surgical Pathology with approval from the institutional review board. Pathology reports and H&E staining of each specimen were reviewed to determine the nature of the disease and the tumor histology. Esophageal cancers were divided into 2 major subtypes according to the WHO guideline[17] as follows: adenocarcinoma (4 cases) and squamous cell carcinomas (18 cases).

In situ *hybridization*

Gli1 (X07384) was cloned into pBluescript M13 + KS using *Hind*III (5′) and *Xba*I (3′). The plasmid was digested with *Nru*I to generate the sense fragment (412 bp) and with *Nde*I to generate the antisense fragment (682 bp). PTCH1 (U59464; cloned into *Xba*I5′ and *Cla*I3′ of pRK5) was digested with *Dra*III to generate a small cDNA fragment (590 bp). Sense and antisense probes were obtained by T3 and T7 *in vitro* transcription using a kit from Roche (Mannheim, Germany). Tissue sections (6 μm thick) were mounted onto poly-L-lysine slides.[18] Following deparaffinization, tissue sections were rehydrated in a series of dilutions of ethanol. To enhance signal and facilitate probe penetration, sections were immersed in 0.3% Triton X-100 solution for 15 min at room temperature, followed by treatment with proteinase K (20 μg/ml) for 20 min at 37°C. The sections were then incubated with 4% (v/v) paraformaldehyde/PBS for 5 min at 4°C. After washing with PBS and 0.1M triethanolamine, the slides were incubated with prehybridization solution (50% formamide, 50% 4 × SSC) for 2 hr at 37°C. The probe was added to each tissue section at a concentration of 1 μg/ml and hybridized overnight at 42°C. After high-stringency washing (2 × SSC twice, 1 × standard saline citrate twice, 0.5 × SSC twice at 37°C), sections were incubated with an alkaline phosphatase-conjugated sheep antidigoxigenin antibody, which cata-

Grant sponsor: The National Institutes of Health; Grant number: R01-CA94160; Grant sponsor: The Department of Defense; Grant number: DOD-PC030429; Grant sponsor: The American Cancer Society; Grant sponsor: The Sealy Foundation for Biomedical Sciences; Grant sponsor: The National Science Foundation of China; Grant number: 30228031.
***Correspondence to:** Jingwu Xie, Sealy Center for Cancer Cell Biology, Departments of Pharmacology, Toxicology and Pathology, University of Texas Medical Branch, Galveston, TX 77555. Fax: +409-747-1938. E-mail: jinxie@utmb.edu or to Hongwei Zhang, Institute of Developmental Biology, School of Life Sciences, Shandong University, Jinan, China 250100. E-mail: zhu@sdu.edu.cn
[†]The first three authors contributed equally to this work.
Received 7 October 2004; Accepted after revision 8 April 2005
DOI 10.1002/ijc.21295
Published online 7 July 2005 in Wiley InterScience (www.interscience.wiley.com).

TABLE I – LIST OF ESOPHAGEAL CANCERS AVAILABLE FOR OUR STUDIES

Number	Age	Sex	Pathology diagnosis	Stage	Gli1/PTCH1	Shh
Control-1			Normal esophagus	Normal	−	−
EC-1	66	F	Squamous cell carcinoma (M)	II	+	+
EC-2	69	F	Squamous cell carcinoma (M)	I	−	−
EC-3	60	M	Squamous cell carcinoma (W)	II	+	+
EC-4	57	F	Squamous cell carcinoma (W)	III	−	−
EC-5	57	M	Squamous cell carcinoma (W)	II	+	+[1]
EC-6	65	M	Squamous cell carcinoma (W)	II	+	+
EC-7	68	M	Squamous cell carcinoma (W)	II	−	−
EC-8	56	F	Squamous cell carcinoma (M)	III	+	+[1]
EC-9	64	M	Squamous cell carcinoma (M)	II	−	−
EC-10	51	M	Squamous cell carcinoma (M)	II	+	+
EC-11	47	F	Squamous cell carcinoma (M)	II	−	−
EC-12	64	F	Squamous cell carcinoma (P)	II	+	+
EC-13	54	M	Squamous cell carcinoma (P)	III	+	+[1]
EC-14	38	F	Squamous cell carcinoma (P)	III	+	+[1]
EC-15	55	M	Squamous cell carcinoma (P)	II	−	−
EC-16	73	M	Squamous cell carcinoma (P)	II	+	+
EC-17	68	M	Squamous cell carcinoma (P)	II	−	−
EC-18	66	M	Squamous cell carcinoma (P)	II	+	+
EC-19	50	M	Adenocarcinomas of thoracic esophagus (M)	I	+	+
EC-20	52	F	Adenocarcinomas of gastroesophageal junction (M)	II	+	+
EC-21	52	M	Adenocarcinomas of lower esophagus (M)	IV	+	+
EC-22	55	M	Adenocarcinomas of lower esophagus (M)	II	+	+

Esophageal cancer specimens and summary of *Shh*, *PTCH1* and *Gli1* expression. These data were derived from *in situ* hybridization, Real-time PCR analyses and immunohistochemistry. Since our data from these 3 approaches were consistent with each other, a list of the data from each method was not necessary. –[1]*Shh* genomic DNA amplification was observed in these tumors (confirmed by real-time PCR and regular PCR). W, well-differentiated tumor; M, moderately differentiated tumor; P, poorly differentiated tumor; EC, esophageal cancer.

lyzed a color reaction with the NBT/BCIP (nitro-blue-tetrazolium/5-bromo-4-chloro-3-indolyl phosphate) substrate (Roche). Blue indicated strong hybridization. As negative controls, sense probes were used in all hybridization and no positive signals were observed.

RNA isolation, PCR and quantitative PCR

Total RNAs were extracted using an RNA extraction kit from Promega (Madison, WI) according to the manufacturer's instructions. The exon II of the *Shh* gene was amplified with the forward primer 5′-TAACGTGTCCGTCGGTGGG -3′ and the reverse primer 5′-TGCTTTCACCGAGCAGTGG-3′ using the following cycles: 96°C for 4 min, 25 cycles of 96°C for 30 sec, 57°C for 45 sec and 72°C for 45 sec, plus 72°C for 5 min (50 ng of total genomic DNA in 25 μl PCR cocktail). D10S222 was amplified using the same condition but with 27 cycles. For real-time PCR analyses, we detected the levels of Shh, Gli1 and PTCH1 transcripts using the Applied Biosystems' assays-by-demand assay mixtures (Applied Biosystems, Foster City, CA) and predeveloped 18S rRNA (VIC dye-labeled probe) TaqMan assay reagent (P/N 4319413E) as an internal control. The procedure was described previously.[13] Rnase P was used as the internal control for detecting genomic amplification of the *Shh* gene. The sequences for primers and probes are available upon request. The amount of target ($2^{-\Delta\Delta CT}$) was obtained by normalization to an endogenous reference (18sRNA or Rnase P) and relative to a calibrator.

Immunohistochemistry

Representative formalin-fixed and paraffin-embedded tissue sections (6 μm thickness) were used for immunohistochemistry with specific antibodies to human Shh and PTCH1 (catalog number 9024 for Shh and 6149 for PTCH1; Santa Cruz Biotechnology, Santa Cruz, CA). All primary antibodies have been previously tested for immunohistostaining.[11,13,19] Immunohistochemistry was carried out as previously reported.[13]

Cell culture, MTT assay, BrdU incorporation, flow cytometry and TUNEL assay

Cell lines (KYSE-180 and KYSE-270, purchased from German Collection of Microorganisms and Cell Cultures, Braunschweig, Germany; and RKO, purchased from American Type Culture Collection, Manassas, VA) were cultured in RPMI-1640 with 10% FBS (KYSE-180), F12/RPMI-1640 (1:1) with 2% FBS (KYSE-270), or DMEM with 10% FBS (RK0), respectively. Cells (0.5% FBS) were treated with KAAD-cyclopamine (at a final concentration of 2 or 5 μM) or Shh neutralizing antibodies (5E1 monoclonal antibody was purchased from the Hybridoma Bank, University of Iowa, and was used at the concentrations of 0.1 or 0.5 μg/ml). For colorimetric MTT assay, culture media (including KAAD-cyclopamine) were changed every 24 hr, and the assay was performed according to our published protocol in the presence of 0.5% FBS.[19] BrdU[20,21] and flow cytometry[20] was performed as previously reported. Ectopic expression of Gli1, under the control of the CMV promoter, in KYSE-180 and KYSE-270 cells was achieved by transient transfection with lipofectAmine 2000,[19,20] and Gli1 was detected by immunofluorescent staining with the Myc tag antibody 9e10 (Sigma, St. Louis, MO).[20] TUNEL assay was performed using a kit from Roche according to the manufacturer's instructions.[19,20]

Results

Expression of hedgehog target genes in esophageal cancers

Hedgehog is a critical endodermal signal for the epithelial-mesodermal interactions during development of the vertebrate gut. In adult esophagus, hedgehog signaling is undetectable.[22,23] To test if hedgehog signaling is activated in primary esophageal cancers, we examined expression of hedgehog target genes *Gli1* and *PTCH1* in 22 cases of esophageal specimens (see Table I for specimen information). Increased levels of PTCH1 and Gli1 transcripts indicate activation of the hedgehog pathway.[1]

We first detected Gli1 and PTCH1 transcripts using *in situ* hybridization. In agreement with published reports,[23] we found that the normal esophageal tissue did not have detectable levels of Gli1 and PTCH1, indicating that the hedgehog pathway is not normally activated in adult esophageal tissues (Fig. 1*a*). In contrast, we detected Gli1 and PTCH1 transcripts in 14 of 22 (∼ 64%) tumor specimens, suggesting that activation of the hedgehog pathway is a common event in esophageal cancers. We observed activation of the hedgehog pathway both in adenocarcinomas and in squamous cell carcinomas. In squamous cell carcinomas, 10 of 18 (∼ 56%) specimens had high levels of Gli1 and PTCH1 transcripts

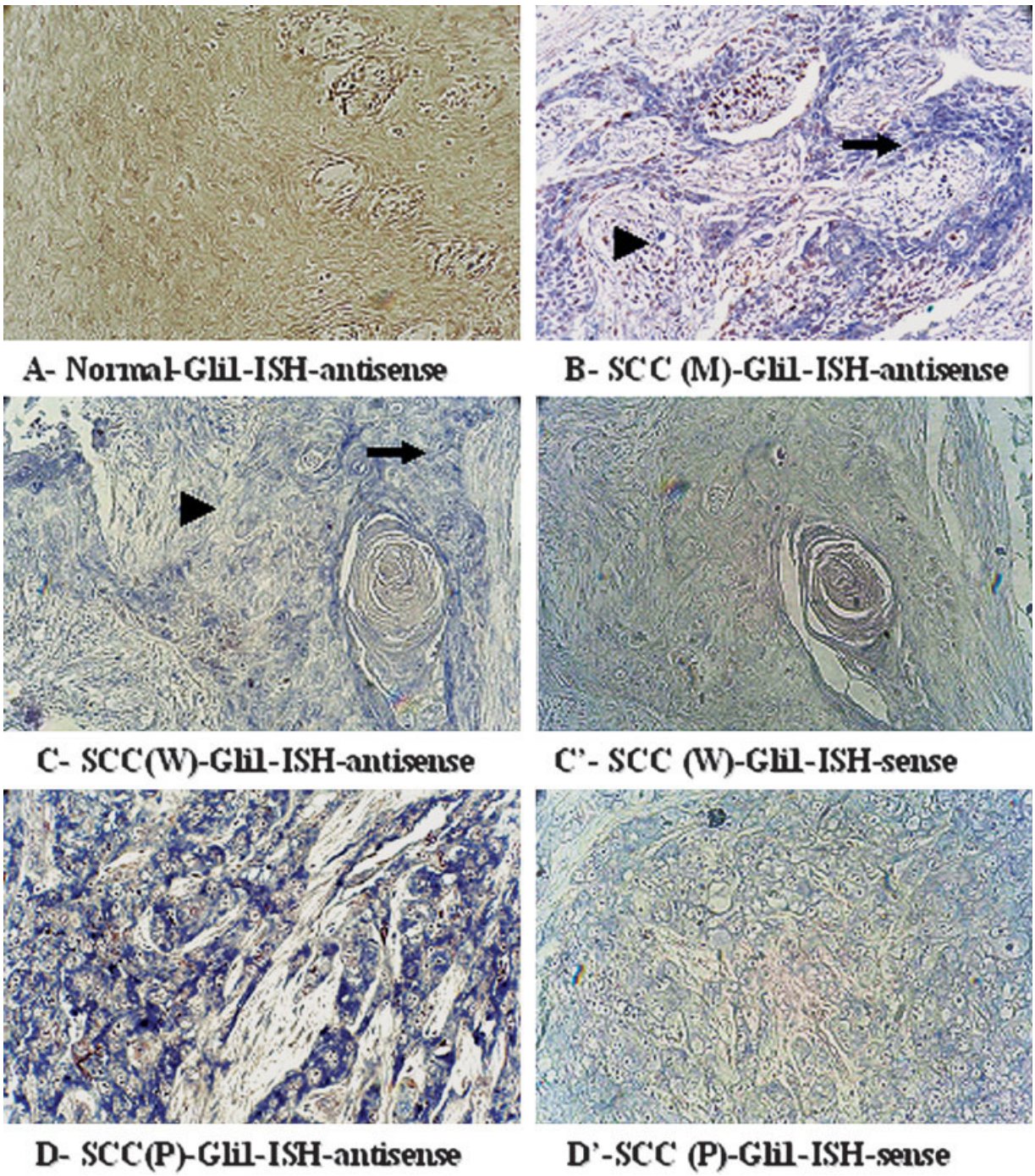

FIGURE 1 – Elevated expression of Gli1 and PTCH1 in primary esophageal tumors. Gli1 transcript (blue as positive) was detected by *in situ* hybridization in the normal control (*a*) and esophageal cancers (*b–d*). (*c′*) and (*c*) are from the same tumor, with (*c′*) being derived from the Gli1 sense probe. Similarly, (*d′*) is the sense probe control of (*d*). Expression of Gli1 transcript was strong in the tumor (indicated by arrows) and weak in the stroma (indicated by arrowheads). The pattern of PTCH1 transcript was similar to those of Gli1 (figures not shown), indicating activation of the hedgehog pathway in esophageal cancers. The data are summarized in Table I.

(see Table I for details). All 4 adenocarcinomas had detectable expression of Gli1 and PTCH1 (Table I). These data indicate that activation of the hedgehog pathway occurs frequently in esophageal cancers.

Further analyses did not reveal any association of hedgehog target gene expression with the tumor stage or differentiation. *In situ* hybridization data indicate that transcripts of Gli1 (Fig. 1*b* and *c*) and PTCH1 (not shown here) are detectable both in the tumor (indicated by arrows) and in the adjacent stroma tissue (indicated by arrowheads). These data suggest that hedgehog signaling may involve epithelium/stroma interactions during development of esophageal cancer.

To confirm the *in situ* hybridization data, we performed real-time PCR analyses to detect the levels of Gli1 and PTCH1 transcripts. We found that Gli1 and PTCH1 transcripts from esophageal tumors were several folds higher than those from

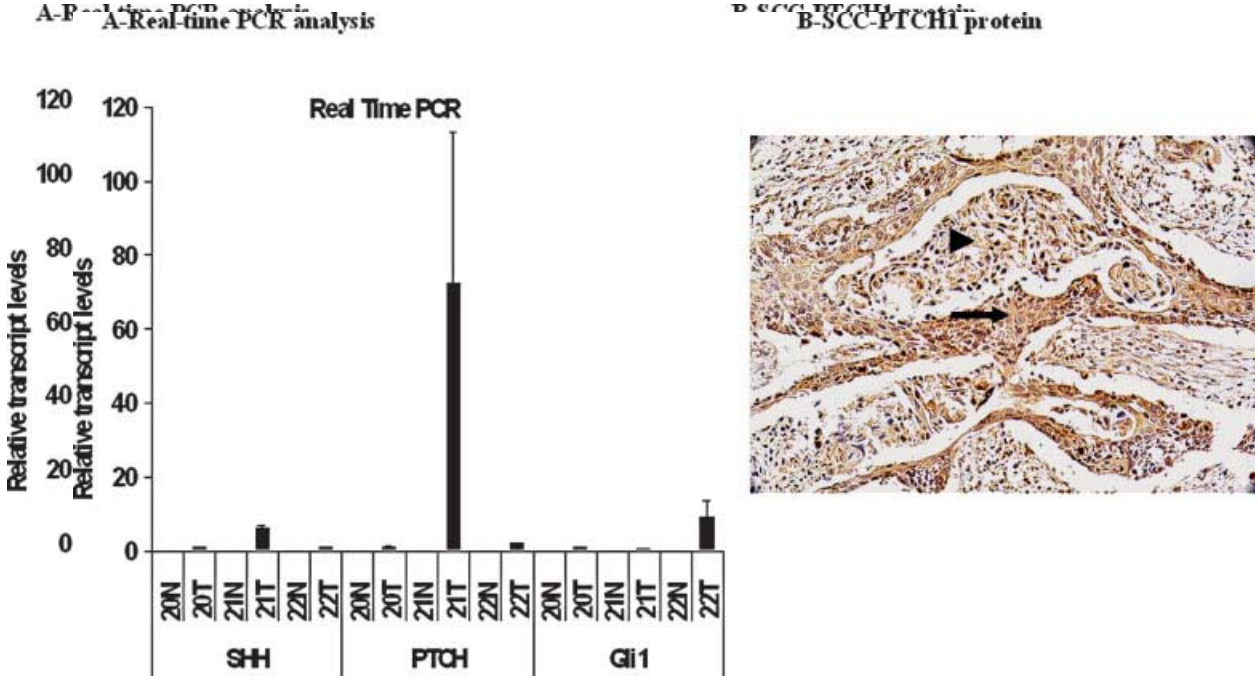

Figure 2 – Elevated PTCH1 transcript and PTCH1 protein in esophageal cancers. To confirm the *in situ* hybridization data, we performed real-time PCR analyses on Shh, PTCH1 and Gli1. Shh, PTCH1 and Gli1 transcripts (*a*) were elevated in 3 primary esophageal tumors. We found that real-time data are consistent with our *in situ* hybridization data. To confirm elevated PTCH1, we performed immunohistochemistry with PTCH1 antibodies.[15] (*b*) shows positive staining of PTCH1 protein (positive in brown) both in the tumor (indicated by an arrow) and in the stroma (indicated by an arrowhead). Our data from real-time PCR analyses are consistent with those derived from *in situ* hybridization, which

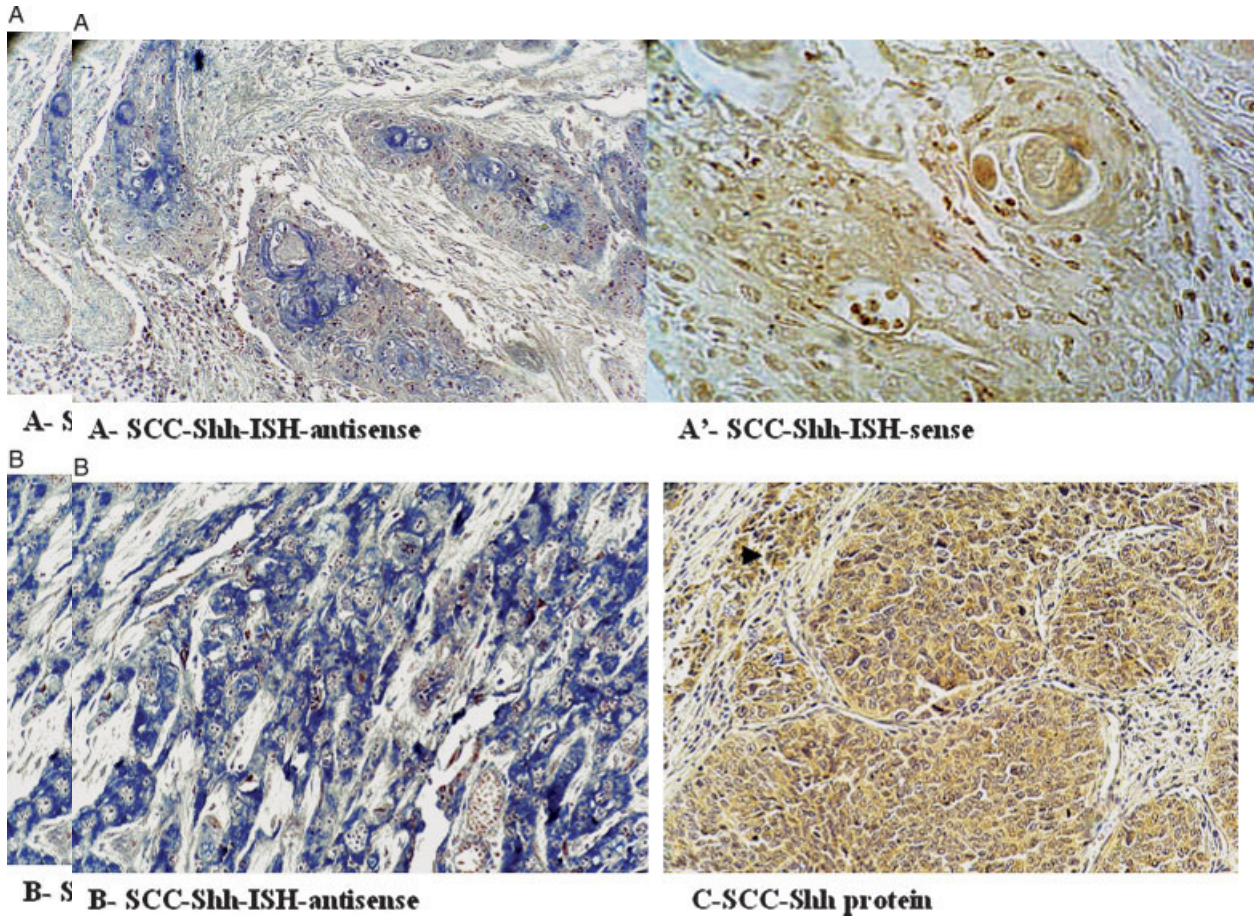

Figure 3 – Expression of Shh in esophageal tumors. *In situ* hybridization was performed to detect Shh transcript in cancerous (*a* and *b*) tissues (positive in blue), and the sense probe did not reveal any positive signals. (*a*′) is the sense probe control of (*a*). Note that no stroma localization of Shh transcript was seen. *In situ* hybridization was confirmed by immunohistostaining of tumor tissues (*c*; positive in brown). Arrowhead indicates stroma expression of Shh protein.

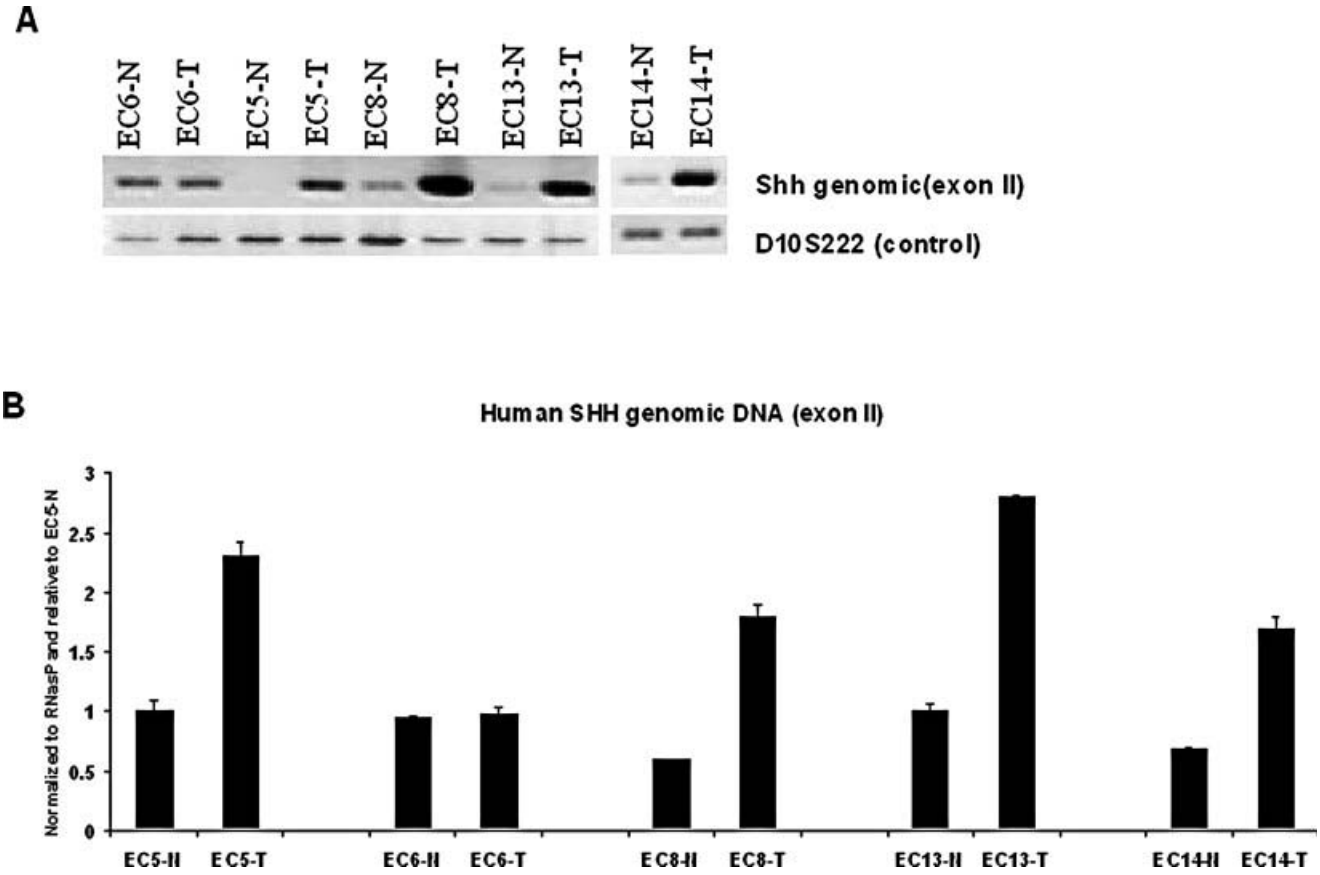

FIGURE 4 – Genomic amplification of the *Shh* exon II in esophageal squamous cell carcinomas. The exon II of *Shh* genomic DNA was initially amplified by regular PCR (see text for details; 25 cycles; nonquantitative PCR). Under the same PCR condition, the levels of PCR products from tumors as well as the matched normal tissues were shown in (*a*). The PCR was repeated 3 times with similar results, suggesting that the *Shh* gene may be amplified in some esophageal tumors. No elevated PCR products were seen from tumors without *Shh* overexpression. To confirm this observation, we performed real-time PCR (see text for details; quantitative analyses). The level of *Shh* genomic fragment was normalized using Rnase P. We noticed that 4 of the esophageal squamous cell carcinomas had 2- to 4-fold increase of *Shh* genomic DNAs over the matched normal tissues (*b*).

the matched normal tissues (Fig. 2*a* shows levels of Shh, PTCH1 and Gli1), confirming that expression of PTCH1 and Gli1 is elevated in the tumor tissues. Expression of PTCH1 in the tumor was further confirmed by immunohistochemistry (Fig. 2*b*).[11,13] All tissues with detectable PTCH1 protein had elevated PTCH1 transcript. In agreement with the *in situ* hybridization results, PTCH1 protein was detected both in the tumor (indicated by an arrow in Fig. 2*b*) and in the stroma (indicated by an arrowhead in Fig. 2*b*). Data derived from *in situ* hybridization, real-time PCR and immunohistochemistry analyses all indicate that activation of the hedgehog pathway is a common event in esophageal cancers.

Expression of Shh in esophageal cancers

It is reported that Shh overexpression may be responsible for activation of the hedgehog pathway in pancreatic cancer and several primary gastric cancers.[11,12] To test this possibility in esophageal cancer, we first examined expression of Shh in esophageal specimens by *in situ* hybridization. As expected, Shh expression was undetectable in the normal esophageal tissue (data not shown). In contrast, many of the primary tumors expressed a high level of Shh transcript (Figs. 2*a* and 3*a* and *b*, Table I). The Shh transcript was detectable specifically in the tumor, not in the stroma (Fig. 3*a* and *b*), suggesting that the tumor cells are the source for Shh expression. Shh expression was associated with detectable levels of Gli1 and PTCH1 transcripts, suggesting an important role of Shh in activating hedgehog pathway in esophageal cancers.

Furthermore, we detected Shh protein by immunohistochemistry using specific antibodies.[11] In agreement with the *in situ* hybridization data, we found that tumors with Shh transcript had higher levels of Shh protein (Fig. 3*c*). As a secreted molecule, sonic hedgehog protein was also detected in the stroma (indicated as arrowhead in Fig. 3*c*). We believe that the secreted sonic hedgehog protein may be responsible for elevated expression of Gli1 and PTCH1 transcripts in the tumor as well as in the stroma (Fig. 1). These results suggest a paracrine signaling mechanism of sonic hedgehog in esophageal cancers.

To identify the mechanisms by which the *Shh* gene was overexpressed in the tumor, we compared genomic DNA of *Shh* from the tumor with that from the adjacent normal tissue. We found that 4 of these tumors with Shh overexpression also had more genomic DNAs (Fig. 4). This observation was initially made using regular PCR amplification PCR (25 cycles, not quantitative) and was confirmed by real-time PCR (quantitative analyses). *Shh* genomic DNA from these tumors, on average, was 3 times more than that from the adjacent normal tissues (Fig. 4*b*). In contrast, we did not observe any elevated *Shh* genomic DNAs in adenocarcinomas of esophagus. These data are in agreement with previous findings that chromosome 7q is frequently overrepresented in esophageal squamous cell carcinomas,[24,25] suggesting that genomic amplifica-

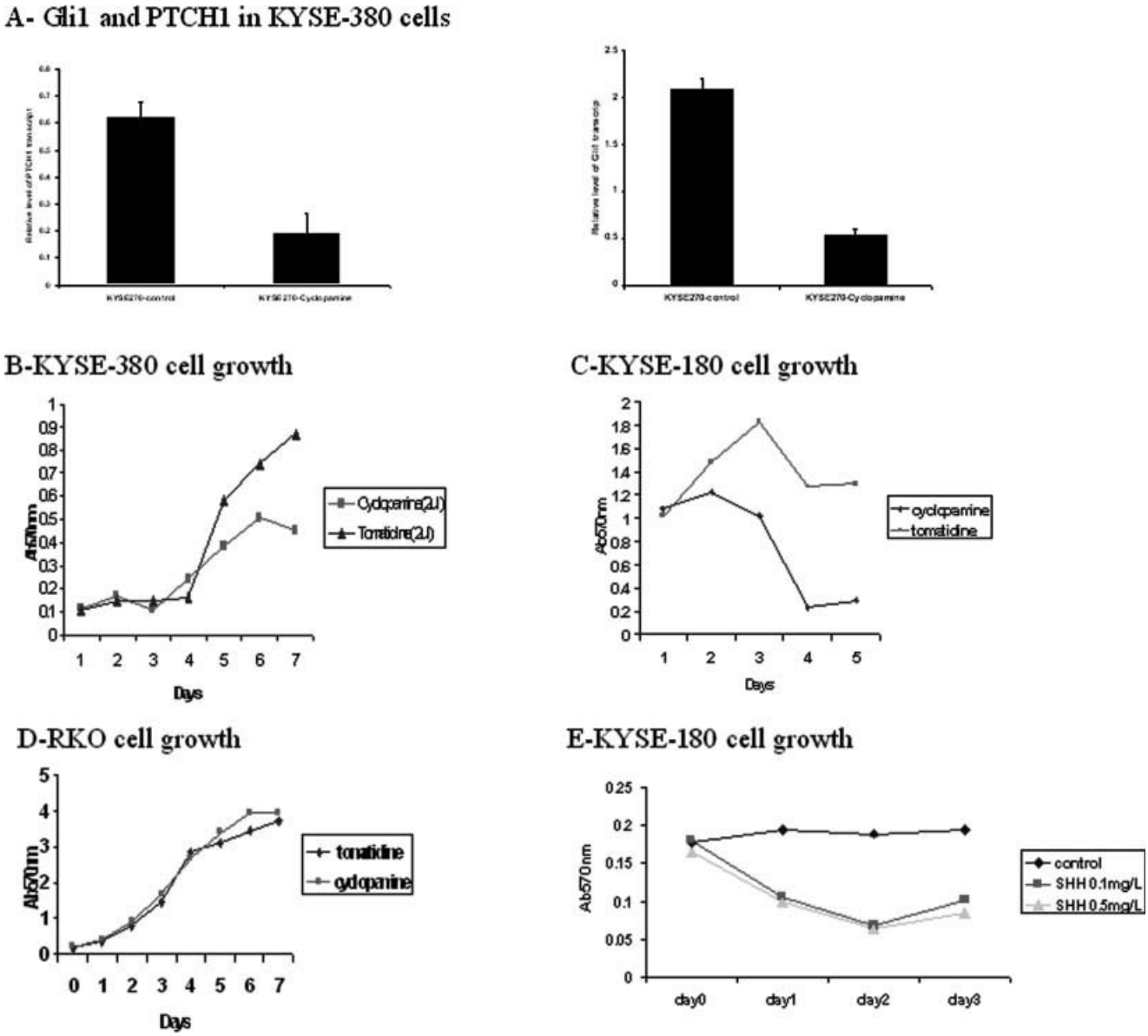

FIGURE 5 – Hedgehog signaling is required for growth of esophageal cancer cells. In the presence of SMO antagonist, KAAD-cyclopamine, the levels of hedgehog pathway target genes (Gli1 and PTCH1) were downregulated (*a* shows data from KYSE-270). Similar data were also obtained from KYSE-180 cells (not shown here). Unlike RKO cells (*d*), which do not have active hedgehog signaling, growth of KYSE-180 (*b*) and KYSE-270 (*c*) cells was inhibited by 2 μM KAAD-cyclopamine. Due to space limit, KAAD-cyclopamine was labeled as cyclopamine. Similarly, incubation of Shh neutralizing antibody 5E1 (0.1 and 0.5 μg/ml) inhibited cell growth of KYSE-180 (*e*) and KYSE-270 (not shown here).

tion of the *Shh* gene in some of these esophageal cancers may be responsible for Shh overexpression.

Targeted inhibition of hedgehog pathway and esophageal cancer cells

If hedgehog pathway activation is required for esophageal cancer development, esophageal cancer cells should be susceptible to treatment of SMO antagonist, KAAD-cyclopamine. Since all available esophageal cancer cell lines have elevated hedgehog signaling,[12] we chose a GI cancer cell line RKO as the negative control (RKO cells do not have elevated levels of Gli1 and PTCH1; data not shown and Berman *et al.*[12]). In this experiment, we used 2 esophageal cancer cell lines (KYSE-180 and KYSE-270) to test the effects of KAAD-cyclopamine. Addition of KAAD-cyclopamine at a final concentration of 2 μM significantly decreased the levels of Gli1 and PTCH1 in both cell lines (Fig. 5*a* shows the data from KYSE-270 cells), indicating that KAAD-cyclopamine inhibits the hedgehog pathway in these cells. The closely related compound tomatidine (2 μM), which does not affect SMO signaling and thus served as a negative control, had little discernible effect on these target genes. As expected, we found that cell growth of esophageal cancer cells, but not RKO cells, was greatly inhibited by KAAD-cyclopamine (Fig. 5*b–d*). We found that cell toxicity of KAAD-cyclopamine at 2 or 5 μM was low (see Fig. S2 for details; supplementary material for this article can be found on the *International Journal of Cancer* website at http://www.interscience.wiley.com/jpages/0020-7136/suppmat/index.html). KAAD-cyclopamine-mediated growth inhibition of KYSE-180 and KYSE-270 cells was dose-dependent (see Fig. S3). Further-

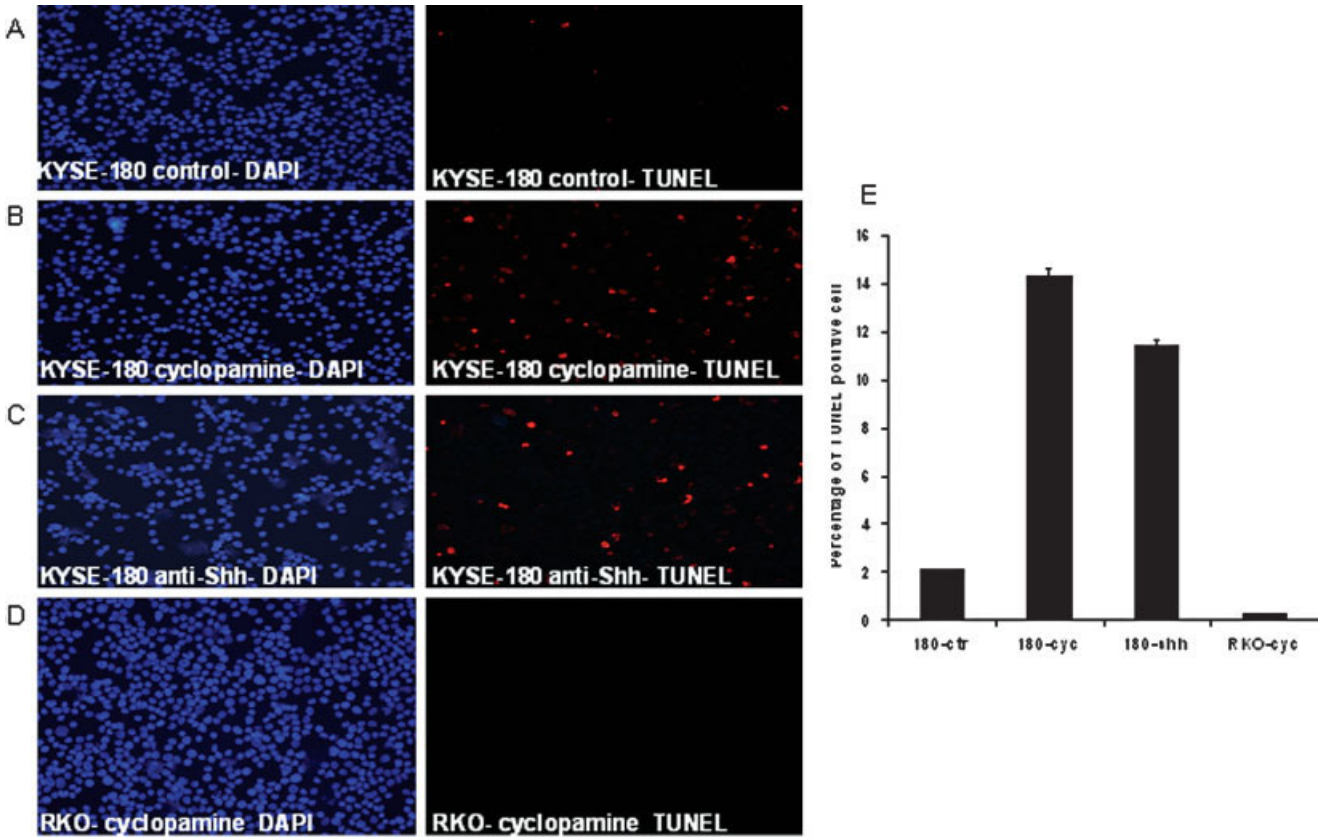

FIGURE 6 – KAAD-cyclopamine and Shh neutralizing antibodies induce apoptosis in esophageal cancer cells. TUNEL assay revealed apoptosis (red) in KYSE180 (*b*) cells, but not in RKO cells (*d*), after treatment with KAAD-cyclopamine (labeled as cyclopamine due to space) for 36 hr. The tomatidine-treated control group had very few TUNEL positive cells (*a* and *e*). Similarly, Shh neutralizing antibody 5E1 (0.1 μg/ml) also caused cell death in KYSE-180 cells (*c*). (*e*) shows the percentage of TUNEL positive cells in each cell lines.

more, KYSE-180 (Fig. 6*b* and *e*) and KYSE-270 cells (not shown here) were TUNEL-positive, indicative of apoptosis after treatment with KAAD-cyclopamine (cell confluence was 15% upon treatment). No apoptosis was observed in RKO cells following addition of 2 μM KAAD-cyclopamine (Fig. 6*d*). Apoptosis was further confirmed by accumulation of sub-G1 cell population (Fig. 7*b*). These results indicate that inhibition of the hedgehog pathway by KAAD-cyclopamine dramatically attenuates the growth of esophageal cancer cells following inhibition of Gli1 and PTCH1 expression, resulting in apoptosis.

If Shh is responsible for hedgehog signaling activation in esophageal cancer cells, inhibition of Shh functions by neutralizing antibodies should reduce cell growth. Indeed, Shh neutralizing antibody 5E1 (at final concentrations of 0.1 μg/ml and 0.5 μg/ml, respectively) significantly inhibited the growth of KYSE-180 cells (Fig. 5*e*), but not that of RKO cells (data not shown). 5E1 IgG also reduced BrdU incorporation in KYSE-180 cells (see Fig. S1). Similar data were also obtained in KYSE-270 cells (data not shown). Flow cytometry analyses indicate an accumulation of sub-G1 cell population after addition of 5E1 IgG in KYSE-180 cells (Fig. 7*c*). This observation was further confirmed by TUNEL analyses (Fig. 6*c*), demonstrating that KYSE-180 cells undergo apoptosis following treatment with 5E1 IgG. Thus, our data support that Shh is responsible for hedgehog-mediated cell proliferation in esophageal cancers.

Our model predicts that overexpression of Gli1 in esophageal cancer cells under a strong promoter (such as the CMV promoter) would constitutively activate the hedgehog pathway, which could render these cancer cells resistant to KAAD-cyclopamine treatment. Indeed, KAAD-cyclopamine did not induce apoptosis in Gli1-expressing KYSE-180 cells, as indicated by lack of TUNEL staining (Fig. 8). Thus, downregulation of Gli1 expression may be an important mechanism by which KAAD-cyclopamine inhibits growth and induces apoptosis of esophageal cancer cells.

Taken together, our findings indicate that activation of the hedgehog pathway is common in esophageal cancers. Activation of the hedgehog pathway is not associated with any specific tumor features (tumor stage, tumor differentiation and tumor subtype). The Shh gene amplification is observed in several esophageal tumors with Shh overexpression. Our data also suggest that downregulation of Gli1 expression is an important mechanism by which KAAD-cyclopamine controls esophageal cancer cell growth. Thus, detection of hedgehog signaling activation may be very useful in cancer diagnosis and targeted cancer treatment of esophageal cancers.

Discussion

Hedgehog signaling activation in esophageal cancers

Hedgehog signaling pathway regulates cell proliferation, tissue polarity and cell differentiation during normal development. Abnormal signaling of this pathway has been reported in a variety of human cancers, including basal cell carcinomas, medulloblastomas, small cell lung cancer and pancreatic cancer.[1] Our findings in this report indicate an important role of the Shh pathway in esophageal cancers. However, not all esophageal squamous cell carcinomas (EC-SCCs) have activated hedgehog signaling, and activation of the hedgehog pathway is not associated with tumor stages or tumor differentiation. In contrast, we found that hedgehog signaling activation in gastric cancers is associated with more

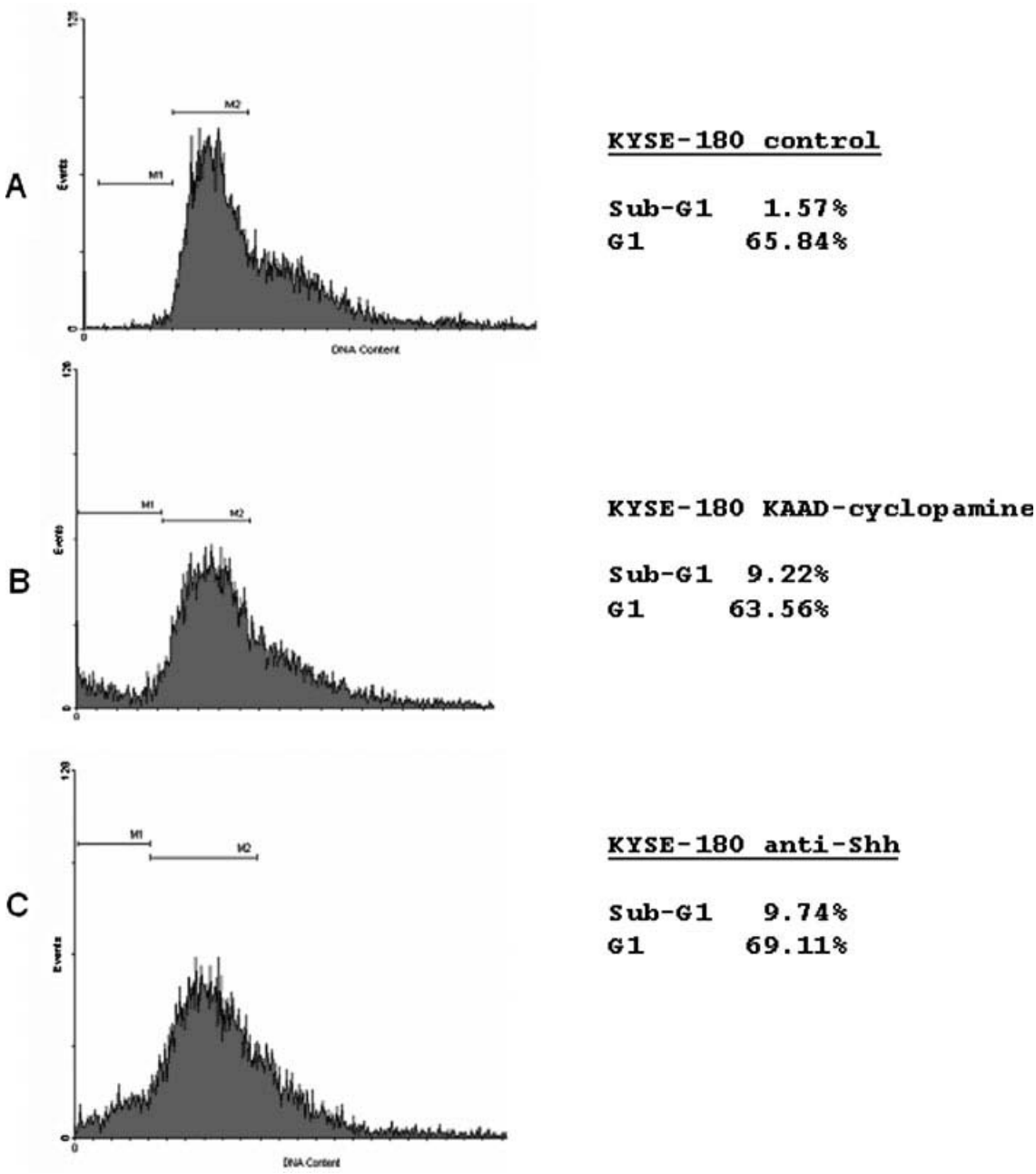

FIGURE 7 – Accumulation of sub-G1 cell population in esophageal cancer cells after hedgehog signaling inhibition. Cells (medium with 0.5% FBS) were treated with 2 μM KAAD-cyclopamine or 0.1 μg/ml Shh neutralizing antibodies for 36 hr before harvest. Flow cytometry was performed as previously reported.[20] KAAD-cyclopamine or Shh neutralizing antibodies increased sub-G1 cell population over 4-fold, from 1.57% to nearly 10% (*a–c*).

poorly differentiated and more aggressive tumors (data not shown). We hypothesize that tumors with activated hedgehog signaling may represent a distinct group of EC-SCCs. Thus, it may be possible to use hedgehog signaling for future molecular classification of EC-SCCs. The actual frequency of hedgehog signaling activation in esophageal cancers, however, should be determined with a large number of primary tumors. It should be interesting to examine the fluency of hedgehog pathway activation in other GI cancers, such as liver, stomach and colon cancers.

Development of esophageal cancer is a multiple-step process, including tumor precursors (Barrett's metaplasia for adenocarcinomas and squamous dysplasia for squamous cell carcinomas), early tumors and tumor metastases. It is of great interests to understand if hedgehog signaling is activated in precursors of esophageal cancers. Similarly, further work is needed to examine if hedgehog signaling is involved in tumor metastases of esophageal cancers. Future understanding of the possible interactions of the hedgehog pathway with other morphogenetic signaling pathways (including wnt and notch pathways) in esophageal cancers will improve our understanding of the etiology of esophageal cancer.

We demonstrated in our studies that amplification of the *Shh* gene may be one mechanism by which Shh is overexpressed in the tumor. Our data are consistent with previous studies, which indicate that gain of 7q is a frequent event in EC-SCCs. Thus, direct detection of

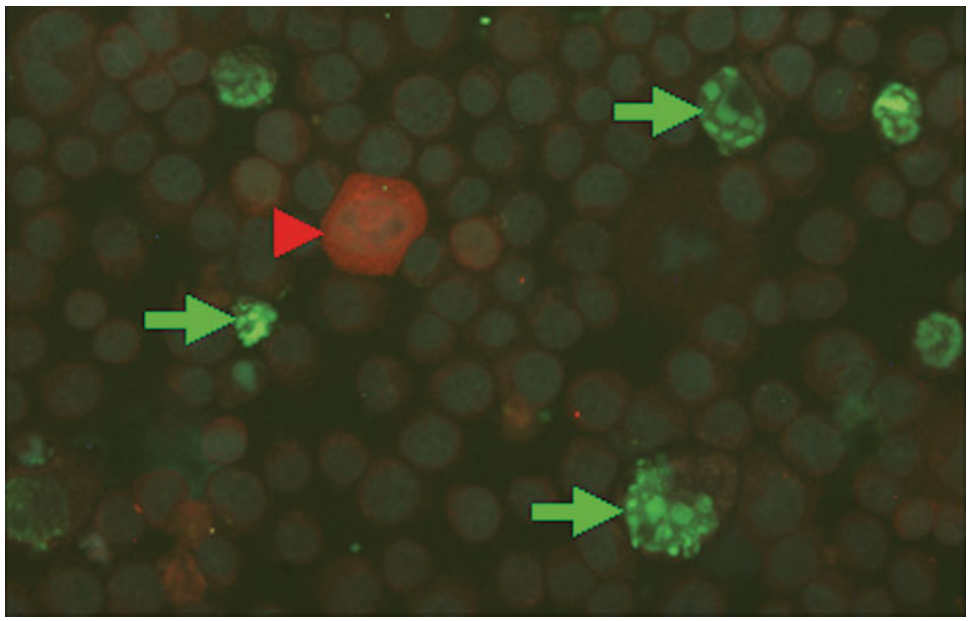

FIGURE 8 – Ectopic expression of Gli1 and cyclopamine sensitivity in esophageal cancer cells. Following ectopic expression of Gli1 under the CMV promoter, KYSE-180 cells became resistant to KAAD-cyclopamine treatment. No apoptosis was detected in over 500 ectopic Gli1 expressing cells (red; indicated by arrowheads), whereas 10–20% Gli1-negative cells underwent apoptosis after KAAD-cyclopamine treatment (green; indicated by arrows).

Shh expression in primary esophageal cancer specimens may be an effective way for diagnosis for subsets of EC-SCC.

Therapeutic perspective of esophageal cancer through targeted inhibition of hedgehog pathway

Addition of smoothened antagonist, KAAD-cyclopamine, or Shh neutralizing antibodies in culture medium of esophageal cancer cells causes inhibition of cell growth, resulting in apoptosis. These data suggest that hedgehog signaling inhibitors may be effective in future treatment of esophageal cancers. Our preliminary data further indicate that activation of caspases-8 and -3 occurs in KYSE-180 cells after treatment with Shh antibodies (data not shown), suggesting that a death receptor pathway is activated. Additional understanding of apoptotic mechanisms will be helpful for future design of novel drugs for esophageal cancers.

We further demonstrated that overexpression of Gli1 prevents cyclopamine-mediated apoptosis in esophageal cancer cells, further supporting the specificity of KAAD-cyclopamine. Our recent studies indicated that chronic oral administration of KAAD-cyclopamine of Ptch1$^{+/-}$ mice did not affect the overall survival of the mice,[20] which provides a foundation for clinical trials of KAAD-cyclopamine on esophageal cancers. Thus, it is quite possible in the future, with availability of a specific SMO antagonist, KAAD-cyclopamine, to treat the subsets of esophageal cancer in which the hedgehog pathway is activated.

Acknowledgements

The authors thank Huiping Guo for technical support in real-time PCR analysis.

References

1. Pasca di Magliano M, Hebrok M. Hedgehog signalling in cancer formation and maintenance. Nat Rev Cancer 2003;3:903–11.
2. Taipale J, Beachy PA. The hedgehog and Wnt signalling pathways in cancer. Nature 2001;411:349–54.
3. Ingham PW. Transducing hedgehog: the story so far. EMBO J 1998; 17:3505–11.
4. Hahn H, Wicking C, Zaphiropoulous PG, Gailani MR, Shanley S, Chidambaram A, Vorechovsky I, Holmberg E, Unden AB, Gillies S, Negus K, Smyth I, *et al*. Mutations of the human homolog of Drosophila patched in the nevoid basal cell carcinoma syndrome. Cell 1996;85:841–51.
5. Johnson RL, Rothman AL, Xie J, Goodrich LV, Bare JW, Bonifas JM, Quinn AG, Myers RM, Cox DR, Epstein EH Jr, Scott MP. Human homolog of patched, a candidate gene for the basal cell nevus syndrome. Science 1996;272:1668–71.
6. Xie J, Johnson RL, Zhang X, Bare JW, Waldman FM, Cogen PH, Menon AG, Warren RS, Chen LC, Scott MP, Epstein EH Jr. Mutations of the PATCHED gene in several types of sporadic extracutaneous tumors. Cancer Res 1997;57:2369–72.
7. Raffel C, Jenkins RB, Frederick L, Hebrink D, Alderete B, Fults DW, James CD. Sporadic medulloblastomas contain PTCH mutations. Cancer Res 1997;57:842–5.
8. Xie J, Murone M, Luoh SM, Ryan A, Gu Q, Zhang C, Bonifas JM, Lam CW, Hynes M, Goddard A, Rosenthal A, Epstein EH Jr, *et al*. Activating smoothened mutations in sporadic basal-cell carcinoma. Nature 1998;391:90–2.
9. Taylor MD, Liu L, Raffel C, Hui CC, Mainprize TG, Zhang X, Agatep R, Chiappa S, Gao L, Lowrance A, Hao A, Goldstein AM, *et al*. Mutations in SUFU predispose to medulloblastoma. Nat Genet 2002; 31:306–10.
10. Watkins DN, Berman DM, Burkholder SG, Wang B, Beachy PA, Baylin SB. Hedgehog signalling within airway epithelial progenitors and in small-cell lung cancer. Nature 2003;422:313–7.
11. Thayer SP, Di Magliano MP, Heiser PW, Nielsen CM, Roberts DJ, Lauwers GY, Qi YP, Gysin S, Fernandez-Del Castillo C, Yajnik V, Antoniu B, McMahon M, *et al*. Hedgehog is an early and late mediator of pancreatic cancer tumorigenesis. Nature 2003;425:851–6.
12. Berman DM, Karhadkar SS, Maitra A, Montes De Oca R, Gerstenblith MR, Briggs K, Parker AR, Shimada Y, Eshleman JR, Watkins DN, Beachy PA. Widespread requirement for Hedgehog ligand stimulation in growth of digestive tract tumours. Nature 2003; 425:846–51.
13. Sheng T, Li C-X, Zhang X, Chi S, He N, Chen K, McCormick F, Gatalica Z, Xie J. Activation of the hedgehog pathway in advanced prostate cancer. Mol Cancer 2004;3:29.
14. Sanchez P, Hernandez AM, Stecca B, Kahler AJ, DeGueme AM, Barrett A, Beyna M, Datta MW, Datta S, Ruiz i Altaba A. Inhibition of prostate cancer proliferation by interference with SONIC HEDGEHOG-GLI1 signaling. Proc Natl Acad Sci USA 2004;101:12561–6.
15. Karhadkar SS, Bova GS, Abdallah N, Dhara S, Gardner D, Maitra A, Isaacs JT, Berman DM, Beachy PA. Hedgehog signalling in prostate regeneration, neoplasia and metastasis. Nature 2004;431:707–12.
16. Pisani P, Parkin DM, Bray F, Ferlay J. Estimates of the worldwide mortality from 25 cancers in 1990. Int J Cancer 1999;83:18–29.
17. Sarbia M, Becker KF, Hofler H. Pathology of upper gastrointestinal malignancies. Semin Oncol 2004;31:465–75.
18. Unden A, Zaphiropoulos PG, Toftgard R, Stahle-Backdahl M. Human patched (PTCH) mRNA is overexpressed consistently in tumor cells of both familial and sporadic basal cell carcinoma. Cancer Res 1997; 57:2336–40.

19. Li C, Chi S, He N, Zhang X, Guicherit O, Wagner R, Tyring S, Xie J. IFNalpha induces Fas expression and apoptosis in hedgehog pathway activated BCC cells through inhibiting Ras-Erk signaling. Oncogene 2004;23:1608–17.
20. Athar M, Li C, Tang X, Chi S, Zhang X, Kim AL, Tyring SK, Kopelovich L, Hebert J, Epstein EH Jr, Bickers DR, Xie J. Inhibition of smoothened signaling prevents ultraviolet B-induced basal cell carcinomas through regulation of Fas expression and apoptosis. Cancer Res 2004;64:7545–52.
21. Xie J, Aszterbaum M, Zhang X, Bonifas JM, Zachary C, Epstein E, McCormick F. A role of PDGFRalpha in basal cell carcinoma proliferation. Proc Natl Acad Sci USA 2001;98:9255–9.
22. van den Brink GR, Hardwick JC, Nielsen C, Xu C, ten Kate FJ, Glickman J, van Deventer SJ, Roberts DJ, Peppelenbosch MP. Sonic hedgehog expression correlates with fundic gland differentiation in the adult gastrointestinal tract. Gut 2002;51:628–33.
23. Arsic D, Keenan J, Quan QB, Beasley S. Differences in the levels of Sonic hedgehog protein during early foregut development caused by exposure to adriamycin give clues to the role of the Shh gene in oesophageal atresia. Pediatr Surg Int 2003;19:463–6.
24. Yen CC, Chen YJ, Chen JT, Hsia JY, Chen PM, Liu JH, Fan FS, Chiou TJ, Wang WS, Lin CH. Comparative genomic hybridization of esophageal squamous cell carcinoma: correlations between chromosomal aberrations and disease progression/prognosis. Cancer 2001;92:2769–77.
25. Walch AK, Zitzelsberger HF, Bruch J, Keller G, Angermeier D, Aubele MM, Mueller J, Stein H, Braselmann H, Siewert JR, Hofler H, Werner M. Chromosomal imbalances in Barrett's adenocarcinoma and the metaplasia-dysplasia-carcinoma sequence. Am J Pathol 2000;156:555–66.